Institut für organische Chemie und Biochemie

Lehrstuhl für Biotechnologie

Mechanistic Insight into the Role of PolyP in Neurodegeneration

Justine Lempart

Vollständiger Abdruck der von der Fakultät für Chemie der Technischen Universität München zur Erlangung des akademischen Grades eines

Doktors der Naturwissenschaften (Dr. rer. nat.)

genehmigten Dissertation.

Vorsitzender:	Prof. Dr. Matthias Feige
Prüfer der Dissertation:	
	1. Prof. Dr. Johannes Buchner
	2. Prof. Dr. Ursula Jakob

Die Dissertation wurde am 21.10.2019 bei der Technischen Universität München eingereicht und durch die Fakultät für Chemie am 03.12.2019 angenommen.

Declaration

I, Justine Lempart, hereby declare that this thesis was prepared by me independently and using only the references and resources stated. This work has not been submitted to any other audit commission. Parts of this work have been published in scientific journals.

Erklärung

Hiermit erkläre ich, Justine Lempart, dass ich die vorliegende Arbeit selbständig verfasst und keine anderen als die angegebenen Quellen und Hilfsmittel verwendet habe. Die Arbeit wurde bisher keiner Prüfungskommission vorgelegt. Teile dieser Arbeit wurde in wissenschaftlichen Journalen veröffentlicht.

Justine Lempart

Munich, 21st of October 2019

Contents

1 ZUSAMMENFASSUNG

PolyP ist aus anorganischen Phosphaten aufgebaut und damit eines der einfachsten Moleküle in der Natur. Trotz seiner simplen Struktur hat das Polyanion eine beeindruckende Anzahl essenzieller Funktionen in verschiedenen Organismen. Kürzlich hat unser Labor die spannende Entdeckung gemacht, dass PolyP die Entstehung von amyloidogenen Fibrillen *in vitro* beschleunigt und neuronale Zellen in Zellkulturexperimenten gegen die Toxizität dieser Fibern schützt. Damit wurde gezeigt, dass das Molekül eine physiologische Rolle bei neurodegenerativen Erkrankungen spielt. In dieser Arbeit habe ich die Interaktion zwischen PolyP und zwei Proteinen, die in neurodegenerativen Erkrankungen involviert sind, untersucht: Alpha-Synuclein ist mit der Pathologie der Parkinson-Krankheit und Tau mit der Pathologie der Alzheimer-Krankheit assoziiert. Hierbei habe ich herausgefunden, dass die Entstehung von α-Synuclein- Fibrillen einen initialen Schritt hat, welcher unabhängig von PolyP ist. In diesem Schritt werden α-Synuclein-Oligomere gebildet, mit welchen PolyP dann interagieren kann, was daraufhin die Entstehung von Fibrillen rapide beschleunigt. Das reversible Binden von PolyP an ausgereifte α-Synuclein- Fibrillen induziert eine veränderte Fibrillen - Struktur. In vorherigen Veröffentlichungen wurde gezeigt, dass diese Struktur stabiler ist und weniger dazu neigt, toxische Intermediate abzusondern. Der PolyP-α-Synuclein-Komplex blockiert ebenfalls die Bindung von α-Synuclein- Fibrillen an die Zellmembran und verhindert dadurch die Aufnahme von Amyloiden in differenzierte neuronale Zellen. Im Gegensatz zu α-Synuclein interagiert das monomere Tau Protein direkt mit PolyP. Durch “single molecule studies” haben wir herausgefunden, dass diese Interaktion zu einer Struktur führt, die eher geneigt ist, Aggregate zu bilden. Aggregationsassays mit verschiedenen Tau-Isoformen haben gezeigt, dass PolyP mehrere Bindestellen an einem Tau-Monomer hat. Durch diese inter- und intramolekularen Interaktionen bildet PolyP ein Gerüst, welches mehrere Tau-Monomere zusammenbringt und die Entstehung von Fibern beschleunigt. Diese Fähigkeit von PolyP ist von der Kettenlänge des Polyanions abhängig.

Zusammengefasst gibt diese Arbeit mechanistische Einsichten in die Rolle von PolyP in amyloidogenen Prozessen. Außerdem bildet sie die Grundlage für die weitere Untersuchung von PolyP als potenzieller therapeutischer Ansatz, um die zelluläre Verbreitung neurodegenerativer Erkrankungen im Gehirn zu verhindern.

2 ABSTRACT

Built as a linear chain of inorganic phosphate units, polyP is one of nature's simplest molecules. Yet, this polyanion exerts a number of crucial functions in organisms. Recent work from our lab identified polyP as a physiological modifier of neurodegenerative diseases by accelerating amyloid fiber formation *in vitro* and protecting neuronal cells against amyloid toxicity in cell culture experiments. In this work, I characterized the interaction between polyP and two proteins involved in neurodegenerative diseases: α-synuclein, a protein associated with the pathology in Parkinson's disease and tau, a protein associated with the pathology in Alzheimer's disease. I found that α-synuclein fiber formation shows an initial polyP-independent step. Subsequent oligomerization of α-synuclein was then rapidly accelerated by the presence of polyP. Reversible binding of polyP to mature α-synuclein fibrils induced altered fiber morphology that was previously shown to make the fibers more stable and less prone to shed off toxic intermediates. The formation of a polyP-α-synuclein fiber complex prevented the association of fibrils with the cell membrane and significantly reduced the internalization of amyloids into differentiated neuronal cells. In contrast to α-synuclein, polyP interacted directly with monomeric tau, leading to the formation of a distinct aggregation-prone conformation that we characterized by single molecule studies. Aggregation assays with various tau isoforms suggested that tau contains several polyP binding sites and revealed a chain length dependency of the inter- and intramolecular scaffolding ability of polyP towards tau. In summary, this study provided novel mechanistic insights into the role of polyP in amyloidogenic processes and form the foundation for polyP as a potential novel therapeutic strategy to prevent the cellular spreading of the diseases.

3 INTRODUCTION

The introduction is adapted from a review, entitled “Role of Polyphosphate in Amyloidogenic Processes”, which I wrote as part of my thesis work (Lempart and Jakob 2019).

3.1 PolyP- A molecule of many functions

PolyP is one of the simplest biomolecules, which has been found in all eukaryotic and almost every prokaryotic organism tested so far (Figure 1) (Kulaev and Vagabov 1983; Wood and Clark 1988; Kumble and Kornberg 1995; Rao, Gomez-Garcia et al. 2009). The negative charge and the high energetic content appear to contribute to some of polyP’s described functions, including the ability to chelate metal ions, and serve as energy source and phosphate buffer (Archibald and Fridovich 1982; Pick and Weiss 1991; Keasling, Bertsch et al. 1993).

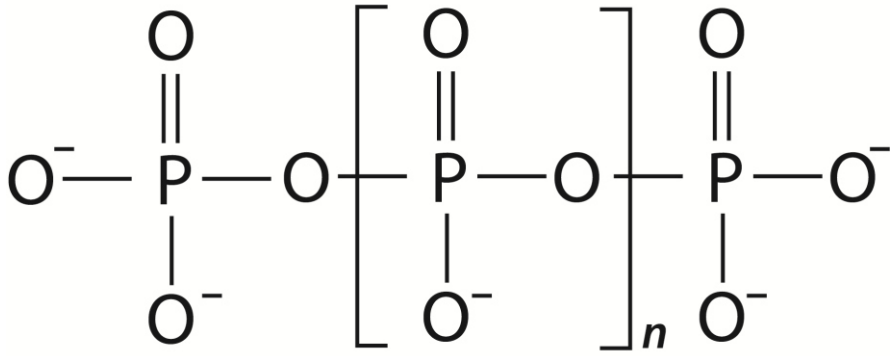

Figure 1: Model structure of polyP*. Inorganic phosphate units are linked through phosphoanhydride bonds in a linear chain (n= between 3 or up to 1000).*

However, the mechanisms for several other cellular functions of polyP, are less likely to be directly mediated by its biophysical features and raised the question how this simple molecule exerts its pleiotropic effects. In unicellular organisms, polyP was found to serve as a modifier of biofilm formation, contributor to virulence and important enhancer of stress resistance (Figure 2) (Kornberg, Rao et al. 1999; Rashid, Rao et al. 2000; Rao, Gomez-Garcia et al. 2009; Docampo, Jimenez et al. 2011; Kulakovskaya, Vagabov et al. 2012). In mammals, polyP takes part in energy homeostasis (Wang, Schroder et al. 2016), blood clotting (Morrissey, Choi et al. 2012), apoptosis (Hernandez-Ruiz, Gonzalez-Garcia et al. 2006), DNA repair and nuclear transcription (Jimenez-Nunez, Moreno-Sanchez et al. 2012; Bru,

Samper-Martin et al. 2017), ion channel function (Kim and Cavanaugh 2007; Zakharian, Thyagarajan et al. 2009), PTP formation (Abramov, Fraley et al. 2007; Seidlmayer, Gomez-Garcia et al. 2012) and cell signaling in the brain (Holmstrom, Marina et al. 2013) (Figure 2).

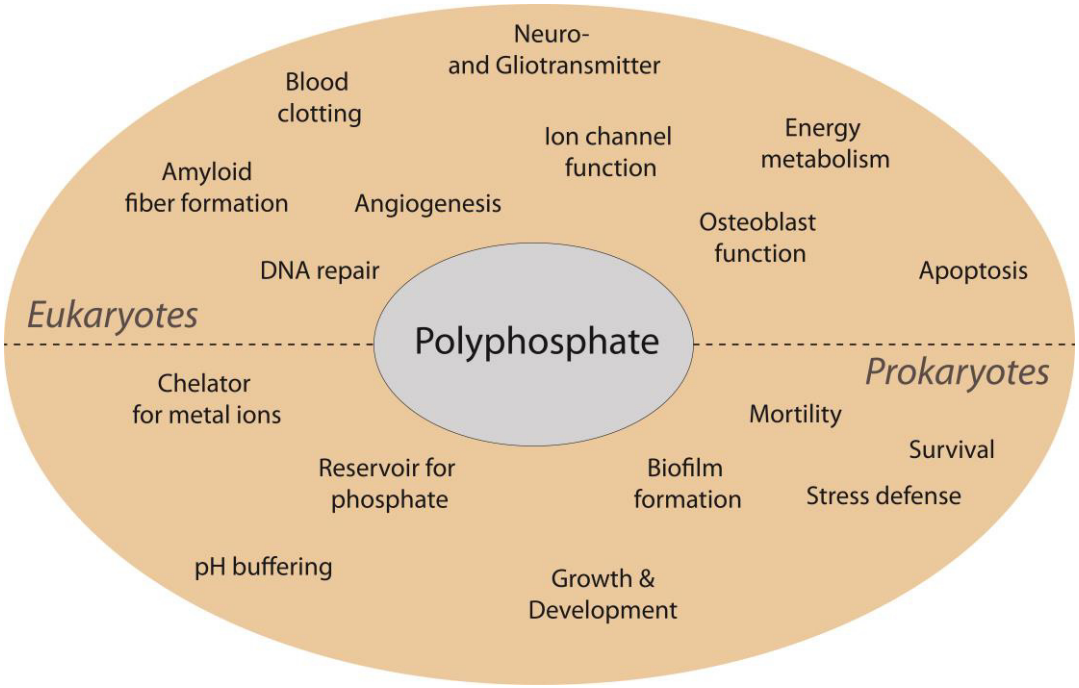

Figure 2: Multi-functionality of polyP in eukaryotes and prokaryotes (Lempart and Jakob 2019).

Recent findings from our lab identified polyP as an ATP-independent chaperone (Gray, Wholey et al. 2014). These results indicated not only that polyP constitutes one of the earliest defense mechanism against cellular stressors, but suggested that part of its multi-functionality might in fact be based on polyP-protein interactions. Endogenous polyP levels have long been known to increase under oxidative stress conditions (Akiyama, Crooke et al. 1992), where bacteria convert over 50% of their cellular ATP into polyP (Gray, Wholey et al. 2014). This energetic redirection of ATP provides two major advantages for the stress-exposed cellular network: ATP depletion effectively down-regulates processes that are highly sensitive to oxidation while polyP-protein interactions prevent irreversible protein aggregation. Upon stress relief, PolyP kinase (PPK) is then able to regenerate ATP from polyP, fueling ATP- dependent chaperones like DnaK, DnaJ or GrpE, which then refold the protected proteins (Gray, Wholey et al. 2014) (Figure 3).

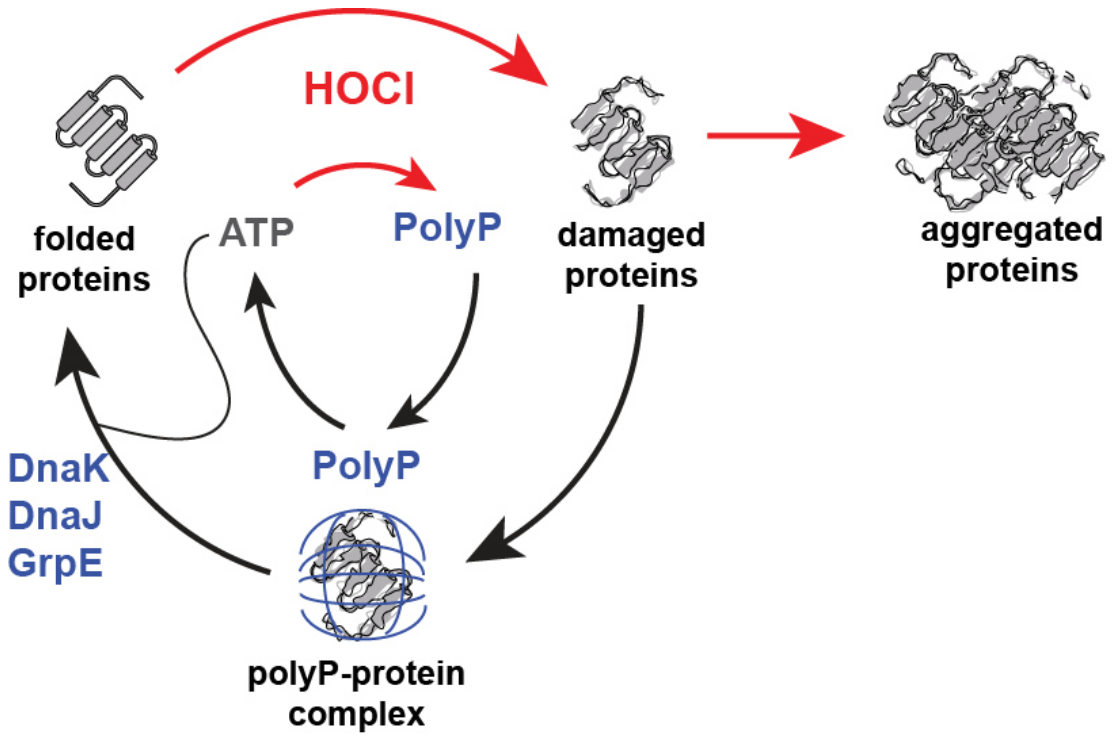

***Figure 3: The role of polyP under cellular stress conditions**. Conversion of ATP into polyP safely stores the cellular energy content and protects proteins from stress-induced aggregation through the formation of a polyP-protein complex. Upon stress relief chaperones like DnaK, DnaJ or GrpE can refold the protein, release polyP and cellular ATP levels can get regenerated (Gray, Wholey et al. 2014).*

In vitro experiments provided first mechanistic insights by demonstrating that polyP concentrations in the micromolar range are sufficient to convert proteins from a thermolabile α-helical into a thermostable β-sheet conformation. Unexpectedly, those structures are capable of inducing increased fluorescence with the amyloid interacting dye Thioflavin T (ThT) (Cremers, Knoefler et al. 2016; Yoo, Dogra et al. 2018). This conversion from unstructured or mainly α-helical proteins into β-sheet rich structures is also the foundation of fibril formation found in many different neurodegenerative diseases and suggested that polyP might serve as a modifier of amyloidogenic processes.

3.2 The role of polyP in amyloidogenesis

3.2.1 The influence of polyP on amyloid formation in bacteria

It has long been known that depletion of polyP reduces bacterial biofilm formation (Rashid, Rumbaugh et al. 2000). This was reasoned with a potentially essential role of polyP in quorum sensing, which - in the absence of the polyanion- would result in the impaired ability of bacteria to respond to their environment (Rashid, Rumbaugh et al. 2000). However, recent work of our lab revealed that polyP directly influences the cross-β-sheet fibril formation of CsgA fibers (i.e, curli), an integral part of the bacterial biofilm matrix. These results suggested a direct involvement of polyP in the formation and/or structural arrangement of the fibril (Rashid, Rumbaugh et al. 2000; Cremers, Knoefler et al. 2016). Indeed, *in vitro* experiments measuring CsgA fiber formation via ThT fluorescence showed that polyP is capable of accelerating this process (Cremers, Knoefler et al. 2016). Studies using Δ*ppk* strains confirmed these *in vitro* findings and revealed that polyP-deficient bacteria show significantly slower biofilm formation compared to wild-type (WT) strains (Rashid, Rumbaugh et al. 2000). Addition of polyP to the media of these mutants rescued the effect and restored biofilm formation (Cremers, Knoefler et al. 2016).

3.2.2 Influence of polyP on disease-associated amyloids

The underlying mechanism of curli formation is based on the conversion of unstructured CsgA into fibrillary cross β-sheet structures on the cell surface (Hufnagel, Tukel et al. 2013). This process comprises mechanistically all characteristics of the amyloid formation that is found to contribute to neurodegenerative diseases, including Alzheimer's disease (AD) and Parkinson's disease (PD) (Soto 2003; Eichner and Radford 2011; Shoffner and Schnell 2016). Subsequent studies with disease-associated amyloids revealed that polyP indeed also accelerates the fiber formation of Aβ, tau (AD) and α-synuclein (PD) (Figure 4) (Cremers, Knoefler et al. 2016). Alpha-synuclein and Aβ fibers form two to three times faster in the presence of polyP than in its absence. Moreover, *in vitro* fibrillation of full-length tau is accelerated from several month ($T_{1/2}$ >9 months) to a few days ($T_{1/2}$ ~50 hours) when polyP is added (Cremers, Knoefler et al. 2016). The polyP effects were shown to be chain-length dependent, with longer polyP (>60 P_i) chains showing a disproportionally higher impact than shorter chains (<14

P_i). Mechanistically it remains elusive whether polyP interacts with the unstructured or α-helical structure of the soluble amyloids and induces their β-sheet formation, or binds and stabilizes β-sheet structures that transiently accumulate during the amyloid fiber formation process. Moreover, it is unknown whether polyP interacts with specific sidechains or the protein backbone of the client protein. The finding that polyP's clients are very diverse supports the idea of polyP-protein backbone interactions (Gray, Wholey et al. 2014; Yoo, Dogra et al. 2018).

3.2.3 Influence of polyP on amyloid structures

Recent studies showed that platelet-derived polyP elicits structural changes in fibrin that generates shorter protofibrils with reduced stiffness and produces a fibrin network with increased knotted regions (Whyte, Chernysh et al. 2016). Similarly, the Jakob lab found that polyP induces a significant morphological change in amyloid fibrils, which normally form two single protofilaments, twisted around each other in a distinct helix (Guerrero-Ferreira, Taylor et al. 2018). In the presence of polyP, however, the fibrils are significantly thinner and lack the characteristic twisted structure (Figure 4) (Cremers, Knoefler et al. 2016). Moreover, fibrils formed in the presence of polyP were about 30% less prone to shedding and found to be more susceptible to degradation by proteases including proteinase K (Figure 4) (Cremers, Knoefler et al. 2016). Easily degradable fibers that are more stable and incapable of disassembling into toxic oligomers suggest that polyP can lower amyloid toxicity through altering fiber structure. Previous studies that have shown different physiochemical properties (i.e pH) (Hoyer, Antony et al. 2002) or different polyanionic modifiers (i.e Heparin) (Cohlberg, Li et al. 2002) to induce similar structural changes that ultimately lead to altered toxicity, stability, seeding behavior and spreading (Bousset, Pieri et al. 2013), agree with this idea and further suggest a physiological and/or pathological relevance of polyP in the context of neurodegeneration.

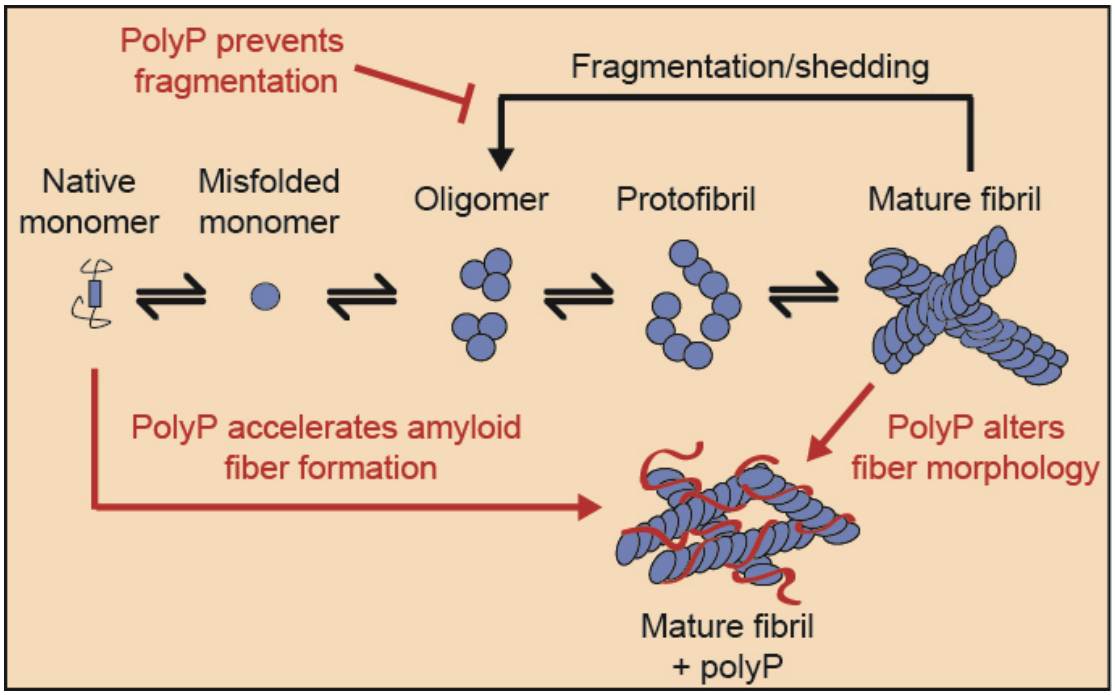

***Figure 4 : The influence of polyP on amyloid fiber formation**. Structural rearrangement of monomeric protein leads to the formation of β-sheet rich monomers, oligomers, protofibrils and eventually mature fibers. PolyP accelerates amyloid fiber formation to mature fibers, alters the fiber morphology and prevents the fragmentation and shedding of oligomers (Lempart and Jakob 2019).*

3.3 PolyP in the mammalian brain

Only limited reports about the role of polyP in mammals are available. This is likely due to the challenges that arise when polyP concentrations are low (Kumble and Kornberg 1995; Kornberg 1999). By studying rats, the group of Kornberg showed that the highest polyP concentrations are found in the brain (25 to 120 µM in Pi units) and the liver (22 and 42 µM in Pi units) (Gabel and Thomas 1971; Kumble and Kornberg 1995) with chain lengths between 50 to 800 residues (Gabel and Thomas 1971; Kumble and Kornberg 1995). However, the length of polyP chains is still under debate with other studies suggesting that polyP chains in mammals are exclusively shorter, i.e. between 10 and 100 phosphates (Lorenz, Munkner et al. 1997; Stotz, Scott et al. 2014). The differences in the reported chain lengths are most likely due to the challenges arising with the detection of low physiological polyP concentrations (Kornberg 1999) and potential differences in polyP levels and lengths during different developmental stages. Indeed, brain polyP levels appear to change over the lifetime of the animals while polyP levels in the liver stayed

constant. The polyP concentrations peaked in young mice (12 month of age) followed by a decrease to about 50% of the maximum in older animals (28 months of age) (Lorenz, Munkner et al. 1997). The decrease was accompanied by changes in endogenous exopolyphosphatase activity and a loss in long- chain polyPs (150mer) (Lorenz, Munkner et al. 1997). In addition to age-associated changes in polyP, the levels of polyP have also been found to change during certain pathological conditions. For instance, it has been reported that the polyP levels in the brains of AD mice are significantly lower than the polyP levels in healthy, age-matched littermates (Cremers, Knoefler et al. 2016). Another study by Angelova et al. detected increased amounts of polyP in cells with PD-related mutations (Angelova, Agrawalla et al. 2014). Although the biosynthesis pathway of polyP in mammals remains elusive, polyP production has been associated with the respiratory chain (Figure 5) (Baev, Angelova et al. 2016; Wang, Schroder et al. 2016). The fact that PD pathology is associated with mitochondrial dysfunction (Burchell, Gandhi et al. 2010; Burchell, Gandhi et al. 2010) and the finding that polyP potentially originating from the organelle could explain the altered polyP levels in the pathological context.

3.3.1 PolyP – A structural component of the mitochondrial permeability transition pore

Studies in bacteria revealed that short to medium chain polyP forms a part of a membrane spanning complex, consisting of polyhydroxybutyrate (PHB) and Ca^{2+} (Reusch and Sadoff 1988). This channel was proposed to serve as a voltage gated ion transporter with polyP penetrating the lipid bilayer and supporting the transport of divalent cations across the membrane (Reusch and Sadoff 1988; Castuma, Huang et al. 1995). Shortly after this discovery, similar PHB-polyP-Ca^{2+} ion channel structures were identified in rat liver mitochondria (Pavlov, Zakharian et al. 2005). Upon purification and *in vitro* reconstitution of the complex, it became clear that this channel resembles the permeability transition pore which is involved in Ca^{2+} mediated cell death (Figure 5) (CROMPTON 1999; Rasola and Bernardi 2011). Indeed, treatment of astrocytes with exogenous polyP led to increased mitochondrial permeability transition pore (mPTP) opening and cell death while downregulation of polyP significantly reduced mPTP opening and ionomycin-induced cell death (Abramov, Fraley et al. 2007). In contrast to the bacterial ion

channels, however, only long-chain polyPs (>120Pi) are effective, and induce opening of the mPTP, Ca^{2+} efflux, and the activation of apoptosis (Angelova, Baev et al. 2016).

3.3.2 PolyP as a glio- and neurotransmitter

Generally very little is known about the distribution of polyP in different cell types and different cell compartments. The group of Morrissey et al has extensively studied polyP in the context of coagulation where they identified that platelets secrete polyP via Ca^{2+}-dependent exocytosis (Muller, Mutch et al. 2009; Sakatani, Fujiya et al. 2016). Similarly, astrocytes depict high levels of polyP in cytoplasmic vesicle-like structures, that get released into the extracellular space in a Ca^{2+}-dependent fashion (Holmstrom, Marina et al. 2013; Stotz, Scott et al. 2014; Angelova, Iversen et al. 2018). Neighboring astrocytes or neurons are then able to bind and internalize polyP, where it works as glio- and neurotransmitter, respectively (Figure 5) (Holmstrom, Marina et al. 2013; Angelova, Agrawalla et al. 2014). As a neurotransmitter, polyP influences the action potential of voltage-dependent Na^{+}, K^{+}, and Ca^{2+} channels in the peripheral and central nervous system (Stotz, Scott et al. 2014; Baev, Angelova et al. 2016). As a gliotransmitter, polyP binds, in a chain length independent manner (Holmstrom, Marina et al. 2013), to the purinergic P2Y1 receptor on the surface of astrocytes leading to the activation of phospholipase C (PLC). PLC, in turn, activates Phosphatidylinositol 4,5-bisphosphate, which leads to the activation of Inositol triphosphate and the cellular depolarization through Ca^{2+} influx from the endoplasmic reticulum (Dinarvand, Hassanian et al. 2014; Baev, Angelova et al. 2016). The depolarized cell releases more polyP into the extracellular space and propagates the signaling wave (Holmstrom, Marina et al. 2013; Dinarvand, Hassanian et al. 2014; Baev, Angelova et al. 2016). The finding of polyP being a glio- and neurotransmitter provides important insight about its role in the mammalian brain and insight into its extracellular and intracellular localization.

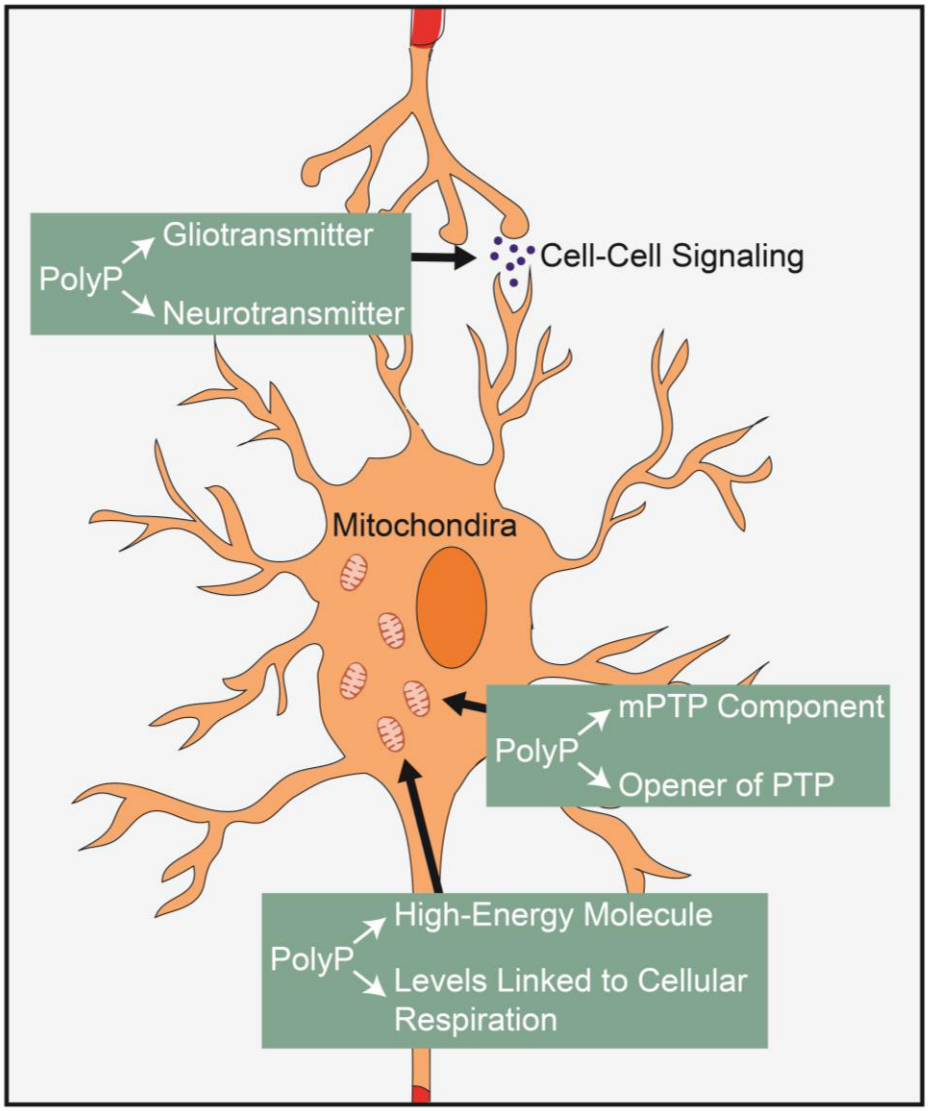

***Figure 5: Role of polyP in the mammalian brain**. PolyP is involved in signaling as a Glio- and Neurotransmitter. In the mitochondria polyP is associated with energy homeostasis and with mPTP formation and apoptosis (changed after (Lempart and Jakob 2019).*

3.4 The pathology of AD and PD

Neurodegenerative diseases like AD and PD share a common pathology, which is based on the conversion of soluble α-helical or intrinsically disordered proteins into insoluble β-sheet rich oligomers and fibers (Eichner and Radford 2011). Occurrence and deposition of mature amyloid fibers has long been thought to cause the observed neurotoxicity. However, the occasional appearance of amyloid deposits in brains of patients lacking symptoms (Ingelsson, Fukumoto et al. 2004) suggested that the underlying toxicity might in fact not be caused by the stable end

product but might be triggered by the fiber formation process itself. Indeed, within the last decade, on or off-pathway oligomers were identified as the primary toxic species responsible for the observed neuroinflammation (Lee, Suk et al. 2010), oxidative stress (Unal-Cevik, Gursoy-Ozdemir et al. 2011) and neurotoxicity (Winner, Jappelli et al. 2011; Diogenes, Dias et al. 2012). Apart from "shedding" of toxic intermediates (Chen, Drakulic et al. 2015) and/or the ability to seed *de-novo* fiber formation, mature fibers are thought to have little to no toxicity themselves.

3.4.1 Amyloid formation and amyloid toxicity in Alzheimer's disease

Patients suffering from AD experience a number of different symptoms, including memory loss, confusion and anxiety (Reisberg, Borenstein et al. 1987; Chung and Cummings 2000). Up to 15 years before the occurrence of the first symptoms, so-called neurofibrillary tangles and amyloid plaques start to form in the brain of affected individuals. Once diagnosed, the median post diagnostic survival of AD patients is only 5 years (Helzner, Scarmeas et al. 2008).

Neurofibrillary tangles are constituted of amyloidogenic tau protein and senile plaques are built-up of amyloidogenic Aβ (Selkoe 1991). Tau is an intrinsically disordered protein that has a variety of isoforms that play an important role in the organization of the cytoskeleton of neuronal cells through stabilization of microtubules (Kempf, Clement et al. 1996; Santarella, Skiniotis et al. 2004; Kellogg, Hejab et al. 2018). During disease development, tau dissociates from microtubules and becomes prone to form amyloid fibrils, ultimately leading to the formation of neurofibrillary tangles (Figure 6) (Alonso, Grundke-Iqbal et al. 1996; Ballatore, Lee et al. 2007).

Aβ is generated through procession of amyloid-β precursor protein via enzyme 1 (BACE1) and γ-secretase giving rise to various different isoforms with $A\beta_{40}$ and $A\beta_{42}$ being the most common (Puig and Combs 2013). The peptide is highly conserved and can be found in all vertebrates, where it is present throughout the whole lives of the animals (Brothers, Gosztyla et al. 2018). *In vivo* and *in vitro* studies have identified that Aβ-levels increase during physiological challenges. The increased Aβ levels then give rise to Aβ's putative functions including a protective role against infections, the restoration of fissures in the blood-brain barrier, the promotion of the recovery from injury as well as a regulatory role in synaptic signaling (Brothers, Gosztyla et al. 2018). While soluble monomeric Aβ has a rapid

turnover in the extracellular space ($T_{1/2}$=0.7 to 2.0 hours) (Savage, Trusko et al. 1998; Abramowski, Wiederhold et al. 2008), oligomeric Aβ is cleared more slowly, hence causing toxicity and leaving it prone to Aβ plaque formation (Masters and Selkoe 2012) (Figure 6).

Although it is mostly enigmatic how tau and Aβ amyloid formation leads to toxicity and subsequent degeneration of the brain, most reports in the last decades identified on- or off-pathway oligomers as toxic species (Chen, Drakulic et al. 2015; Tipping, Karamanos et al. 2015). Tau oligomers induce mitochondrial abnormalities, synaptic dysfunction and inhibit fast axonal transport (LaPointe, Morfini et al. 2009; Morfini, Burns et al. 2009; Lasagna-Reeves, Castillo-Carranza et al. 2012; Lasagna-Reeves, Castillo-Carranza et al. 2012). Aβ oligomers were shown to accumulate in synaptic sites. Here the amyloids disrupt cell-to-cell signaling which eventually results in neuronal cell death (Selkoe 2002). Although the overall connection between tau and Aβ amyloid formation stays enigmatic, growing evidence suggests that once oligomers are formed tau and Aβ amyloids might act synergistically to promote synaptic dysfunction what ultimately leads to the neuronal loss.

3.4.2 Amyloid formation and toxicity in Parkinson's disease

The pathology of PD goes hand in hand with the appearance of insoluble α-synuclein deposits in Lewy bodies of cells of the substantia nigra (Spillantini, Schmidt et al. 1997) (Figure 6). Subsequent loss of motor neurons contributes to the common symptoms of PD, including rigidity, slow movement and tremors (Dunnett and Björklund 1999; Dawson 2000). The progression of PD is slower than the progression of AD with a speculated median survival of 40 years after the first non-motor featured symptoms occur (Hawkes, Del Tredici et al. 2010).

The physiological role(s) of the 14 kDa soluble α-synuclein protein have not been fully identified but seem to be associated with its specific localization at nerve terminals (George, Jin et al. 1995; Iwai, Masliah et al. 1995). Evidence exist that α-synuclein influences vesicle transport by regulating the amount and the release of SNARE complexes (Burre, Sharma et al. 2010; Bendor, Logan et al. 2013). Triggers for α-synuclein amyloid formation are still enigmatic except for certain mutated forms and overexpression that were shown to cause a higher risk of developing PD (Polymeropoulos, Lavedan et al. 1997; Kruger, Kuhn et al. 1998).

Similarly to AD pathology, the toxicity observed in PD is associated with α-synuclein intermediates that form on the fiber formation pathway. Where monomeric α-synuclein has a physiological role in synaptic vesicle trafficking the oligomers disrupt SNARE complex formation, dopamine release and synaptic vesicle motility (Choi, Choi et al. 2013; Wang, Das et al. 2014). Moreover, α-synuclein toxicity is associated with several organelle dysfunctions, disrupting the nucleus, mitochondria, ER/Golgi and lysosomes (Outeiro and Lindquist 2003; Cuervo, Stefanis et al. 2004; Kamp, Exner et al. 2010; Nakamura, Nemani et al. 2011).

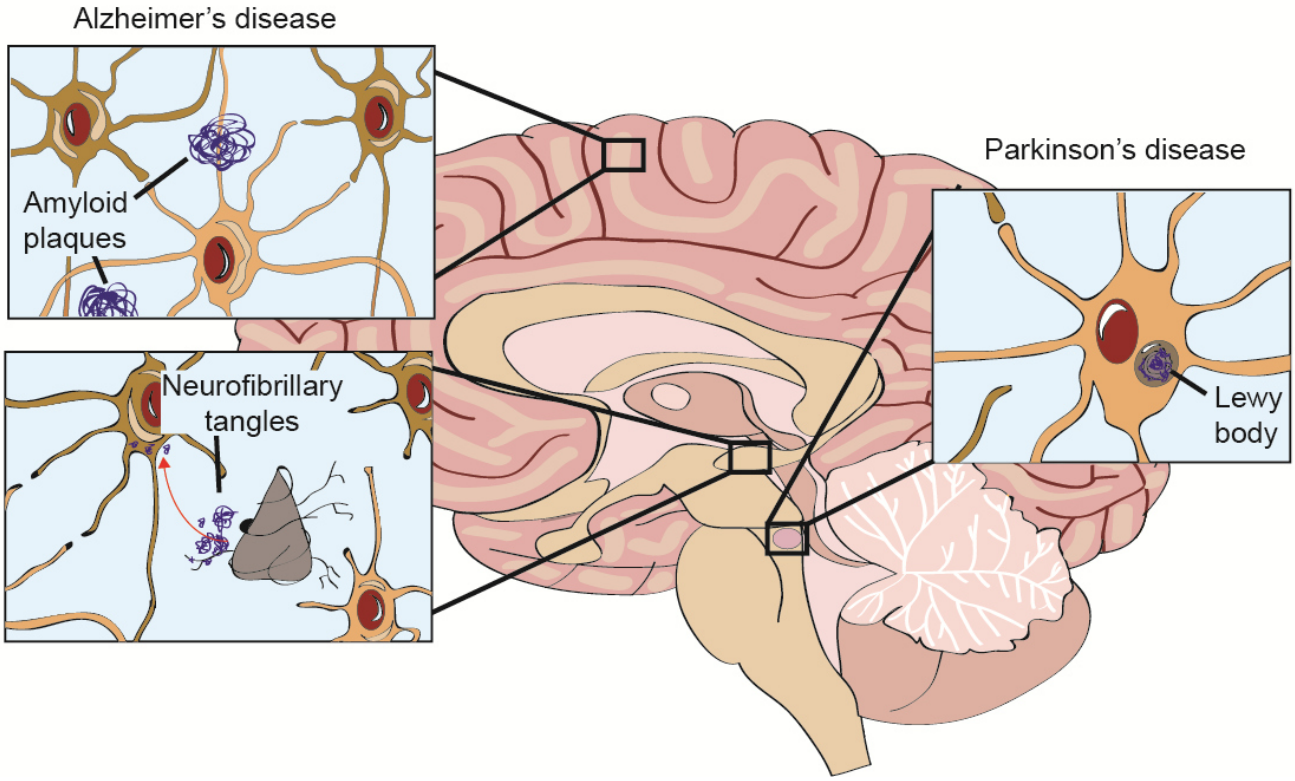

***Figure 6: Neurodegenerative diseases are characterized by aggregate formation in the brain**. AD toxicity is associated with extracellular amyloid plaque formation and intracellular neurofibrillary tangle formation. PD toxicity goes hand in hand with Lewy body formation in motor neurons of the substantia nigra.*

3.4.3 Prion-like spreading of amyloids contributes to disease progression

Up to this date therapies for the treatment of PD and AD are limited to the treatment of the symptoms (Szeto and Lewis 2016). The lack of preventative or disease altering drugs is due to the limited mechanistic insight into the

development and the sporadic occurrence of neurodegeneration. One novel therapeutic attempt, that tries to alter the disease progression, targets the prion-like spreading of amyloids. Studies with tau, Aβ and α-synuclein showed that amyloids self-amplify, and propagate between cells (Hansen, Angot et al. 2011; Domert, Sackmann et al. 2016), contributing to disease progression (Figure 7) (Jucker and Walker 2013; Guo and Lee 2014). Stereotypical and topographical pattern of progression and spread of protein aggregates in the CNS of AD and PD patients supports this idea (Braak, Del Tredici et al. 2003; Kordower, Chu et al. 2008; Li, Englund et al. 2008; Masuda-Suzukake, Nonaka et al. 2013; Paumier, Luk et al. 2015). In addition, intrastriatal injection of preformed α-synuclein fibrils into the brain of WT rodents induces α-synuclein pathology and shows that the amyloids propagate throughout anatomically connected brain regions (Luk, Kehm et al. 2012; Paumier, Luk et al. 2015). The propagation patterns in the brain of AD and PD patients as well as the rodent experiments suggests that the amyloids spreads through the brain in a hierarchical pattern (Braak, Muller et al. 2006). Oligomeric α-synuclein species are particularly prone to be dispersed in a prion-like fashion (Figure 7) (Danzer, Krebs et al. 2009; Danzer, Kranich et al. 2012): Active secretion into the extracellular space is followed by internalization by neighboring cells (Reyes, Olsson et al. 2015) via micropinocytosis and GAG receptors (i.e heparan sulfate) (Nakase, Tadokoro et al. 2007; Holmes, DeVos et al. 2013; Gustafsson, Loov et al. 2018). Once inside the cells, the amyloids are processed via the endosomal-lysosomal pathway (Figure 7) (Karpowicz, Haney et al. 2017). Therapies targeting the uptake mechanism via antibodies (Tran, Chung et al. 2014; Schofield, Irving et al. 2019) show first successes in rodent models and raise the hope for a novel therapeutic attempt that is aiming to prevent the spreading of neurodegenerative diseases throughout the brain.

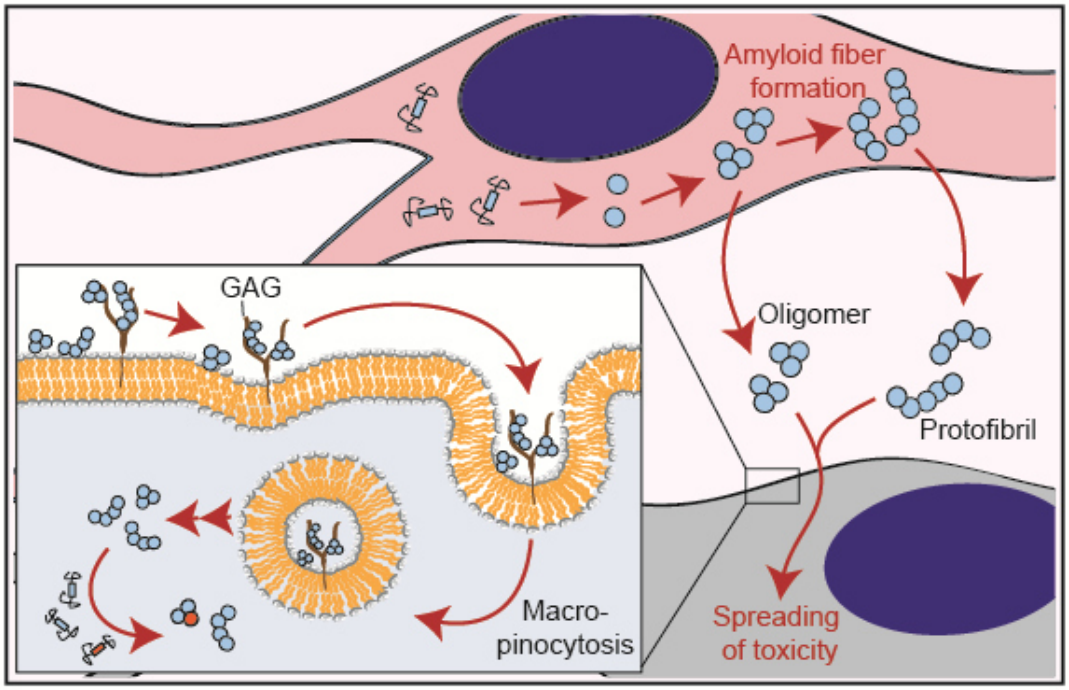

***Figure 7: Prion-like spreading of amyloidogenic protein**. Cells form amyloid fibers that can be released into the extracellular space. Neighboring cells take up the amyloids via GAG and micropinocytosis. Misfolded proteins then spread the toxicity by sequestering native protein for amyloid formation.*

3.5 PolyP as a modifier of neurodegeneration

Previous studies from the Jakob lab showed that polyP significantly decreases the toxicity of amyloidogenic proteins in differentiated neuronal cells (Cremers, Knoefler et al. 2016). Alpha-synuclein fibrils that were merely preformed in the presence of polyP completely lack the toxic effect on differentiated SH-SY5Y or PC-12 cells compared to α-synuclein fibrils formed in the absence of polyP (Cremers, Knoefler et al. 2016). Part of the protective effect could be attributed to polyP's stabilizing ability towards the fibrils, preventing the "shedding" off of toxic intermediates. In a similar experiment the group tested the toxicity of fibrils incubated under destabilizing conditions and was able to show that the presence of polyP during that incubation time abolishes the toxic effect of fibrils towards differentiated SH-SY5Y cells in a subsequent toxicity assay (Cremers, Knoefler et al. 2016). DIC imaging of the cells supported the outcome of the toxicity assays and showed that polyP preserves axon contacts between differentiated neuronal cells in the presence of amyloidogenic α-synuclein while cells treated without polyP show distinct axon retraction.

Assays using C.*elegans* models showed the protective effect of polyP *in vivo* by effectively delaying $A\beta_{1-42}$ induced paralysis in the worms (Cremers, Knoefler et al. 2016). The animals were shown to be able to ingest polyP fed to them for 5.5 hours. 24 hours later, worms treated with polyP showed 25% less paralysis compared to untreated worms (Cremers, Knoefler et al. 2016). In line with those findings are reports by Mueller et al. The group independently confirmed the protective effect of polyP by showing a decreased neurotoxicity of $A\beta_{25-35}$ in the presence of the polyanion (Muller, Wang et al. 2017). Pre-incubation of primary cortical neurons with polyP nanoparticles was able to increase the cellular survival in the presence of $A\beta_{25-35}$ peptide by 30-50% compared to the cells without polyP (Muller, Wang et al. 2017).

3.6 Objective

Accumulating evidence suggests polyP as a modifier of amyloidogenic processes, and raises the question as to how polyP affects fiber formation and protects cells against amyloid toxicity. The goal of my thesis project was to answer these important questions. The first aim of my work was to identify the underlying mechanism by which polyP accelerates fiber formation. I focused on the fiber formation of the two structurally unrelated proteins, i.e. α-synuclein and tau, which were previously shown by our lab to be strongly influenced by polyP. Utilizing various biophysical and biochemical assays, I aimed to identify when and to what extent polyP interacts with these peptides. SmFRET studies in collaboration with the Rhoades lab of the University of Pennsylvania enabled us to conduct in-depth single molecule studies of polyP-induced conformational changes of tau. My second aim was to investigate the mechanism behind the protective role of polyP against α-synuclein toxicity. I addressed this question by investigating in detail how polyP affects internalization and localization of monomeric and fibrillary α-synuclein in differentiated SH-SY5Y cells.

4 MATERIAL AND METHODS

Chemicals used in this study were obtained from Thermo Scientific, Invitrogen, MP Biomedicals, Roche or Sigma Aldrich. Vendors for enzymes, specific chemicals or equipment are listed in the brackets.

4.1 Protein purification

4.1.1 Alpha-synuclein purification

Alpha-synuclein WT or α-synuclein A90C mutant were purified as described (Jain, Bhasne et al. 2013; Cremers, Knoefler et al. 2016) with slight modifications. In brief, *E. coli* strain BL21 (DE3) containing the α-synuclein-expressing vector pT7-7 was grown in Luria Broth (LB) with 200 µg/mL ampicillin until OD_{600} of 0.8-1.0 was reached. Protein expression was induced with 0.8 mM Isopropyl β-D-1-thiogalactopyranoside (IPTG) for 4 hours and bacteria were harvested at 4,500 x g for 20 minutes and 4°C. After the pellet was resuspended in 50 ml lysis buffer (10 mM Tris-HCl, pH 8.0, 1 mM EDTA, Roche Complete protease inhibitor cocktail), the lysate was boiled for 15-20 minutes. The aggregated proteins were removed by centrifugation at 13,500 x g for 30 minutes and 136 µl/ml of a 10% w/v solution streptomycin sulfate solution and 228 µl/ml glacial acetic acid were added to the supernatant. After an additional centrifugation step at 13,500 x g for 30 minutes, the supernatant was removed and mixed in a 1:1 ratio with saturated ammonium sulfate and incubated stirring at 4°C for 1 h. The mixture was spun down at 13,500 x g for 30 minutes and the pellet was resuspended in 10 mM Tris-HCl, pH 7.5. The pH was adjusted to pH 7.5 with concentrated NaOH and the protein was dialyzed against 10 mM Tris-HCl pH 7.5, 50 mM NaCl, filtered and loaded onto three connected 5 ml HiTrap Q HP columns (GE Healthcare). After washing with 10 mM Tris-HCl pH 7.5, 50 mM NaCl, the protein was eluted with a linear gradient from 50 mM to 500 mM NaCl. Protein-containing fractions were combined and dialyzed against 50 mM ammonium bicarbonate, pH 7.8. Oligomeric α-synuclein species were removed by filtering the protein through a 50-kDa cut-off column (Amicon, Millipore) and aliquots of the protein were prepared, lyophilized and stored at -80°C.

4.1.2 ScPPX purification

Saccharomyces cerevisiae exopolyphosphate (ScPPX) was purified according to Pokhrel et al (Pokhrel, Lingo et al. 2019) with slight modifications. In brief, MJG317 (BL21, pScPPX2, i.e., S.c. PPX1 in pET-15b) was incubated overnight at 37°C without shaking in LB containing 100 µg/ml ampicillin. The following day, the cultures were shaken for 30 min at 180 rpm at 37°C until they reached an OD_{600} of 0.4 - 0.5. Additional 100 µg/ml ampicillin and isopropyl IPTG were added to a final concentration of 1 mM and the protein was expressed by incubating the cells for 4 hours at 37°C with shaking at 180 rpm. The cells were harvested by centrifugation for 20 min at 4,000 rpm at 4°C, and the pellet was resuspended in 50 mM sodium phosphate buffer, 500 mM NaCl, 10 mM imidazole (pH 8). Subsequently, 1 mg/ml lysozyme, 2 mM $MgCl_2$, and 50 U/ml Benzonase were added. The solution was incubated for 30 min on ice. Cells were sonicated with two cycles of 50% power pulsing 5 s on and 5 s off for 2 min with 2 min rest between cycles. The protein lysate was spun down at 20,000 g for 20 min at 4°C to remove cell debris and the supernatant was loaded onto a nickel-charged chelating column. After a washing step with first 50 mM sodium phosphate buffer, 0.5 M NaCl, 10 mM imidazole (pH 8) and then 50 mM sodium phosphate buffer, 0.5 M NaCl, 20 mM imidazole (pH 8), the protein was eluted with 50 mM sodium phosphate buffer, 0.5 M NaCl, 0.5 M imidazole (pH 8). Fractions containing ScPPX were pooled and dialyzed twice against 2 l of 20 mM Tris-HCl (pH 7.5), 50 mM KCl, and 30 % (v/v) glycerol. Precipitated protein was removed via centrifugation for 20 min at 20,000 g at 4°C. The supernatant was supplemented with 50% glycerol and the protein was stored at -80°C.

4.1.3 Tau purification

His-tagged Tau wildtype and mutant constructs were purified by Sanjula Wickramasinghe as described in (Wickramasinghe, Lempart et al. 2019).

4.1.4 Determination of protein concentration

The protein concentrations were determined spectroscopically at 280 nm using a Jasco spectrophotometer V-550. The extinction coefficient for tau (1490 $M^{-1}cm^{-1}$) and α-synuclein (5940 $M^{-1}cm^{-1}$) was determined according to their amino acid sequence via the PDB at 280 nm. The concentration of labeled proteins was

determined via the respective absorption maximum and the specific extinction coefficient provided by the vendor.

	extinction coefficient	Excitation maximum
AF488-maleimide (Invitrogen)	72,000 $M^{-1}cm^{-1}$	490 nm
AF594-cadaverine (Life technologies)	105,000 $M^{-1}cm^{-1}$	590 nm

The concentration of labeled tau was determined by Sanjula Wickramasinghe as described in (Wickramasinghe, Lempart et al. 2019).

4.2 Fluorescence labeling

4.2.1 Preparation of fluorescently labeled α-syn^{PFF}

For crosslinking of α-synuclein-A90C with Alexa Fluor 488 – maleimide (Invitrogen), 100 µM of purified protein was first incubated with 1 mM tris(2-carboxyethyl)phosphine (Invitrogen) for 30 min at room temperature in the dark. Alexa Fluor 488 – maleimide was added in a 6-fold excess to the concentration of polyP chains and the mixture was incubated over night at 4°C. The reaction was stopped by adding 2 mM dithiothreitol (DTT). The free dye was removed using a NAP column (GE Healthcare) and the concentration of dye and protein were determined by measuring absorbance at 488 and 280 nm, respectively. To generate α-syn$^{PFF\text{-}AF488}$, 760 µM freshly purified α-synuclein monomers were incubated with 40 µM labeled α-synuclein-AF488 in 40 mM KPi, 50 mM KCl, pH 7.5 for 24 hours at 37°C under continuous shaking using two 2 mm borosilicate glass beads (Aldrich) in clear 96-well polystyrene microplates (Corning) (Giehm and Otzen 2010). Samples from the 96-well plate were combined in Eppendorf tubes and the fibers were collected via centrifugation at 20,000 x g, 20 min, room temperature. The pellets were washed twice with 40 mM KPi, 50 mM KCl, pH 7.5 to remove smaller oligomers. After the final spin, the pellets were resuspended in 40 mM KPi, 50 mM KCl, pH 7.5 and sonicated 3 x 5 seconds on ice with an amplitude of 50%. For structural analysis by transmission electron microscopy (TEM), samples before and after sonication were saved for negative staining. The concentration of fibrils was determined by incubating a small aliquot of α-syn$^{PFF\text{-}AF488}$ in 8 M urea, 20 mM Tris pH 7.5, measuring the absorbance at 280 nm and

calculating the concentration with the extinction coefficient of 5960 mol^{-1} cm^{-1} (see above). Aliquots were taken and stored at – 80°C.

4.2.2 Preparation of fluorescently labeled $polyP_{300}$

Defined chain length polyP was a kind gift from Dr. Toshikazu Shiba (Regenetiss, Japan). PolyP was labeled with Alexa Fluor-647 as described in (Choi, Collins et al. 2010) with slight modifications. In brief, 125 µM (in Pi units) of $polyP_{300}$ was incubated with 2.5 mM Alexa Fluor 647 cadaverine (Life Technologies) and 200 mM 1-ethyl-3- (3-dimethylaminopropyl) carbodiimide (EDAC) (Invitrogen) in water for 1 hour at 60°C. The reaction was stopped on ice and labeled $polyP_{300\text{-}AF647}$ was separated from free dye and unlabeled polyP via a NAP-5 column (GE Healthcare) that was equilibrated with 40 mM KPi, pH 7.5. The concentration of polyP was determined via a toluidine blue (TBO) assay (Mullan, Quinn et al. 2002). In this assay, polyP was mixed with 6 mg/l TBO and the absorbance was measured at 530 and 630 nm. The 530 nm / 630 nm absorbance ratio was determined and the concentration was calculated based on a $polyP_{300}$ standard curve.

4.2.3 Preparation of fluorescently labeled tau

Tau protein was labeled by Sanjula Wickramasinghe as described in (Wickramasinghe, Lempart et al. 2019).

4.3 Thioflavin T fluorescence

Alpha-synuclein or tau monomers (concentration given in figure legends) were incubated in 40 mM KPi, 50 mM KCl, pH 7.5 at 37°C with 10 µM thioflavin T (ThT; Sigma) under continuous shaking. Two 2 mm borosilicate glass beads (Aldrich) were present in the α-synuclein incubation reaction. PolyP or heparin were added either at the beginning of the polymerization reactions or at indicated time points during the experiment. The polyP concentration is given in Pi-units. The heparin concentration (18 µM) was chosen to match the amount of negative charge of the 1 mM polyP. Heparin charge concentrations were calculated to match polyP assuming 1.5 to 2 charges per saccharide and an average molecular weight of 665 g/mol (Heuck, Schiele et al. 1985). The mixture was set up in black 96-well polystyrene microplates with clear bottoms (Greiners) and ThT fluorescence was detected in 10 min intervals in a Synergy HTX MultiMode Microplate Reader (Biotec). Excitation was measured at 440 nm and emission at 485 with a gain 40.

4.4 Fluorescence polarization

To monitor the binding of polyP to α-synuclein during fibril formation, samples were pipetted into 96-well polystyrene microplates with clear bottoms (Greiners) and two 2 mm borosilicate glass beads (Aldrich). Experimental conditions were identical to the ones used to measure ThT fluorescence. Fluorescence polarization was measured in a Tecan Infinite M1000 Microplate reader, using an excitation of 635 nm and an emission of 675 nm. Measurements were taken in 10-min intervals parallel to ThT measurements.

4.5 Anisotropy measurements to detect polyP binding and competition

Anisotropy measurements were conducted in a Varian Cary eclipse Fluorescence Spectrophotometer, using an excitation of 640 nm and an emission of 675 nm (PMT value set between 50 and 100). The baseline was established with 50 µM $polyP_{300\text{-}AF647}$ in 40 mM KPi, 50 mM KCl, pH 7.5 at 37°C. At the indicated time points, 30 µM of α-synuclein monomers, α-synuclein fibrils or $\alpha\text{-syn}^{PFF\text{-}AF488}$ were added and anisotropy was further monitored over time. For competition experiments, α-synuclein fibrils were formed in the presence of $polyP_{300\text{-}AF647}$ as before. At defined time points, unlabeled $polyP_{14}$ or $polyP_{300}$ was added, and the anisotropy signal was monitored over time. The difference between the $polyP_{300\text{-}AF647}$ baseline signal and the maximum signal that was reached with addition of 30 µM α-synuclein fibers was set to 100%.

4.6 Structural analysis of α-synuclein

4.6.1 Negative staining and transmission electron microscopy (TEM) analysis

To form fibrils for TEM analysis, 300 µM freshly prepared α-synuclein monomers were incubated either in the absence of polyP (i.e., $\alpha\text{-syn}^{alone}$), or in presence of 7.5 mM (in Pi units) $polyP_{300}$ (i.e., $\alpha\text{-syn}^{polyP}$) for 24 hours at 37°C with 2 mm borosilicate glass beads under continuous shaking in 40 mM KPi, 50 mM KCl, pH 7.5. $Alpha\text{-syn}^{alone}$ fibrils were then either left untreated or were incubated with 7.5 mM $polyP_{300}$ for 20 min (i.e. $\alpha\text{-syn}^{alone \rightarrow polyP}$) and put onto grids. For PPX treatment, the polyP-α-synuclein fiber mixture was incubated with 44 µg/ml ScPPX and 1 mM $MgCl_2$ for 2-16 hours at RT and put on the girds. Samples were negatively stained with 0.75% uranyl formate (pH 5.5-6.0) on thin amorphous carbon layered 400-mesh copper grids (Pelco) in a procedure according to (Ohi, Li et al. 2004). Briefly,

5 µl of the sample was applied onto the grid and left for 3 min before removing it with Whatman paper. The grid was washed twice with 5 µl ddH_2O followed by three applications of 5 µL uranyl formate (vendor). The liquid was removed using a vacuum. Grids were imaged at room temperature using either a Morgagni (CCD camera pixel size: 5 µm, (2.1 Å/pixel @ 22,000x)) or a Fei Tecnai 12 microscope operating at 120kV (US 4000 CCD camera at 66873x resulting in a sampling of 2.21 Å/pixel). For quantitative analysis, about 45 individual α-synuclein filaments were selected across 10 micrographs of each sample and the filament widths were determined using the micrograph dimensions as a reference. Pixel widths were converted into angstroms using the program imageJ. Images were taken with a Fei Tecnai 12 microscope and the respective analysis was conducted in collaboration with Eric Tse (Southworth lab UCSF).

4.6.2 X-ray fiber diffraction

Alpha-synuclein fibrils were grown with and without polyP as described above. Prior to the measurements, 1-2 ml of a solution containing 100 µM α-synuclein fibrils were washed 3 times with 10 mM Tris pH 7. Then, fibrils were pelleted by centrifugation (15,000xg, 5min, RT). The supernatant was removed, and the pellet was resuspended in 5-10 µl 10 mM Tris pH 7.0. Then, 5 µl of the fibril pellet was placed between two fire-polished silanized glass capillaries and oriented by air-drying. The glass capillaries with the aligned fibrils were mounted on a brass pin. Diffraction patterns were recorded using 1.13 Å X-rays produced by a 21-ID-D beamline, Argonne Photon Source (APS). All patterns were collected at a distance of 200 mm and analyzed using the Adxv software package (Arvai 2015). X-ray fiber diffraction was conducted in collaboration with Magdalena Ivanova (University of Michigan)

4.7 ScPPX treatment and determination of polyP concentration using molybdate assay

40 µM of α-synuclein monomers or fibrils, prepared in 40 mM Hepes, pH 7.5 and 50 mM KCl, were incubated with the indicated concentrations of $polyP_{300}$ for 10 min at room temperature in a clear 96-well plate (Corning). The samples were either used directly or spun down at 20,000 x g for 20 minutes at room temperature to remove any unbound polyP. The pellets were resuspended in 40 mM Hepes (pH 7.5), 50 mM KCl. Next, 8 µg/ml ScPPX and 1 mM $MgCl_2$ was added to each

sample and the incubation was continued for 105 min (for spin down) or 120 min (for titration) at room temperature. To stop the reaction and detect P_i, 25 µl of a detection solution containing 600 mM H_2SO_4, 88 mM ascorbic acid, 0.6 mM potassium antimony tartrate, and 2.4 mM ammonium heptamolybdate was added (Christ and Blank 2018; Pokhrel, Lingo et al. 2019). The reactions were developed for 30 min. Then, the precipitated proteins were re-solubilized with 100 µl of 1 M NaOH, and the absorbance was measured at 882 nm using a Tecan M1000 plate reader. The free phosphate concentration was determined with a standard curve of sodium phosphate, which was prepared in parallel with each experiment. After the spin down, the phosphate measured in the supernatant was considered free, and the phosphate measured in the pellet was considered bound. The bound and protected fraction was calculated according to the equation below (1), with c_{total} being the total amount of polyP used in the assay, $c_{supernatant}$ being the amount of polyP in the supernatant and c_{pellet} being the amount of polyP in the pellet that is not protected from degradation through PPX.

$$c_{bound+protected} = c_{total} - c_{supernatant} - c_{pellet} \qquad (1)$$

4.8 Cell culture and α-synuclein uptake experiments

Human neuroblastoma cells SH-SY5Y cells (ATCC CRL-2266) were cultured in DMEM/F12 (Thermo Fisher) medium supplemented with 10% (v/v) heat inactivated fetal bovine serum (Sigma-Aldrich), 1% (w/v) penicillin/streptomycin (Life Technologies) at 37°C and 5% CO_2. The media was changed every 2–3 days and cells were split 1–2 times per week with 0.25% trypsin-EDTA (Thermo Fisher Scientific). Cells were maintained to a maximum passage number of 25.

For microscopy experiments, 60 000 cells/ml were seeded in 8 well Nunc™ Lab-Tek™ II Chambered Coverglass (Thermo Fisher) and differentiated for 5-7 days with addition of 10 µM all trans retinoic acid (Sigma-Aldrich) every other day.

4.8.1 Alpha-synuclein uptake

Cells were treated with 3 µM α-syn$^{PFF\text{-}AF488}$ or α-syn$^{mon\text{-}AF488}$ in the presence or absence of the indicated concentrations and chain lengths of polyP. The cells were incubated for indicated times either at 37ºC or 4ºC. Before imaging, the media was changed to DMEM/F12 without phenol red (Thermo Fisher) and supplemented with 10% (v/v) heat inactivated fetal bovine serum (Sigma-Aldrich), 1% (w/v)

penicillin/streptomycin (Life Technologies). To distinguish between the inside and outside signals, the cells were incubated with 3 µM α-syn$^{PFF-AF488}$ or α-syn$^{mon-AF488}$ for 3 hours at 37˚C as before. Then, cells were treated with or without 0.05% of the membrane impermeable dye Trypan blue for 15 sec prior to the imaging to quench extracellular fluorescence (Karpowicz, Haney et al. 2017). Subsequently the cells were washed carefully with PBS and the media was change to DMEM/F12 without phenol red (Thermo Fisher) supplemented with 10% (v/v) heat inactivated fetal bovine serum (Sigma-Aldrich), 1% (w/v) penicillin/streptomycin (Life Technologies). To enrich for endogenous polyP, SH-SY5Y cells were seeded and differentiated as described above. Once differentiated, cells were either left untreated or incubated with 250 µM polyP$_{300-AF647}$ (in Pi units) for 24 hours. Subsequently, fresh media was added to the cells for 6 hours. Afterwards, cells were incubated with 3 µM α-syn$^{PFF-AF488}$ for 24 hours. Before imaging the media was changed to DMEM/F12 without phenol red (Thermo Fisher) supplemented with 10% (v/v) heat inactivated fetal bovine serum (Sigma-Aldrich), 1% (w/v) penicillin/streptomycin (Life Technologies). To test the influence of polyP during the α-syn$^{PFF-AF488}$ uptake, differentiated SH-SY5Y cells were incubated with 3 µM α-syn$^{PFF-AF488}$ at 37°C. After 2, 4 or 6 hours, 250 µM polyP$_{300-AF647}$ was added to the cells. Cells were imaged at time points 1, 2.5, 5, 7 and 24 hours. To test for co-localization of α-syn$^{PFF-AF488}$ and polyP$_{300-AF647}$, cells were incubated with 3 µM α-syn$^{PFF-AF488}$ at 37°C. After 6 h, 250 µM polyP$_{300-AF647}$ was added and cells were imaged after 7 h. Cells were imaged with a confocal laser scanning Leica SP8 high resolution microscope with a white light (470-670nm) laser systems. Leica HyD detectors were used to measure the emitted light.

4.8.2 Uptake of TAT-TAMRA in the presence of polyP

Differentiated SH-SY5Y cells were incubated with 5 µM TAT-TAMRA (AnaSpec), for 3 hours either in the presence or in the absence of 250 µM polyP$_{300}$. The uptake of 3 µM α-syn$^{PFF-AF488}$ in the presence and absence of 250 µM polyP$_{300}$ was monitored as controls. TAT-TAMRA was excited at 565 nm. The detection range was adjusted according to the emission spectra suggested by the Leica LAS X navigating software.

4.9 Sample preparation for SDS-PAGE and Western blots

150 000 SH-SY5Y cells/ml were seeded in 6 well plates (3 ml total volume) and differentiated for 5-7 days with addition of 10 µM all trans retinoic acid (Sigma-Aldrich) every other day. Subsequently cells were treated with 3 µM α-syn^{PFF} or α-syn^{mon} and 250 µM polyP was added at indicated time points. After 24 hours of incubation the cells were washed 2 times with ice cold PBS and lysed with 300 µl RIPA buffer (50 mM Tris pH 7.5, 150 mM NaCl, 1 x protease inhibitor cocktail, 1 % Triton X 100, 0.5 % deoxycholic acid, 0.1 % SDS). To ensure that the cells are fully lysed the mixture was homogenize (Power Gen 125, Fisher Cientific, setting 5) for 20 seconds. The protein concentration was determined via a Bradford assay and samples were prepared to a concentration so 20 µg of protein were loaded per lane on the gel. 150 ng of purified α-synuclein was used as positive control.

4.10 Bradford assay

5 µl of the sample was combined with 195 µl Bradford solution (Bradford reagent (BioRad) in a 1:5 ratio in ddH_2O). The absorbance was measured at 595 nm in a Tecan M1000 plate reader and the protein concentration was determined with a BSA standard curve (0.25 -1.5 mg/ml).

4.11 SDS-PAGE and Western blots

Proteins were separated on SDS-PAGE gels (12 % TGX-gel (BioRad). Before loading, samples were diluted in a 1:5 (v/v) ratio in 5x Laemmli buffer (final concentration: 60 mM Tris, 12.5% glycerol, 2% SDS, 0.01% bromphenol blue, +/- 125 mM β-mercaptoethanol). Samples were then boiled at 95˚C for 5 min, loaded onto the SDS-PAGE and separated following the manufacturer's specifications in SDS running buffer (25 mM Tris, 192 mM glycine, 0.1% SDS). The proteins were either visualized on the gel by Coomassie blue staining (Wong et al., 2000) or transferred onto a PVDF membrane (polyvinylidene difluoride membrane, Immobilon-P, Millipore) by a semi-dry electrophoretic transfer (western blot) technique (Biorad). The membrane was incubated in 2% bovine serum albumin solution in TBS-T (25 mM Tris, 0.05% (v/v) Tween, 137 mM NaCl, 3 mM KCl, pH 7.5) solution for 2 hours at RT, or ON at 4°C to minimize unspecific antibody binding. The membranes were incubated in anti-α-synuclein antibody (BD Bioscience, catalogue number 610789), which was diluted 1:1500 in 2% BSA in PBS-T. After 2h of incubation, all unbound antibody was removed by three

consecutive washing steps with TBS-T for 10 min. Then, the secondary anti-mouse antibody (ThermoScientific, catalogue number 31430) was applied dilution 1:10000 in 2% BSA in PBS-T for 1 hour at RT. Subsequent washing 3x with TBS-T removed all unbound antibody before the signal was detected using the SuperSignal West Pico Chemiluminescent substrate (ThermoScientific) kit according to the manufacturers specifications.

4.11.1 smFRET instrument and data analysis

SmFRET experiments were prepared by Sanjula Wickramasinghe as described in (Wickramasinghe, Lempart et al. 2019).

4.12 Statistical analysis

Two-tailed Students t-tests were performed when two groups were compared. One-way ANOVA was performed when comparing more than two groups. P-values under 0.05 were considered significant. All data are displayed as +/- SD except for FRET and FCS with are displayed as SEM. Replicate numbers (n) are listed in each figure legend and a minimum of n= 3 was used. Prism 7.04 (GraphPad) was used to perform statistical analysis. SEM of diffusion times are shown from at least three repeats of measurements. SEM of ET_{eff} was calculated as described in (Wickramasinghe, Lempart et al. 2019).

5 RESULTS

The work on polyP and α-synuclein is published in “Mechanistic Insights into the Protective Roles of Polyphosphate Against Amyloid Cytotoxicity” (Lempart, Tse et al. 2019).

5.1 PolyP binds to oligomeric α-synuclein and accelerates fiber formation after an initial polyP-independent step

The unexpected discovery that polyP accelerates fiber formation of several unrelated amyloids, including Tau, Aβ and α-synuclein raised the question as to the underlying mechanism of polyP action (Cremers, Knoefler et al. 2016). One common feature of these proteins is their tendency to convert from soluble, unstructured or α-helical monomers into cross β-sheet rich fibrils (Eichner and Radford 2011), a process that can be measured via ThT fluorescence. The ThT binding kinetics follow a characteristic sigmoidal curve, starting with a nucleation (or lag) phase, in which ThT-negative monomers and small soluble oligomers are present, an elongation (or growth) phase, in which oligomers associate to larger ThT-binding assemblies, and a plateau phase, where the mature fibrils accumulate (Figure 8A) (Shoffner and Schnell 2016). The fluorescent dye ThT intercalates along the long axis of amyloid oligomers and fibrils, spanning across the β-strands of four consecutive monomers (Krebs, Bromley et al. 2005; Biancalana, Makabe et al. 2009; Wu, Biancalana et al. 2009). This interaction leads to a strong fluorescence signal at 482 nm when excited at 450 nm (Naiki, Higuchi et al. 1989). In this work, a ThT concentration of 10 µM was used. An amount that gives sufficient fluorescent signal without influencing the aggregation process itself (Xue, Lin et al. 2017).

Previous work has shown that polyP effectively accelerates α-synuclein fiber formation. Presence of polyP increases the rate of fiber formation from several days or weeks to only a few hours (Cremers, Knoefler et al. 2016). To investigate how polyP accelerates this process, I first focused on identifying when polyP starts to interact with α-synuclein during the fiber forming process. I monitored ThT fluorescence to detect α-synuclein fiber formation and, in parallel, conducted fluorescence polarization (FP) measurements to detect polyP-α-synuclein interaction. FP is based on measuring the change in the rotation angle of polarized

light, which is different for bound vs unbound molecules (Figure 8B) (Jameson and Croney 2003).

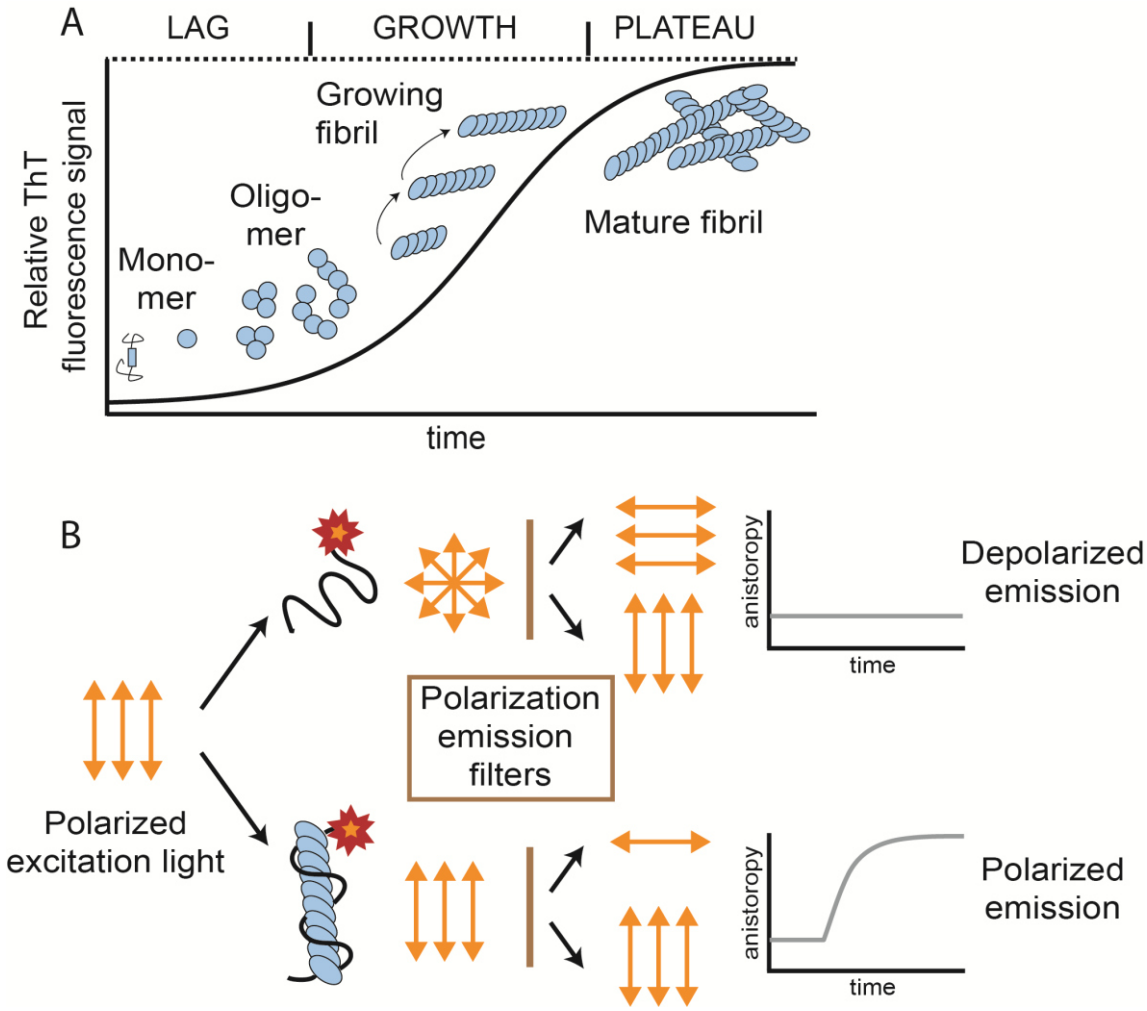

***Figure 8: Schematic model for ThT fluorescence and fluorescence polarization**. (A) When measured with ThT fluorescence, fiber formation follows a characteristic sigmoidal kinetic, including a lag phase, growth phase and plateau phase (Lempart, Tse et al. 2019). (B) Model for anisotropy/fluorescence polarization measurements with fast tumbling (unbound) molecules leading to depolarized emission while slow tumbling (bound) molecules lead to polarized emission.*

In our setup, I labeled polyP with the fluorescent dye Alexa Fluor 647 (from here on referred to as $polyP_{300\text{-}AF647}$). Consistent with previously published data (Cremers, Knoefler et al. 2016), the addition of $polyP_{300\text{-}AF647}$ to α-synuclein (100 µM) significantly shortened the lag phase and accelerated the elongation phase (green circles, Figure 9A) compared to the polyP-free control (grey triangles, Figure 9A).

The FP measurement showed initially no binding between $polyP_{300\text{-}AF647}$ and α-synuclein monomers. After 3 to 4 hours, however, both FP and ThT signals increased steadily until they reached a plateau after about 15 hours (Figure 9A, B). In order to compare the curve of fiber formation and polyP-binding, I normalized the values to a set point (10 hours) during the elongation phase. The graph shows that binding to polyP (red squares, Figure 9C) slightly precedes the fiber formation (green circle, Figure 9C). The elongation rate, however, appears to be very similar. This result indicates that polyP does not interact with α-synuclein monomers but a species that requires some time to form under these conditions. However, once this species has formed, the binding of polyP rapidly accelerates the fiber formation process.

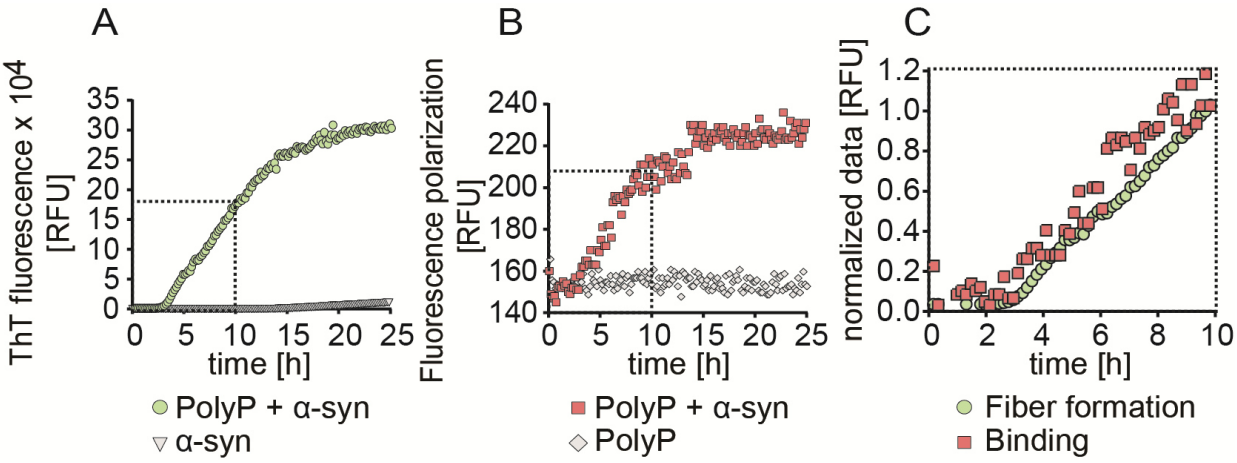

***Figure 9: PolyP binds ThT positive α-synuclein species**. (A) Fiber formation of α-synuclein (100 µM) in the presence (green) and absence (grey) of $polyP_{300\text{-}AF647}$ (500 µM in Pi units) at 37ºC under constant shaking measured via ThT fluorescence. (B) Fluorescence polarization measurements were conducted in parallel to detect interaction between $polyP_{300\text{-}AF647}$ and α-synuclein. (C) Normalization of ThT fluorescence and FP to values measured within the elongation phase (10 hours). Experiments were conducted at least 3 times and representative kinetic traces are shown (Lempart, Tse et al. 2019).*

To more closely investigate when polyP binds during the lag phase, I added polyP at different time points during the lag and elongation phase. Alpha-synuclein fiber formation (300 µM) was then measured in 10 min intervals via ThT fluorescence. In the absence of polyP, the ThT signal started to increase after about 9 hours of incubation. The presence of polyP from the beginning shortened this lag phase to 1 hour (blue circles, Figure 10A). Addition of polyP after 2 hours, shortened the

remaining lag phase to 30 min (green squares, Figure 10A), whereas an immediate jump in ThT fluorescence could be observed with polyP addition after 5 hours (purple diamond, Figure 10A), 8.5 hours (red triangle, Figure 10A) or 19 hours (black triangle, Figure 10A). The later polyP was added, the bigger the immediate jump in ThT fluorescence. These findings suggest that polyP accelerates fiber formation once an oligomeric nucleator is formed.

Next, I wanted to test the influence of different polyP and different α-synuclein concentrations on the initial oligomer formation. I reasoned that the concentration of the polyanion or the amyloidogenic peptides are crucial for duration of the lag phase. I incubated increasing concentrations of α-synuclein (100-640 µM) with 0, 50 or 100 µM of polyP (in Pi-units) and investigated the time until an initial increase in ThT fluorescence could be observed. The lag phase, when using 100 µM α-synuclein was found to be about 16 hours in the absence and 2- 5 hours in the presence of polyP (Figure 10B). Increasing the α-synuclein concentration to 200 or 400 µM decreased the lag phase in the absence of polyP to 14 hours and 5 hours, respectively, while the lag phase in the presence of 50 or 100 µM polyP remained largely unchanged. Increasing the α-synuclein concentration from 400 to 640 µM did not decrease the lag phase any further neither in the absence nor in the presence of polyP (Figure 10B). These findings indicate that there is an α-synuclein concentration-independent nucleation step that initializes α-synuclein fiber formation, and which cannot be accelerated by polyP. This idea would explain the lack of fiber formation in healthy individuals even though both polyP and α-synuclein are present in the same cells of the brain (Jakes, Spillantini et al. 1994; Holmstrom, Marina et al. 2013).

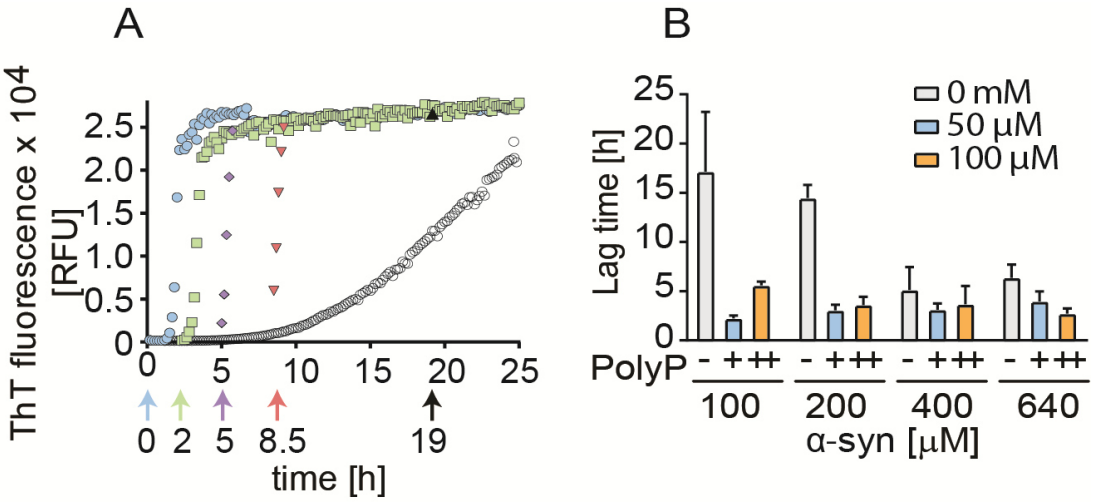

Figure 10: Alpha-synuclein fiber formation shows a rate limiting polyP independent step. *(A) Addition of 500 µM polyP$_{300}$ (in Pi units) after 0, 2, 5, 8.5 and 19 hours of α-synuclein fiber formation (300 µM). ThT fluorescence was monitored in 10 minute intervals. Experiment was conducted at least 3 times and representative kinetic traces are shown. (B) Lag phase of α-synuclein fiber formation formed with different α-synuclein concentrations (100, 200, 400 and 640 µM) and different polyP concentrations (0, 50 and 100 µM in Pi units). ThT fluorescence was measured and lag phase was determined. Experiment was repeated four times and +/- SD is shown (Lempart, Tse et al. 2019).*

5.2 PolyP alters the morphology of preformed α-synuclein fibers

To independently confirm that polyP does not interact with monomeric α-synuclein but readily binds to mature fibers, we conducted anisotropy measurements. For these experiments, I formed α-synuclein fibers, harvested and washed them to ensure the absence of any smaller soluble species and added those or freshly dissolved α-synuclein monomers to $polyP_{300\text{-}AF647}$ and measured the interaction with anisotropy. The addition of α-synuclein fibers to $polyP_{300\text{-}AF647}$ immediately increased the signal, indicating that polyP binds to mature fibers (Figure 11A). In agreement with our previous results (Figure 9), the addition of monomers has no effect on the tumbling rate of polyP, confirming a lack of interactions between polyP and freshly prepared α-synuclein monomers (Figure 11A).

Previous findings have shown that the presence of polyP during fiber formation significantly alters the fiber morphology (Cremers, Knoefler et al. 2016). The fact that polyP binds to preformed fibrils led me to test whether polyP can also induce structural changes when added to pre-formed fibers. To test this idea, I formed α-synuclein fibers and treated them with or without polyP for 20 min. As a control, I used fibers that were formed in the presence of polyP (Cremers, Knoefler et al. 2016). The samples were subsequently fixed on grids and visualized using Transmission Electron Microscopy (TEM). Fibers that were incubated with polyP for just 20 min showed the same characteristics than fibers that were formed in the presence of polyP (Figure 11B). Both types of fibers are, on average, 5 nm thinner and less twisted than fibers that were formed without polyP (Figure 11B). X-ray fiber diffraction experiments conducted in collaboration with Magdalena Ivanova (University of Michigan) confirmed these conformational changes and provided a more detailed image of the polyP-induced structural changes in α-synuclein fibers (Figure 11C-E). The equatorial plot of radial intensities showed polyP induced changes in the packaging of β-sheet in the amyloid fibrils (Figure 11E). The strand-to-strand packing was not influenced by polyP as shown by the lack of changes in the median signal. These experiments illustrate that the interaction with polyP has a significant effect on the fiber morphology and that the fiber structure is highly dynamic and can be altered by polyP.

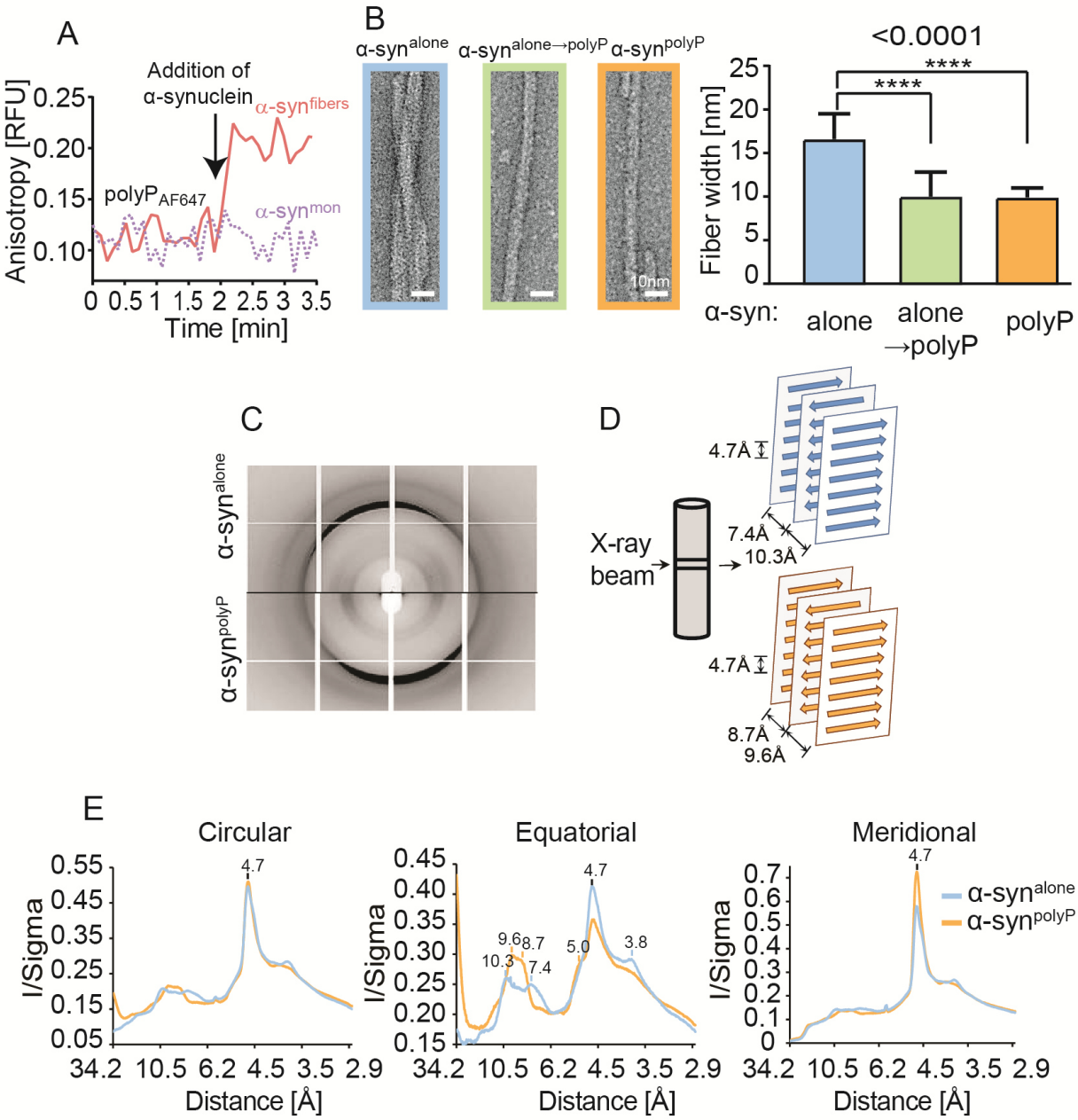

Figure 11: Addition of polyP to preformed α-synuclein fibers significantly alters the fiber morphology. *(A) 30 µM α-synuclein fibers or monomers were added to 50 µM polyP$_{300\text{-}AF647}$ and binding was measured via anisotropy. (B) TEM analysis of α-synuclein fibers formed without polyP (α-syn^{alone}), with polyP (α-syn^{polyP}) or without polyP and then treated with polyP for 20 min (α-syn$^{alone\rightarrow polyP}$). Between 30 and 40 fibrils were quantified over 10 micrographs. Error bars are shown +/-SD and statistical analysis was prepared with one-way ANOVA (****, p-value <0.0001). (C-E) X-ray fiber diffraction formed in the presence and absence of polyP$_{300}$. (C) Intensities were averaged circular (360), equatorial (+/-30) or meridional (+/-30 around the Y-axis). (D) Model for potential β-sheet packaging in the amyloids (E) Circular and meridional diffraction patterns show a sharp peak at 4.7 Å that is uninfluenced by polyP. Equatorial diffraction pattern show polyP induced shifts (Lempart, Tse et al. 2019).*

5.3 PolyP - α-synuclein fiber interaction is reversible and chain length dependent

To further characterize the polyP-α-synuclein interaction, I determined reversibility and chain length dependency. Previous work showed that longer polyP chains (n> 60) are significantly more effective in accelerating α-synuclein and Aβ fiber formation than shorter chains (Cremers, Knoefler et al. 2016). To identify whether this effect is correlated with the binding affinity, I tested for their ability to compete for the binding sides on the fibers. In detail, I pre-incubated $polyP_{300\text{-}AF647}$ with preformed fibrils to form a complex and added unlabeled $polyP_{14}$ or $polyP_{300}$ to the mixture. This set-up was to test whether unlabeled polyP was able to compete for binding to α-synuclein fibers. Indeed, addition of unlabeled polyP of either chain length caused an immediate drop in the anisotropy signal (Figure 12A). Moreover, longer polyP chains were more effective in competing with $polyP_{300\text{-}AF647}$ for binding than $polyP_{14}$ (Figure 12B).

To test whether polyP chain length also affects fiber morphology, α-synuclein fibers were formed in the absence or presence of $polyP_{14}$ or $polyP_{300}$ and the mature fibrils were loaded onto grids for analysis via TEM. Both chain lengths induced the previously described structural changes, including a less twisted morphology and thinner fibrils (Figure 12C). These results revealed that the morphological changes are independent of the polyP chain length while the competition for binding is highly chain length dependent. This would suggest that different polyP chain lengths have different binding affinities towards α-synuclein fibers, but that binding overall is sufficient for polyP to execute its structure-altering effect on fibrils.

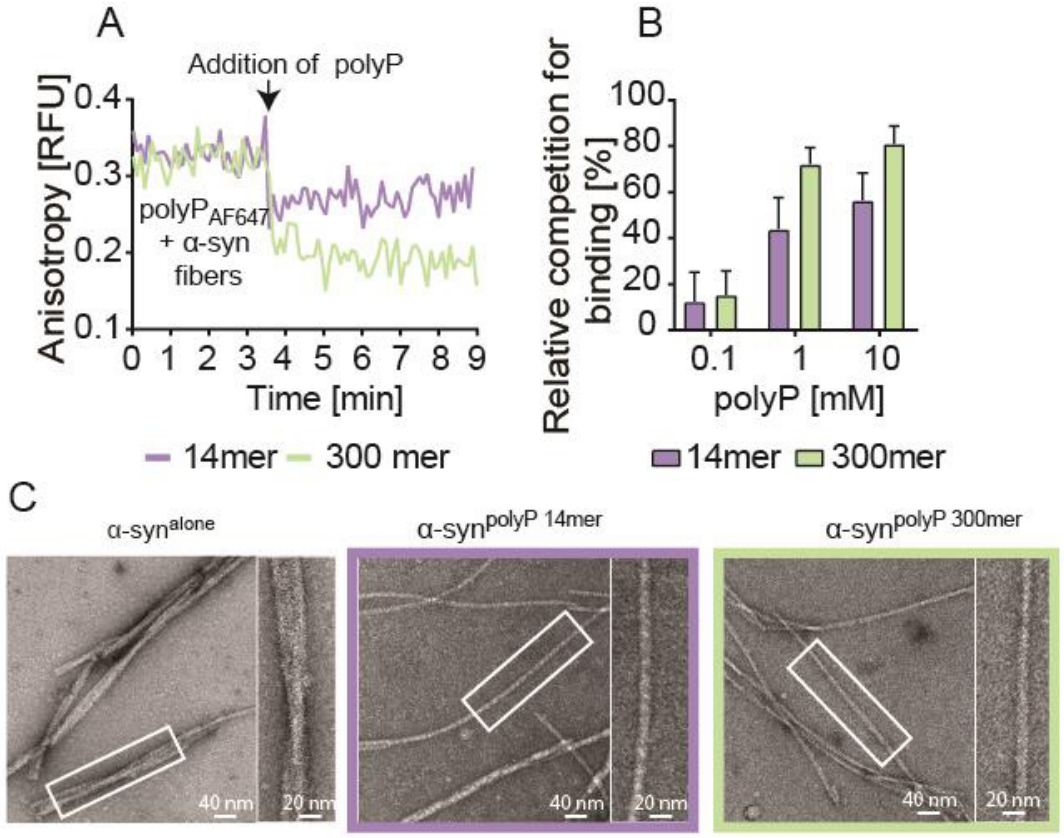

Figure 12: PolyP-α-synuclein interaction is reversible and polyP chain-length dependent. *(A) 50 µM polyP$_{300\text{-}AF647}$ (in Pi units) were pre-incubated with 30 µM α-synuclein fibers to form a polyP$_{300\text{-}AF647}$- α-synuclein complex. Anisotropy of the mixture was measured and at indicated time points 10 mM unlabeled polyP$_{300}$ or polyP$_{14}$ (in Pi units) was added to test for competition and chain length dependency (Lempart, Tse et al. 2019). (B) The drop in signal after addition of 0.1, 1 or 10 mM unlabeled polyP$_{300}$ or polyP$_{14}$ was measured. The signal of polyP$_{300\text{-}AF647}$ without the addition of any α-synuclein fibers gives a baseline signal. The values are shown as relative competition normalization to the decrease in signal to the difference between the signal of polyP$_{300\text{-}AF647}$-α-synuclein-complex and the polyP$_{300\text{-}AF647}$ baseline. Experiment was repeated four times and values are shown +/-SD. (C) TEM analysis of α-synuclein fibers (300 µM) formed in the absence of polyP (α-syn^{alone}) or in the presence of 7.5 mM polyP$_{14}$ (α-syn^{polyP14}) or 7.5 mM polyP$_{300}$ (α-syn^{polyP300}).*

5.4 PolyP - α-synuclein fiber interaction prevents polyP degradation by PPX

Our results clearly suggested that polyP-fiber interactions are reversible. To test whether the addition of polyphosphatase (PPX), a highly active exopolyphosphatase (Wurst and Kornberg 1994), is capable of also reversing the polyP-induced structural changes in α-synuclein fibers, I formed polyP-α-synuclein fibrils and incubated them with purified yeast PPX (scPPX). Structural changes were identified via TEM. I was unable to observe any morphological differences upon addition of PPX (Figure 13A), suggesting either that the morphological changes that were induced by polyP binding are irreversible or that PPX is unable to degrade polyP when bound to the fibers. In order to test for both possibilities, I incubated 40 µM of α-synuclein monomers or fibers with increasing concentrations of polyP, added PPX and monitored Pi hydrolysis using the molybdate assay (Christ and Blank 2018) (Assay was prepared in collaboration with Nicholas Yoo, Jakob lab). While polyP that was incubated with α-synuclein monomers was rapidly and completely hydrolyzed to the corresponding amount of Pi, almost 50% of polyP was protected against hydrolysis in the presence of α-synuclein fibrils (Figure 13B). Similar results were obtained when supernatant and pellet of 40 µM α-synuclein monomer or fibrils incubated with 500 µM polyP were incubated with PPX. Whereas the majority of PPX-sensitive polyP was found in the supernatant when monomers of α-synuclein were used, about half of polyP co-precipitated with α-synuclein fibrils. Of this amount, the majority was again protected from degradation (Figure 13C). This experiment shows that polyP-fiber interactions are protecting against the enzymatic degradation of polyP *in vitro.*

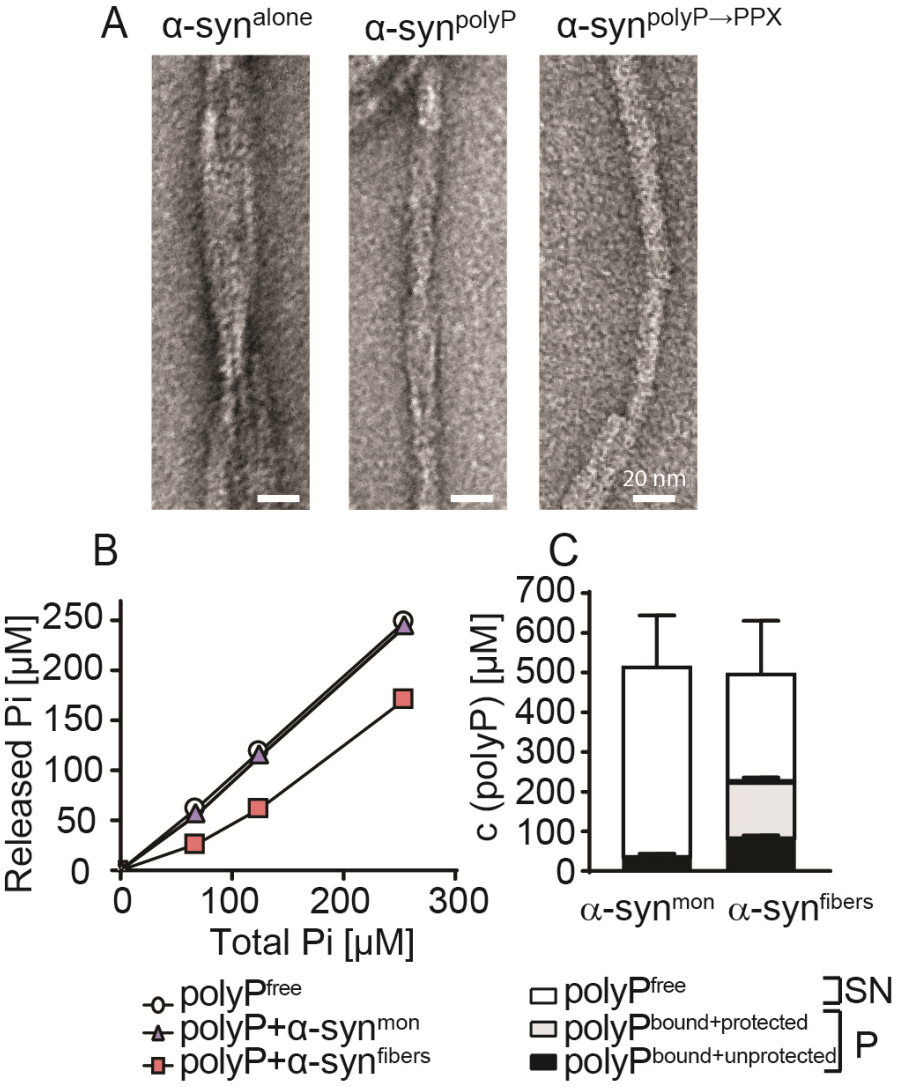

Figure 13: PolyP is protected from degradation by PPX when bound to α-synuclein fibers. *(A) TEM analysis of fibers formed in the absence of polyP (α-syn^{alone}), in the presence of polyP (α-syn^{polyP}) or in the presence of polyP with subsequent PPX treatment (α-syn$^{polyP→PPX}$). (B) PPX hydrolysis of indicated polyP concentrations in the presence and absence of 40 µM of α-synuclein monomers or α-synuclein fibers measured via molybdate assay. The experiment was repeated three times and a representative graph is shown. (C) 500 µM polyP (in Pi units) was spun down in the presence of 40 µM α-synuclein monomers or fibers. Supernatant (SN) and pellet (P) were treated with PPX for polyP hydrolysis and inorganic Pi was detected via molybdate assay. Sample in the pellet was considered bound and sample in the supernatant was considered free (Lempart, Tse et al. 2019).*

5.5 PolyP prevents the intracellular enrichment of α-synuclein fibers

The topographical pattern of AD and PD progression and spreading of toxicity suggested that amyloids are capable of cell-to-cell propagation and self-amplification in a prion-like fashion (Braak and Braak 1991; Braak, Del Tredici et al. 2003; Braak, Muller et al. 2006; Jucker and Walker 2013; Guo and Lee 2014). *In vitro* and *in vivo* studies confirmed this hypothesis by showing entry, recruitment and spreading of misfolded α-synuclein and tau seeds to neighboring cells and/or anatomically connected brain regions (Costanzo and Zurzolo 2013; Guo and Lee 2014). Active secretion of amyloids into the extracellular space is followed by their uptake by neighboring recipient cells (Reyes, Olsson et al. 2015), where the fibrils sequester endogenous protein and cause amyloid fiber formation (Danzer, Krebs et al. 2009).

PolyP was shown to protect differentiated SH-SY5Y cells against Aβ and α-synuclein toxicity (Cremers, Knoefler et al. 2016). Based on our *in vitro* results, which showed that polyP accelerates fiber formation, we reasoned that the polyP-mediated redirection of the equilibrium from toxic oligomers towards mature non-toxic fibers might serve as the underlying mechanism for its cytoprotective effect. Alternatively, it is feasible that the polyP-induced alteration of fiber morphology causes a change in fiber stability, toxicity and/or cell-to-cell spreading. Lastly, it is also conceivable that polyP influences the uptake and/or intracellular turnover of amyloids. In order to unravel the mechanism of polyP's cytoprotective role, I focused on studying the cellular localization of α-synuclein in the absence and presence of polyP. Therefore, I labeled α-synuclein with Alexa Fluor 488 and monitored the uptake of monomeric (α-syn$^{mon\text{-}AF488}$) or fibrillary (α-syn$^{PFF\text{-}AF488}$) protein into neuronal cells via microscopy in the presence and absence of polyP. The experiment was conducted at 37°C, where endocytosis takes place and at 4°C where the endocytotic uptake is significantly decelerated. As expected and shown before, α-syn$^{mon\text{-}AF488}$ is readily being taken up by cells at 37°C but not at 4°C (Tomoda, Kishimoto et al. 1989). Neither the absence nor presence of polyP had any influence on this process (Figure 14A). Alpha-syn$^{PFF\text{-}AF488}$ were also readily taken up at 37°C. In addition, a substantial amount of the signal was membrane associated, consistent with previous results (Karpowicz, Haney et al. 2017). In the presence of polyP, however, we observed neither a significant intracellular α-syn$^{PFF\text{-}AF488}$ signal nor a membrane-associated signal (Figure 14A), suggesting that

polyP interferes with the uptake of α-synuclein fibrils. To independently validate the microscopy findings, I tested the amount of α-synuclein monomer and amyloid uptake via western blot. As before, cells were incubated with α-syn^{mon} or α-syn^{PFF} for 24 hours at 37°C in the presence and absence of polyP. Then, the cells were washed, lysed, run on a SDS-PAGE and blotted onto a membrane for detection with α-synuclein antibody. Consistent with our microscopy data, I found an overall much higher amount of α-syn^{PFF} in the absence of polyP than in its presence (Figure 14B). These results suggested that polyP effectively inhibits the membrane association and internalization of α-syn$^{PFF\text{-}AF488}$ while leaving the uptake of α-syn$^{mon\text{-}AF488}$ unaffected.

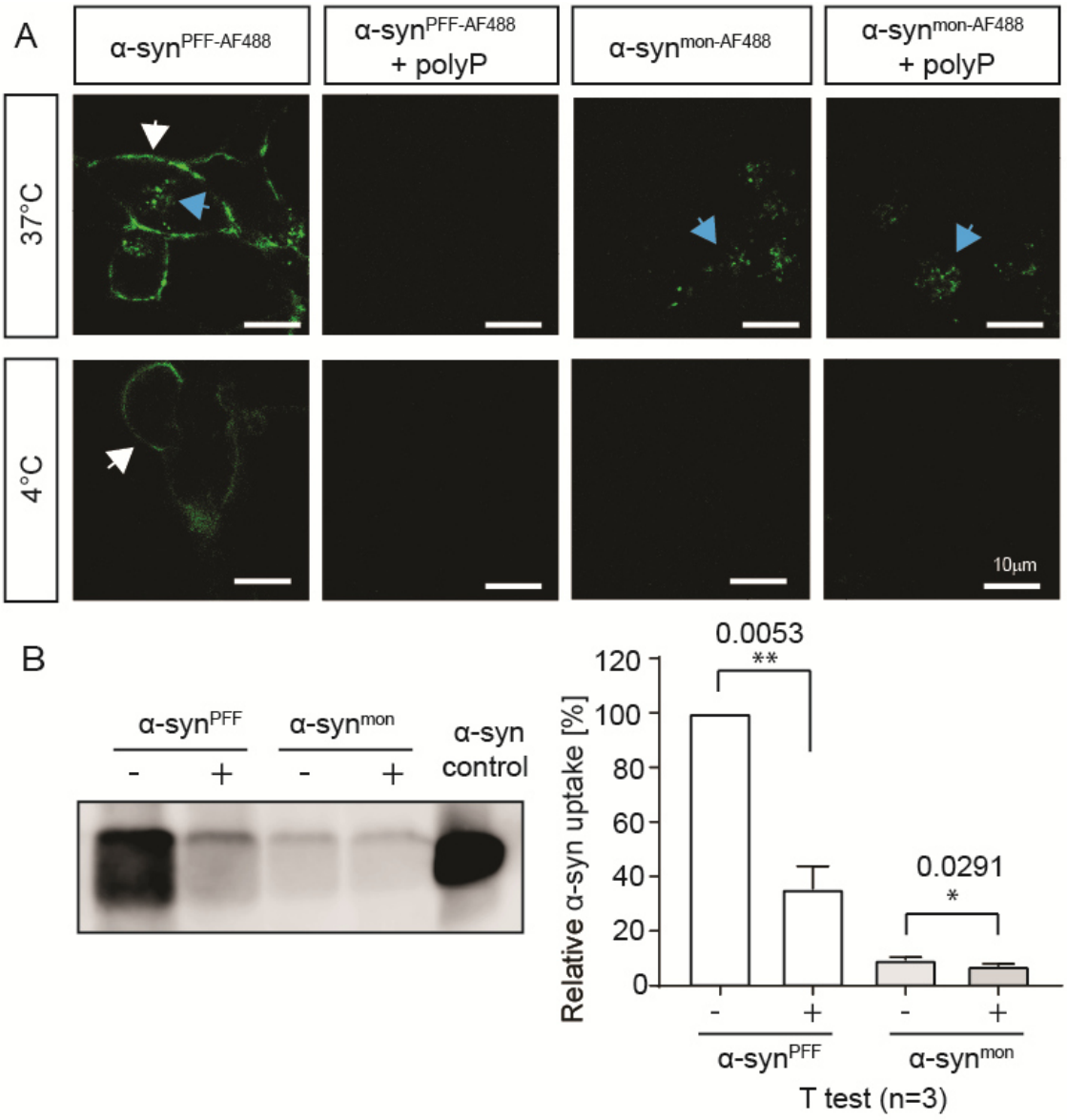

Figure 14: PolyP inhibits the endocytotic uptake of fibrillary α-synuclein. *(A) Differentiated SH-SY5Y cells were treated with 3 µM α-syn$^{mon\text{-}AF488}$ or α-syn$^{PFF\text{-}AF488}$ at 4ºC or 37ºC in the presence or absence of 250 µM polyP$_{300}$ (in Pi units) and uptake was monitored via fluorescence microscopy. Intracellular signal is indicated with blue arrows and extracellular signal with white arrows (Lempart, Tse et al. 2019). (B) Western blot for the detection of α-synuclein of differentiated SH-SY5Y cells treated with α-syn$^{mon\text{-}AF488}$ or α-syn$^{PFF\text{-}AF488}$ in the presence (+) or absence (-) of 250 µM polyP (in Pi units) for 24 hours at 37ºC. Three repeats were quantified and normalized to the α-syn^{PFF} signal respectively. Statistics were prepared with one-way ANOVA (*p<0.05, **<0.01)*

5.5.1 PolyP binds to sonicated and unsonicated α-synuclein fibers with the same affinity

Preformed α-synuclein fibrils are a widely used tool to study the uptake and spreading of α-synuclein fibers (Wood, Wypych et al. 1999; Luk, Song et al. 2009; Volpicelli-Daley, Luk et al. 2014). Unlike the fibers used in the *in vitro* assays of this work, PFF are sonicated to generate a mixture of short fibrils, protofibrils and oligomers (Luk, Kehm et al. 2012). To characterize the sonicated species I tested the interaction between $polyP_{300\text{-}AF647}$ and $\alpha\text{-syn}^{PFF}$ via anisotropy. As control, I used unsonicated fibers that were previously shown to have a strong interaction with polyP (Figure 11A). Displayed is the increase in anisotropy signal after addition of sonicated or unsonicated α-synuclein fibrils to $polyP_{300\text{-}AF647}$ normalized to the addition of 10 µM unsonicated α-synuclein fibers. Both unsonicated and sonicated fibers readily bind to two different concentrations (5 µM and 10 µM) of polyP (Figure 15A). Visualizing the structure of sonicated or unsonicated fibrils via TEM imaging shows that the sonicated fibers are shorter in length with a higher amount of oligomeric species compared to the unsonicated amyloids (Figure 15B). Like previously reported, these results confirm that sonication leads to shorter α-synuclein fibrils with a higher content of oligomeric species. The observation that polyP binds to $\alpha\text{-syn}^{PFF}$ with the same affinity than to unsonicated fibers suggests that polyP could potentially interact with $\alpha\text{-syn}^{PFF}$ in the previously described uptake experiment (Figure 14).

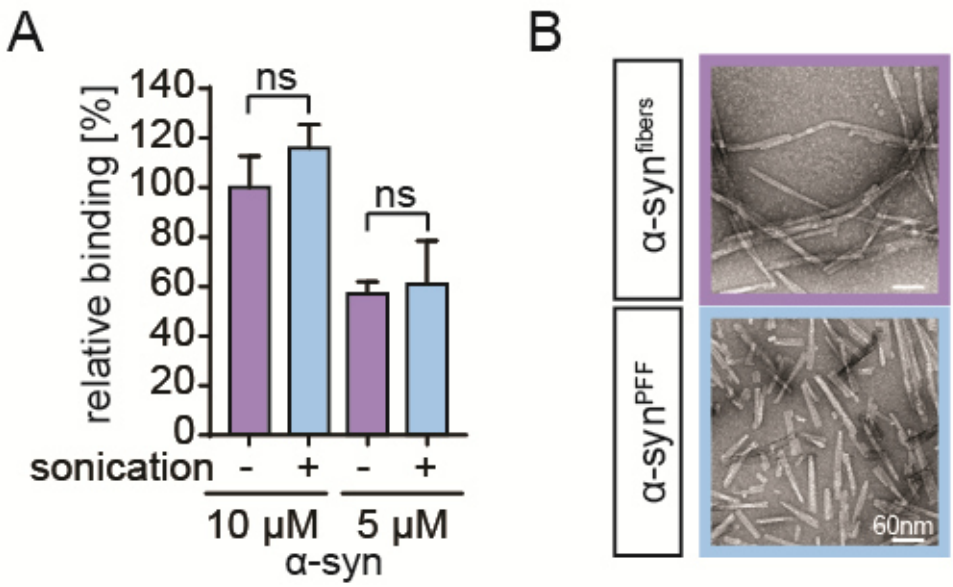

Figure 15: Characterization of sonicated vs unsonicated α-synuclein fibers. *(A) Comparison of binding of 50 µM polyP$_{300\text{-}AF647}$ (in Pi units) to sonicated (+) or unsonicated (-) fibers measured with FP. The drop in signal was normalized to the difference of polyP-α-synuclein signal and polyP signal alone. Statistics were prepared with one-way ANOVA (*p<0.05). (B) Characterization of α-syn$^{PFF\text{-}AF488}$ via TEM shows sonicated fibrils to be shorter in size and a higher amount of oligomeric species (Lempart, Tse et al. 2019)*

5.5.2 Membrane associated fibrils can easily be distinguished from internalized protein via distinct patterns

To validate our results and clearly distinguish between the extracellular and intracellular localization of α-syn$^{PFF\text{-}AF488}$ and α-syn$^{mon\text{-}AF488}$, I used the fluorescent quencher Trypan blue (TB). This membrane impermeable fluorescence dye is capable of interacting with and quenching the signal of fluorescently labeled molecules on the outside but not the inside of cells (Loike and Silverstein 1983; Hed, Hallden et al. 1987; Wan, Park et al. 1993). I therefore incubated differentiated SH-SY5Y cells with either α-syn$^{PFF\text{-}AF488}$ or α-syn$^{mon\text{-}AF488}$ for 3 hours and quenched the samples with TB for 15 seconds. While a clear fluorescent signal shaping the outline of the cell was detectable when cells were incubated with α-syn$^{PFF\text{-}AF488}$ in the absence of TB (white arrow), this signal was completely lost in its presence (Figure 16A). No difference was observed for the intracellular signals consistent with the membrane-impermeable character of TB (Mulcahy, Pink et al. 2014). In the case of α-syn$^{mon\text{-}AF488}$, no significant difference between TB treated or untreated samples was detected, indicating that α-synuclein was almost exclusively in the intracellular space. In summary, these results suggest that polyP prevents the uptake of α-syn$^{PFF\text{-}AF488}$ potentially by interfering with the membrane association of fibrillar α-synuclein.

5.5.3 PolyP degradation by PPX abrogates the uptake inhibition

To verify that the observed inhibition of α-synuclein uptake is due to the polyP chain and not simply due to the large amounts of negative charges, I pre-incubated polyP with PPX to hydrolyze the chain into inorganic phosphate (Pi) units before adding α-syn$^{PFF\text{-}AF488}$. When polyP was treated with PPX, α-syn$^{PFF\text{-}AF488}$ was readily internalized into the cell (Figure 16B). In the absence of PPX, polyP clearly inhibited the uptake of α-syn$^{PFF\text{-}AF488}$ as seen before (Figure 14A). This experiment highlights that the negatively charged chain and not the negative charge alone is essential for inhibiting the uptake of α-syn$^{PFF\text{-}AF488}$.

5.5.4 Physiological polyP concentrations are highly effective in α-syn^{PFF} uptake inhibition

Physiological polyP concentrations in the brain were shown to be between 50 and 130 µM (Kumble and Kornberg 1995; Kornberg 1999). To test the relevant concentrations that leads to uptake inhibition, I incubated differentiated SH-SY5Y

cells with α-syn$^{PFF-AF488}$ in the absence and presence of 10, 100, 250 and 500 µM polyP (in Pi units) and monitored the uptake after 24 hours with fluorescence microscopy. Indeed, concentrations between 100-500 µM polyP (in Pi units) significantly prevented the internalization, whereas 10 µM only slightly reduced the uptake (Figure 16C). This result supports the idea that physiological levels of polyP might play a role in the development or progression of amyloid-related neurodegenerative diseases.

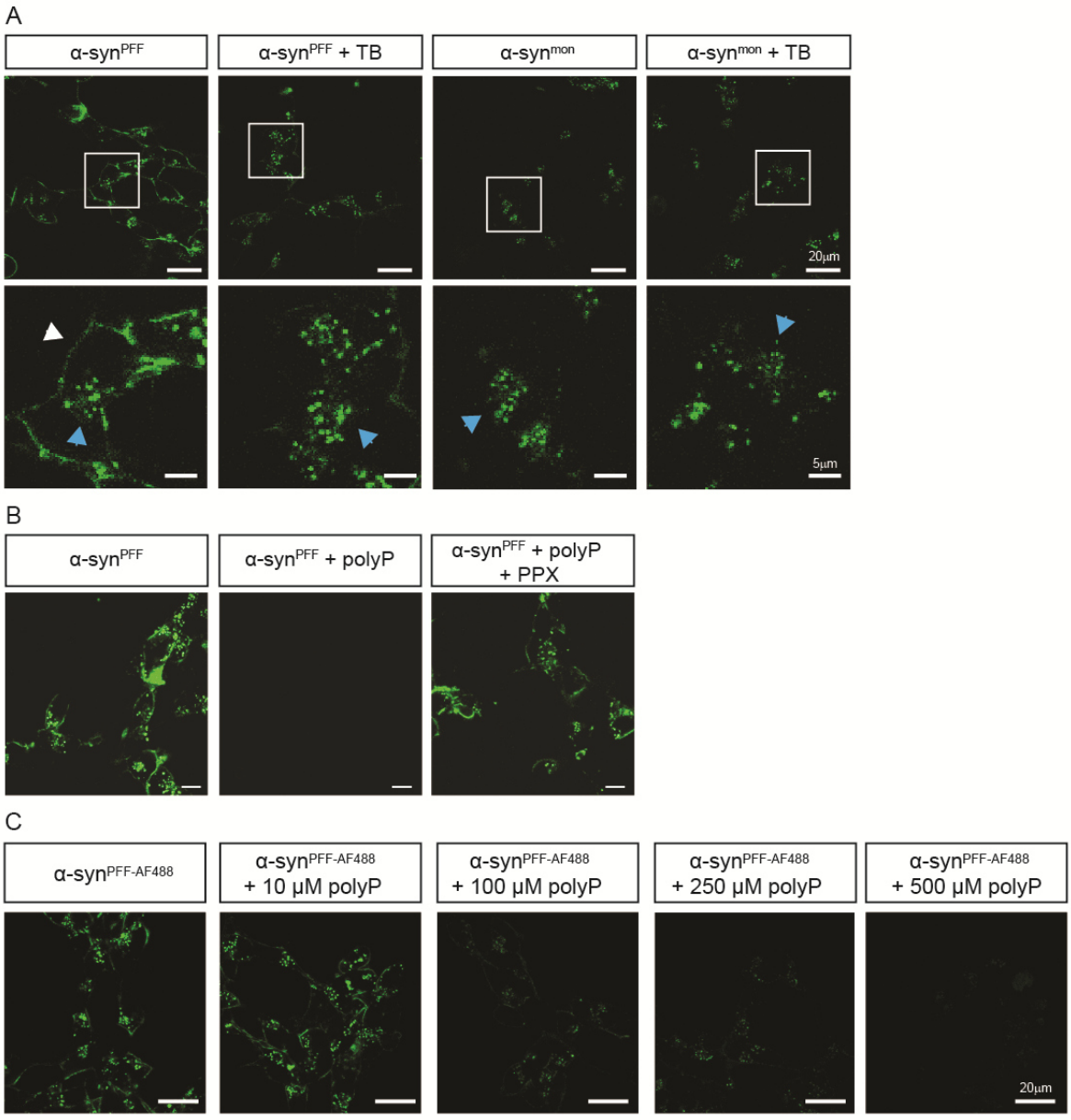

Figure 16: Characterization of the α-synuclein fiber uptake inhibition through polyP. *(A) Differentiated SH-SY5Y cells were treated with 3 µM α-syn$^{mon\text{-}AF488}$ or α-syn$^{PFF\text{-}AF488}$ for 3 hours. One set of samples was treated with the membrane impermeable dye Trypan blue (0.05%) for 15 seconds to quench extracellular fluorescence and localization of α-synuclein was monitored via fluorescence microscopy. Intracellular signal is indicated with a blue arrow and extracellular signal with a white arrow. (B) Differentiated SH-SY5Y cells were treated with 3 µM α-syn$^{PFF\text{-}AF488}$ in the absence of polyP, in the presence of 250 µM polyP (in Pi units) or in the presence of 250 µM polyP (in Pi units) pretreated with PPX. (C) The influence of 10, 100, 250 and 500 µM polyP (in Pi units) were tested on α-syn$^{PFF\text{-}AF488}$uptake inhibition. Differentiated SH-SY5Y cell were treated for 24 hours with α-syn$^{PFF\text{-}AF488}$ in the presence or absence of indicated polyP concentrations at 37ºC and the uptake was monitored via fluorescence microscopy.*

5.6 Presence of polyP stops the uptake of fibers

5.6.1 Pre-incubation of cells with polyP has no influence on the fiber uptake

With physiological relevant polyP concentrations effectively inhibiting the membrane association and uptake of amyloidogenic α-synuclein, it was of great interest to gain more insight into the underlying mechanism. To address this question, I tested whether and how intracellular polyP enrichment affects the α-synuclein uptake. For these experiments, I treated differentiated SH-SY5Y cells with $polyP_{300\text{-}AF647}$ for 24 hours, and confirmed the uptake of $polyP_{300\text{-}AF647}$ via fluorescence microscopy (Figure 17). I then incubated the cells with $\alpha\text{-syn}^{PFF\text{-}AF488}$ for 24 hours and monitored the uptake of $\alpha\text{-syn}^{PFF\text{-}AF488}$ as before. While presence of extracellular polyP (i.e. control) showed the previously observed decrease in $\alpha\text{-syn}^{PFF\text{-}AF488}$, the uptake of $\alpha\text{-syn}^{PFF\text{-}AF488}$ signal was not affected by the enrichment of intracellular polyP (Figure 17). Moreover, an overlay of the polyP and $\alpha\text{-syn}^{PFF\text{-}AF488}$ signal showed no prominent co-localization between the two signals, suggesting that the two molecules do not interact directly with each other in the cell. This experiment shows that elevated intracellular polyP levels have no influence on the internalization of $\alpha\text{-syn}^{PFF\text{-}AF488}$ and suggests that the extracellular presence of polyP is crucial for uptake inhibition.

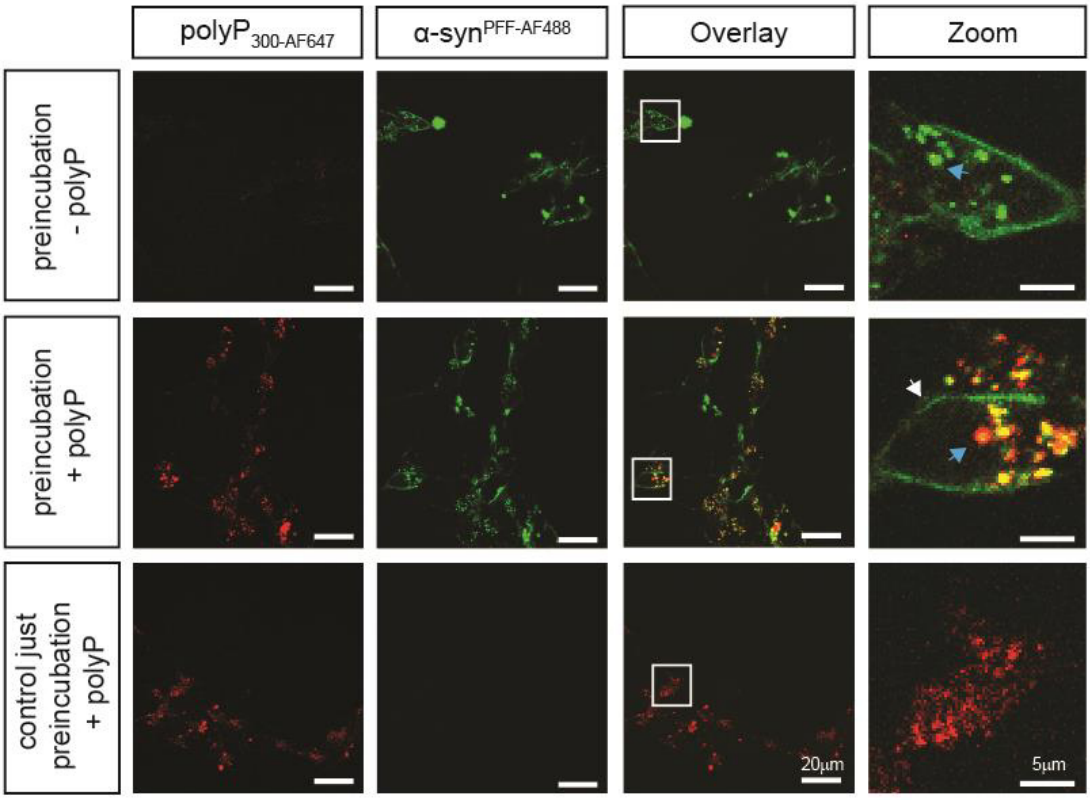

Figure 17: Elevated intracellular polyP levels have no influence on α-syn$^{PFF-AF488}$ uptake. *Differentiated SH-SY5Y cells were treated with 250 µM polyP$_{300-AF647}$ (in Pi units) for 24 hours and subsequently with 3 µM α-syn$^{PFF-AF488}$ for 24 hours. Internalization of both molecules was monitored with fluorescence microscopy. As control cells were left without polyP$_{300-AF647}$ pretreatment or pre-treated cells were not incubated with α-syn$^{PFF-AF488}$ (Lempart, Tse et al. 2019).*

5.6.2 Alpha-syn$^{PFF\text{-}AF488}$ uptake is stopped with the addition of polyP

In order to verify the importance of the extracellular presence of polyP for uptake inhibition, I first incubated the cells with α-syn$^{PFF\text{-}AF488}$ and then added polyP after 2, 4 and 6 hours of incubation and observed the uptake of the labelled amyloids after 2.5, 5, 7 and 24 hours, respectively. In the absence of polyP, α-syn$^{PFF\text{-}AF488}$ gets internalized into the cell and the signal steadily increases over the measured time points. With the addition of polyP after 2 hours of pre-incubation, the α-syn$^{PFF\text{-}AF488}$ signal measured after 2.5, 5, 7 and 24 hours was significantly reduced compared to the control without polyP (Figure 18A). Addition of $polyP_{300}$ after 4 and 6 hours leads to a similar reduction in α-syn$^{PFF\text{-}AF488}$ uptake. Western blot performed after 24 hours of incubation with or without $polyP_{300}$ addition after 2, 4 and 6 hours, confirmed the microscopy results and showed that addition of polyP significantly reduced the amount of internalized protein compared to the control without polyP (Figure 18B). These experiments agree well with our previous results and indicate that the extracellular presence of polyP is effective in rapidly interfering with the uptake of amyloidogenic α-synuclein fibrils.

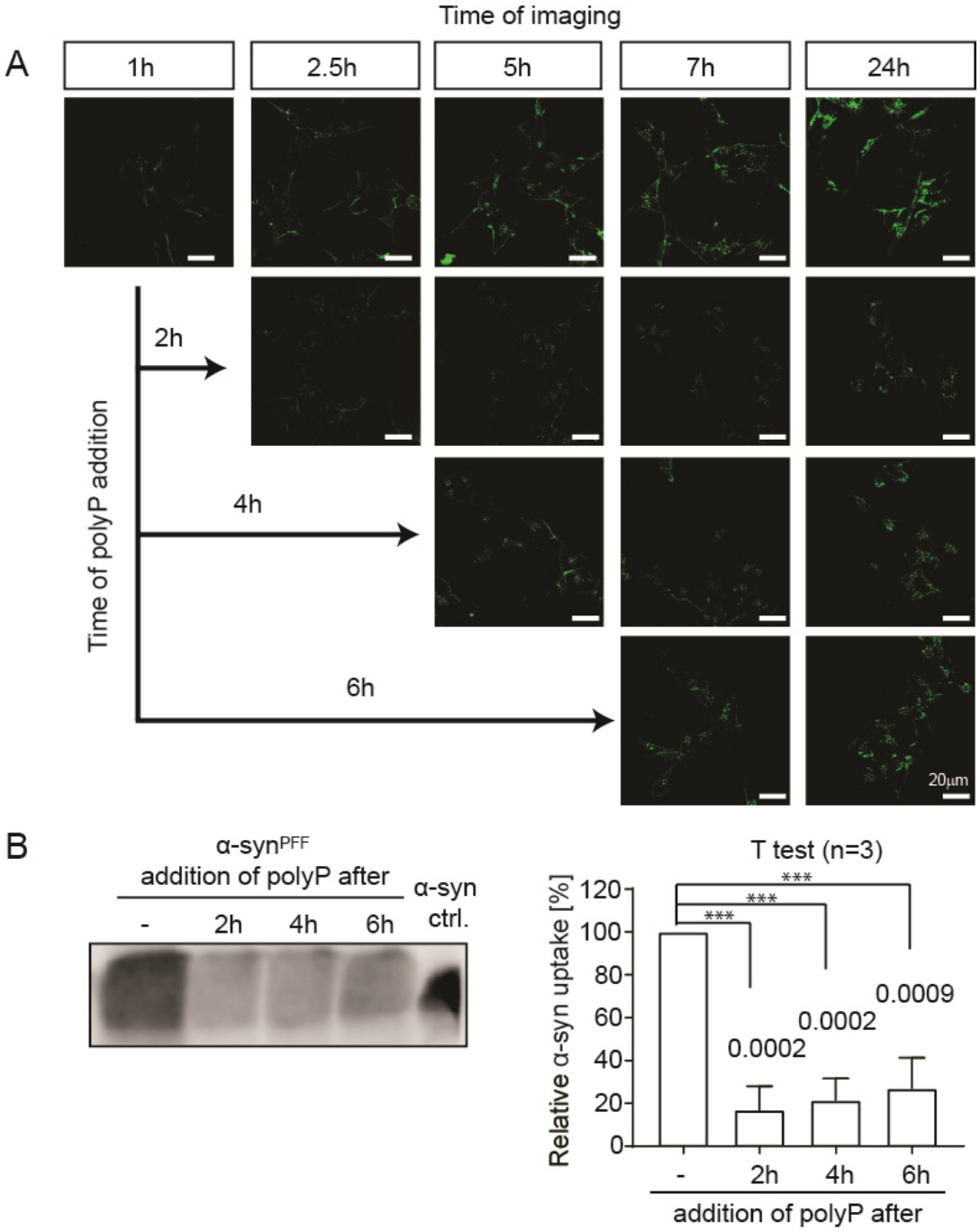

Figure 18: Addition of polyP immediately stops the uptake of α-syn$^{PFF\text{-}AF488}$. *(A) Time course experiment monitoring the uptake of 3 µM α-syn$^{PFF\text{-}AF488}$ into differentiated SH-SY5Y cells after 1, 2.5, 5, 7 and 24 hours. At 2, 4 and 6 hours 250 µM polyP$_{300}$ (in Pi units) is added, respectively (Lempart, Tse et al. 2019). (B) Western blot for the detection of α-synuclein in the cell lysate of differentiated SH-SY5Y cells treated with α-syn^{PFF} for 24 hours when 250 µM polyP$_{300}$ (in Pi units) was added after 2, 4 and 6 hours after treatment. Three repeats were quantified and normalized to the α-syn^{PFF} signal respectively. Statistics were prepared with one-way ANOVA (*p<0.05,**<0.01)*

5.7 PolyP co-localizes with α-syn$^{PFF\text{-}AF488}$ on the cell membrane

The receptor responsible for the macropinocytotic uptake of α-syn$^{PFF\text{-}AF488}$ is the highly negatively charged GAG receptor heparin sulfate (Holmes, DeVos et al. 2013; Reyes, Olsson et al. 2015; Gustafsson, Loov et al. 2018). Since polyP is one of the most densely negative charged molecule, we now reasoned that polyP binding to the α-synuclein fibrils interferes with the binding of α-synuclein to the heparin sulfate receptor. In order to test this idea, I investigated whether polyP interacts with α-syn$^{PFF\text{-}AF488}$ on the membrane. To capture the exact moment when polyP prevents the uptake of α-syn$^{PFF\text{-}AF488}$, I used the same experimental setup of the previous experiment (Figure 18A). Alpha-syn$^{PFF\text{-}AF488}$ was added to differentiated SH-SY5Y cells and the cells were incubated for 6 hours with the amyloid before polyP$_{300\text{-}AF647}$ was added. I then imaged the sample after 1 hour of incubation. As before, I observed the α-synuclein signal both intracellularly (blue arrow) and associated with the membrane (white arrow) (Figure 19A). The polyP$_{300\text{-}AF647}$ signal, on the other hand, was mainly observed on the cell surface, where it completely co-localized with the membrane associated signal of α-syn$^{PFF\text{-}AF488}$. A surface blot analysis along a diagonal arrow through one cell in the image confirmed this result and showed that the intracellularly polyP signal is very faint and not co-localized with α-syn$^{PFF\text{-}AF488}$ while the membrane associated signal shows prominent co-localization between the two molecules (Figure 19B). Together with the *in vitro* finding that polyP readily interacts with α-syn^{PFF} this experiment strongly suggests polyP-α-synuclein interaction as basis for the mechanism of the uptake inhibition.

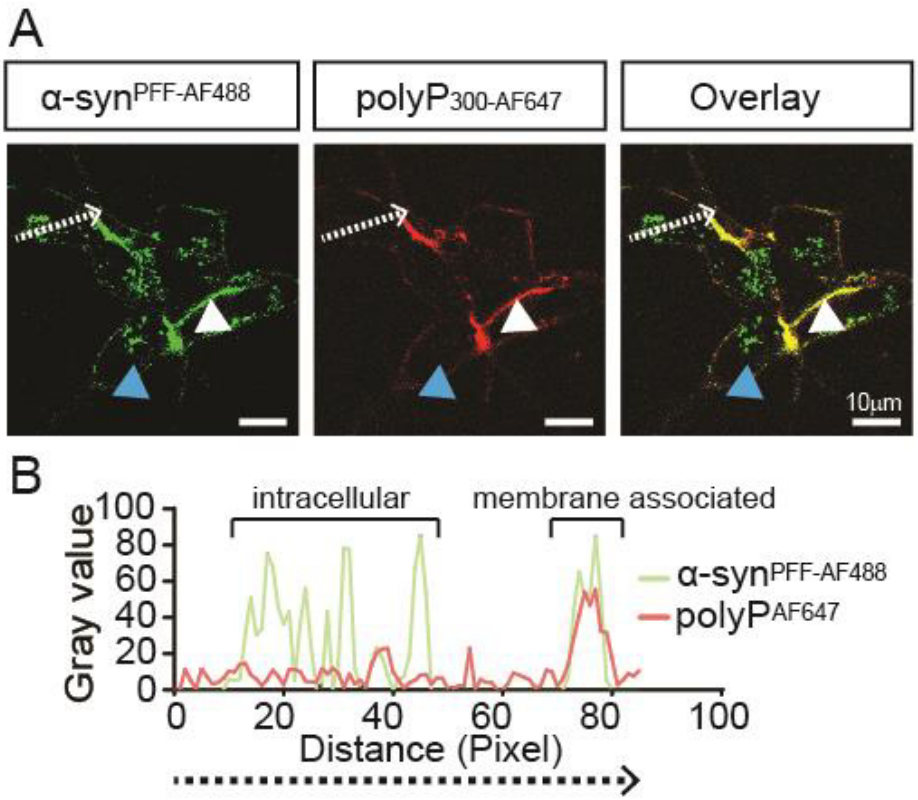

Figure 19: PolyP co-localizes with α-synuclein fibers outside of the cell. *(A) Differentiated SH-SY5Y cells were treated with 3 µM α-syn$^{PFF\text{-}AF488}$ for 7 hours. After 6 hours 250 µM polyP$_{300\text{-}AF647}$ (in Pi units) was added to the cells and the localization of the fluorescently labeled molecules was monitored via microscopy. White arrows indicate membrane associated signal while blue arrows indicate internalized signal. (B) Surface blot of α-syn$^{PFF\text{-}AF488}$ and polyP$_{300\text{-}AF647}$ along the white dashed arrow marked in the upper image (Lempart, Tse et al. 2019).*

5.8 PolyP inhibits fiber uptake in a chain length dependent manner

Previous work showed polyP accelerating amyloid fiber formation in a chain length dependent manner with longer chains (n > 60) being disproportionally more potent than shorter chains (Figure 2E in (Cremers, Knoefler et al. 2016)). To test whether the fiber uptake shows a similar chain length dependence, I incubated differentiated SH-SY5Y cells with α-syn$^{PFF-AF488}$ in the absence or presence of 250 µM polyP$_{14}$, polyP$_{130}$ and polyP$_{300}$ and monitored the uptake after 24 hours using fluorescence microscopy. In agreement with our previous results, I found a clear intracellular α-syn$^{PFF-AF488}$ signal after 24 hours in the absence of polyP and a lack in signal in the presence of the polyP$_{300}$ (Figure 20). While the slightly shorter polyP$_{130}$ chain was similarly potent in preventing the α-syn$^{PFF-AF488}$ uptake, the fiber uptake in the presence of polyP$_{14}$ was only modestly affected (Figure 20). These results indicate that physiological polyP concentrations and chain lengths are highly effective in preventing the uptake of α-synuclein fibrils.

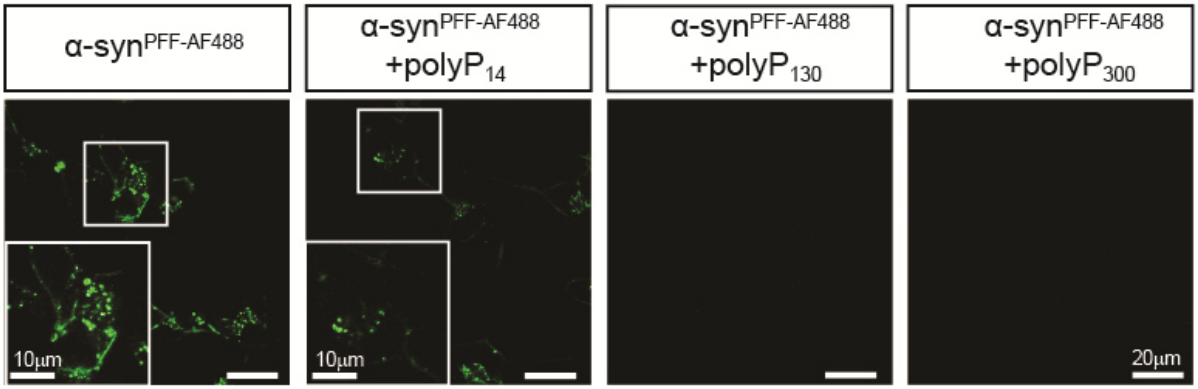

Figure 20: The effect of polyP shows chain length dependency. *Differentiated SH-SY5Y cells were incubated with 3 µM α-syn$^{PFF-AF488}$ for 24 hours in the absence or presence of different chain length of 250 µM polyP (in Pi units) (14mer, 130mer, 300mer). Long polyP chains (130mer and 300mer) completely inhibit the uptake where the 14mer shows a weaker effect (Lempart, Tse et al. 2019).*

5.9 PolyP-induced uptake inhibition is specific for α-synuclein fibers

Our results unequivocally showed that polyP has a significant impact on the uptake of α-syn$^{PFF\text{-}AF488}$. To test whether this effect is specific of α-synuclein fibrils or whether polyP generally interferes with endocytic pathways, I decided to test the uptake TAT-TAMRA, a small 20 kDa protein that gets internalized via the micropinocytosic pathway (Wadia, Stan et al. 2004; Kaplan, Wadia et al. 2005). As before, I monitored the TAT-TAMRA and α-syn$^{PFF\text{-}AF488}$ into differentiated SH-SY5Y cells for 3 hours in the presence or absence of polyP$_{300}$. The amount of internalized protein was determined via fluorescence microscopy. Under the tested conditions, polyP had no significant effects on the uptake of TAT-TAMRA and only interfered with the uptake of α-syn$^{PFF\text{-}AF488}$ (Figure 21). This experiment shows that polyP uptake inhibition is specific for amyloidogenic α-synuclein.

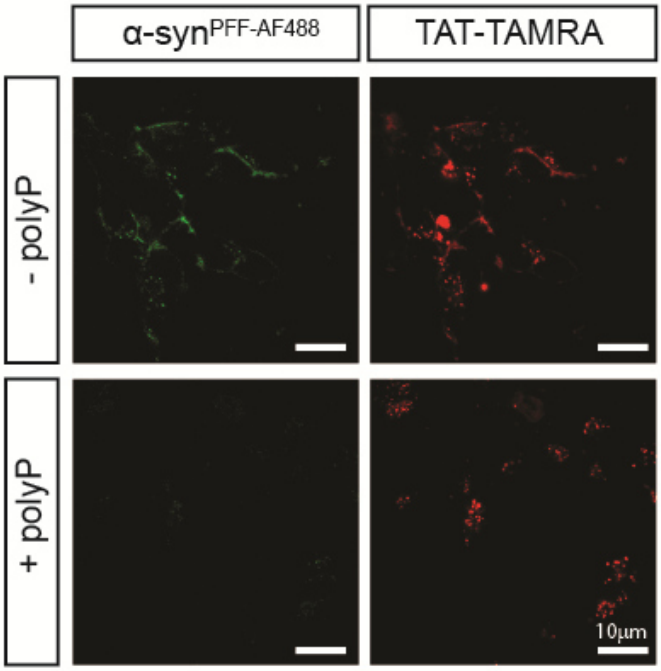

Figure 21: PolyP uptake inhibition is specific for α-syn$^{PFF\text{-}AF488}$. *Differentiated SH-SY5Y cells were treated with 3 µM α-syn$^{PFF\text{-}AF488}$or 5 µM TAT-TAMRA. The uptake of the samples was monitored with fluorescence microscopy at their respective wave length in the absence and presence of 250 µM polyP (in Pi units) (Lempart, Tse et al. 2019).*

5.10 PolyP induces structural changes in tau proteins

This chapter reports work that was conducted in close collaboration with the Rhoades Lab from the University of Pennsylvania and is published in "Polyphosphate Initiates Tau Aggregation through Intra- and Intermolecular Scaffolding" (Wickramasinghe, Lempart et al. 2019). Experiments conducted by our collaborators are indicated in the text.

Previous *in vitro* work from our lab demonstrated that polyP has the most significant effect on tau fiber formation (Cremers, Knoefler et al. 2016). Full length tau alone takes months to form fibrils even at very high protein concentrations (Goedert, Jakes et al. 1996). Yet, in the presence of polyP, the $T_{1/2}$ is reduced to less than 2 days (Cremers, Knoefler et al. 2016). To obtain more detailed mechanistic insights into how polyP affects Tau fiber formation, we focused on the polyP-mediated structural rearrangements of Tau in the early stages of its aggregation. In collaboration with the Rhoades lab, which has successfully established single-molecular Förster resonance energy transfer (smFRET) as an approach to characterize the conformations of aggregation-prone proteins (Trexler and Rhoades 2010; Elbaum-Garfinkle and Rhoades 2012), we worked on identifying polyP-induced structural differences in various tau isoforms. Structurally, tau can be divided into four major domains: the N-terminal domain, the microtubule binding domain region (MTBR), the proline rich region (PRR) and the C-terminal domain (Figure 22). MTBR is involved in microtubule and soluble tubulin binding, which is enhanced by PRR and the C-terminus. MTBR also forms the core of paired helical filaments. The N-terminal domain is less well understood but is thought to regulate microtubule (Derisbourg, Leghay et al. 2015) and neuronal membrane (Brandt, Leger et al. 1995) interaction.

Physiologically, tau occurs in a variety of splicing variants. Alternate splicing of the second repeat (R2) domain of the MTBR gives rise to isoforms containing three (3R) or four (4R) repeat regions with zero (0N), one (1N) or two (2N) N-terminal inserts (Goedert, Spillantini et al. 1989). 3R and 4R have different binding affinities and different assembly activities towards microtubules (Goode, Chau et al. 2000; Panda, Samuel et al. 2003) and were shown to differ in their ability to form aggregates *in vitro* (von Bergen, Friedhoff et al. 2000; Li and Lee 2006). This is due to the fact that one of the two hexapeptide sequences, which are crucial for

aggregation, are located in the R2 domain. With this region being absent in the 3R domain, the 4R domain is generally more prone for aggregation (von Bergen, Friedhoff et al. 2000; Li and Lee 2006).

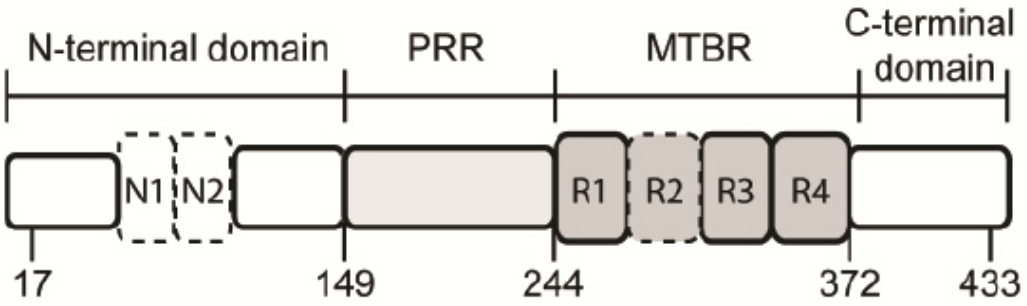

Figure 22: Schematic model of full length tau (2N4R). *The peptide is built-up of the N terminal domain, the proline rich region (PRR), the microtubule binding domain (MTBR) and the C-terminal domain. Labeling sites are marked respectively. Alternative splicing of N1, N2 and R2 leads to the six physiological human tau isoforms (Wickramasinghe, Lempart et al. 2019).*

5.10.1 PolyP interacts with the MTBR and PRR region of Tau

Our previous studies using α-synuclein revealed that polyP only interacts once ThT positive oligomers have formed. To test when polyP begins to interact with tau, full-length tau as well as six tau fragments, the peptides were labeled with a single fluorophore and tested for their ability to interact with $polyP_{14}$ and $polyP_{300}$ using fluorescence correlation spectroscopy (FCS) (Experiment prepared by Rhoades lab). FCS measurements are based on detecting the change in diffusion time through the altered mass and/or hydrodynamic radius resulting from polyP-client interaction. The full-length peptide as well as the fragments including 4R and 3R (MTBR of 244-372), 2N4R and 2N3R (244-372) and P1P2 (PRR 148-245) with the only exception of NT (N-terminus 1-152) all exhibited an increase in diffusion time from 11 to 24% in the presence of $polyP_{300}$ (Figure 23), indicative of binding. Fragments lacking the R2 domain (P2-3R and 3R) were found to have a reproducibly smaller increase in diffusion time upon polyP addition compared to their 4R counterparts (P2-4R and 4R), suggesting that the presence of R2 enhances the interaction with polyP (Figure 23). Addition of the shorter $polyP_{14}$ showed similar trends but was less effective compared to $polyP_{300}$. This

experiment identified the PRR and MTBR as polyP binding sites and suggested that polyP differs in its interactions between tau and α-synuclein.

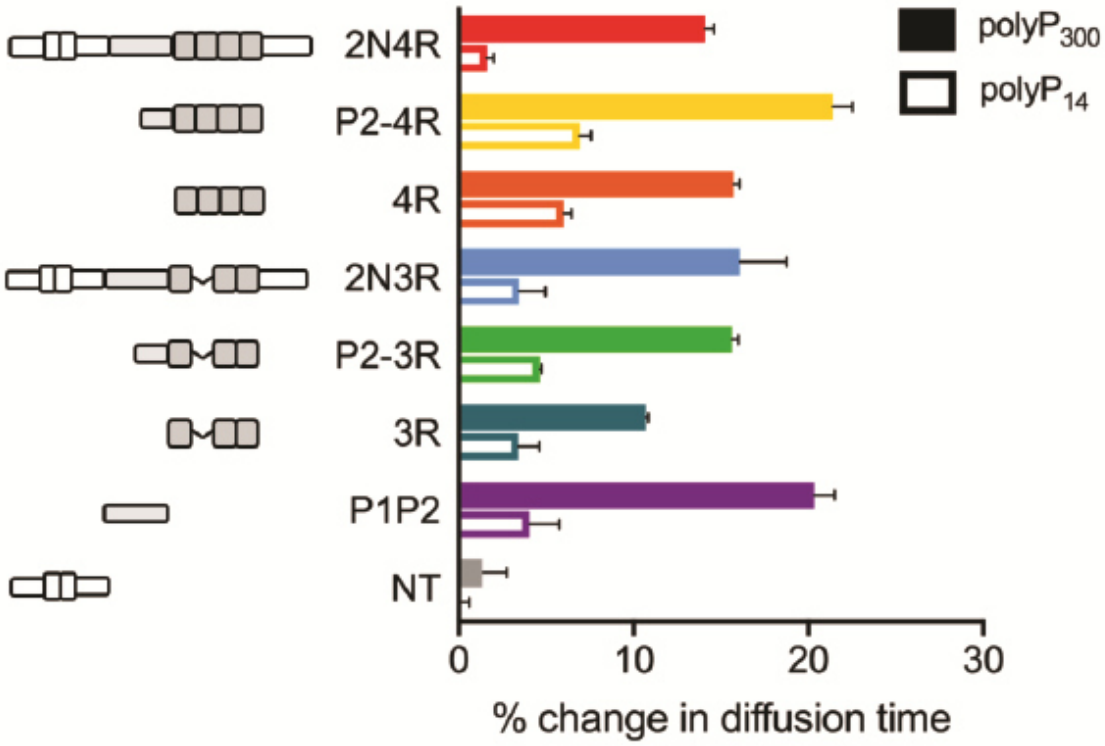

Figure 23: PolyP interacts with different monomeric tau fragments. *FCS measurements show the changes in diffusion times of single-labeled tau constructs with addition of 20 µM polyP$_{300}$ (in Pi units) (solid bars) or polyP$_{14}$ (open bars). Experiments were repeated three times and shown +/- SEM (Wickramasinghe, Lempart et al. 2019).*

5.10.2 PolyP induces compaction of the MTBR and elongation of end-to-end distances

To test whether polyP binding triggers conformational changes in tau that might be responsible for the accelerating effects of polyP on tau fiber formation, the Rhoades lab introduced cysteine residues at specific labeling positions for single molecule FRET studies (smFRET). Sites in the 2N4R and 2N3R that were introduced span either the whole protein (C17-C433), the NT domain (C17-C149), the PRR and MTBR (C149-C375), the MTBR (C244-C372), the PRR (C149-244) or the CT domain (C372-C433). SmFRET experiments were conducted in the presence (solid lines) or in the absence (dashed lines) of polyP$_{300}$ (Experiment

prepared by Rhoades lab). The donor and acceptor fluorophores were Alexa Fluor 488 maleimide and Alexa Fluor 594 maleimide, respectively. FRET efficiencies (ET_{eff}) from individual photon bursts were calculated as a ratio of the intensity of the acceptor over the sum of the intensities of the donor and acceptor. High ET_{eff} values correspond to a shorter distances between donor and acceptor dyes while lower ET_{eff} reflect longer distances. In order to determine the peak ET_{eff} position, the ET_{eff} values were plotted as a histogram and fit with a sum of Gaussian distributions. Presented is the mean ET_{eff} obtained from fitting to reflect the average of tau's conformational ensemble for a given measurement.

Addition of $polyP_{300}$ resulted in a decreased ET_{eff} for both the 2N4R and 2N3R domains, reflecting an increase in end-to-end distance of tau. This result suggested that polyP disrupts long-range electrostatic interactions responsible for tau's relatively compact conformation ensemble in solution (Figure 24A). In contrast, addition of polyP caused a shift to higher ET_{eff} in constructs testing the PRR and MTBR region (Figure 24A, B). This result was confirmed in other constructs, including PRR alone, 2P-3R and 2P-4R as well as 4R and 3R (Figure 24B). P2-4R and P2-3R showed a similar effect although with smaller magnitude compared to the full length protein (Figure 24B). PolyP did not cause any significant shifts in the ET_{eff} values of the isolated MTBR fragments 4R and 3R despite the clear binding signal in the FCS measurements (Figure 24B). Comparison of full-length tau or the P2-4R and P2-3R constructs revealed a shift in their peaks towards the isolated MTBR fragments 4R and 3R, suggesting that these isolated domains already have a more compacted structure. In longer tau constructs, this compact structure seems only to be achievable with inducers like polyP. The PRR alone also shows compaction in the presence of polyP. These results are reminiscent of previous studies conducted with heparin (Elbaum-Garfinkle and Rhoades 2012), and suggest conserved features in the aggregation prone conformational ensemble that are sensitive to polyanionic inducers like polyP and heparin.

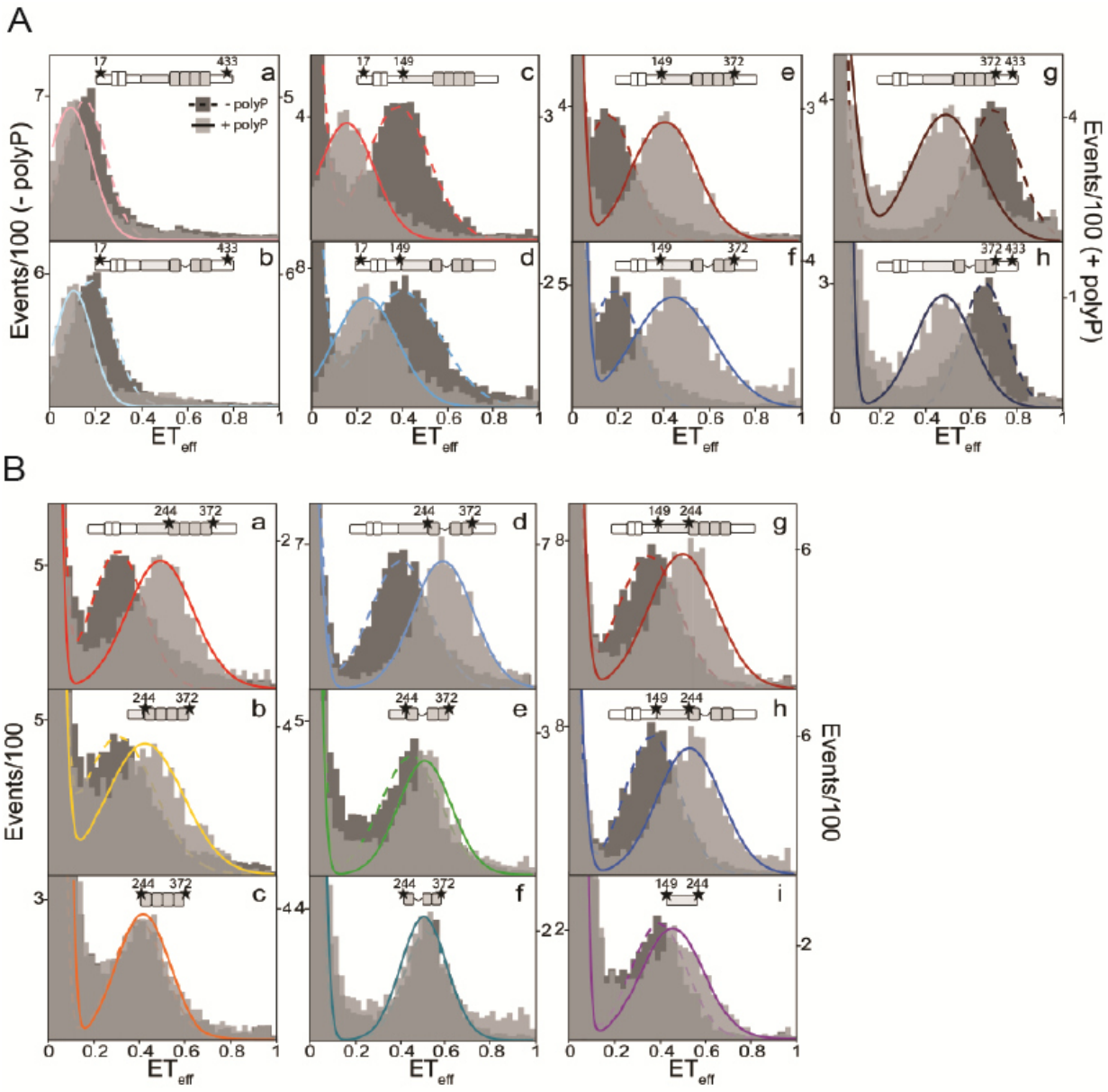

Figure 24: PolyP induces structural changes in tau including the compaction of the PRR and MTBR region and extending the end-to-end distances. *SmFRET histograms measured in the absence (dark gray and dashed lines) or presence of 20 µM polyP$_{300}$ (in Pi units) (light gray and solid lines). Labeling throughout the full length constructs 2N4R (upper row) and 2N3R (lower row) at positions at C17-433 (a, b), C17-C149 (c, d), C149-C372 (e, f) and C372-C433 (g, h). (A) and of the MTBR and PRR region with specific sites of C244-C372 in 2N4R (a), P2-4R (b), 4R (c), 2N3R (d), P23R (e) and 3R (f) and C149-C244 for 2N4R (g), 2N3R (h) and P1P2 (i) (B).Tau models above the respective histogram depict isoforms and labeling positions. Each experiment was repeated at least three times and shown histograms are representatives (Wickramasinghe, Lempart et al. 2019).*

5.10.3 PolyP differentially affects fiber formation of different tau isoforms

To test the effect of polyP induced structural changes towards different tau isoforms on their ability to form amyloids, I carried out ensemble of aggregation experiments, using the various MTBR isoforms including 3R and 4R and their PPR-containing counterparts 2P-3R and 2P-4R. I monitored fiber formation using ThT fluorescence and quantified via $T_{1/2}$. Consistent with previous findings that found the 4R fragment to be more aggregation prone than the 3R fragment (von Bergen, Friedhoff et al. 2000; Barghorn and Mandelkow 2002; Li and Lee 2006), I found that the 4R has a $T_{1/2}$ of 10 min in the presence of $polyP_{300}$ compared to the 3R fragment with a $T_{1/2}$ of 5 hours (Figure 25A, B). Presence of the 2R-region seemed to only affect the fiber formation of the 3R fragment, whose $T_{1/2}$ time was reduced from 4 hours to 1 hour in the presence of $polyP_{300}$. In contrast, the aggregation of the 2P-4R barely changed compared to the $T_{1/2}$ of 4R ($T_{1/2}$=10 min) (Figure 25A, B). Presence of $polyP_{14}$ caused the same trends although the $T_{1/2}$ were generally longer, ranging from 5 hours for the 4R up to 40 h for the 3R (Figure 25A, C). The significant difference between the $polyP_{14}$ and $polyP_{300}$ in this and previous experiments led us to test a wider range of polyP chain lengths and compare those to heparin (Figure 25D,E). The acceleration of the 4R domain had a strong chain length dependency with longer polyP chains ($polyP_{300}$) causing the shortest $T_{1/2}$ time. The half time of fiber formation gradually increased with the chain length from 1 hour in the presence of $polyP_{130}$, to 3 hours in the presence of $polyP_{60}$ and 6 hours when $polyP_{14}$ was added (Figure 25D). However, even the shortest polyP chain was more efficient in acceleration tau fiber formation than heparin, which led to a $T_{1/2}$ of 15 hours. We obtained very similar results with the 3R domain but the measured half times were overall longer (Figure 25E). These results together with the binding data support the conclusion that polyP binds to both the R2 and the PRR domain for most effective acceleration of aggregation. Moreover, they show that the aggregation-prone compaction of the MTBR is necessary but not sufficient for reaching maximal acceleration of fiber formation. Instead, a combination of induced structural changes and the scaffolding ability of polyP seem to be crucial for the observed accelerated fiber formation.

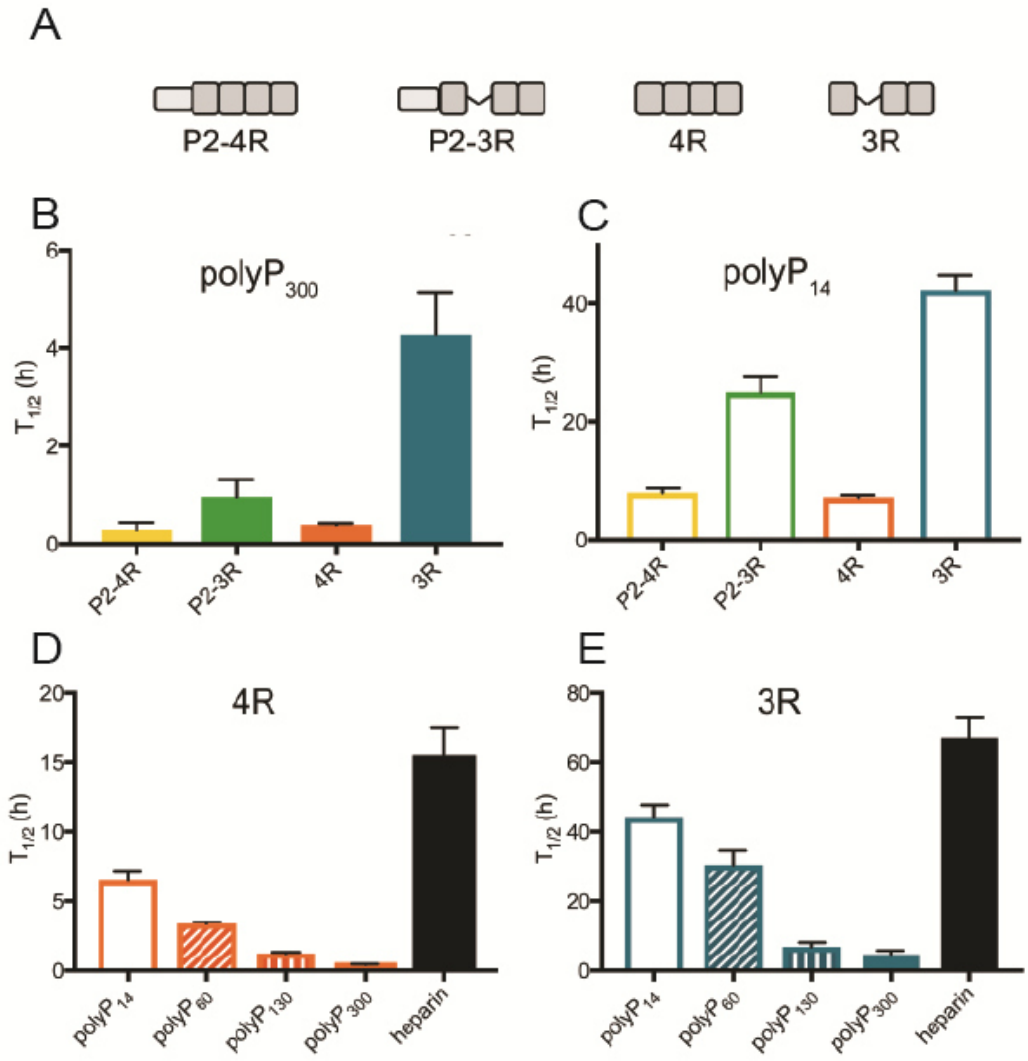

Figure 25: PolyP accelerates tau aggregation dependent on polyP chain length and different tau isoforms*. (A) Schematic of the tau constructs used for aggregation experiments. Fiber formation of 25 µM of different tau fragments P2-4R, P2-3R, 4R and 3R was measured in the presence of 1 mM of either polyP$_{300}$ (B) or polyP$_{14}$ (C) (in Pi units) via ThT fluorescence and the time to reach half the signal of the plateau ($T_{1/2}$) is displayed. For fragment 4R (D) and 3R (E) fiber formation in the presence of 1 mM of various polyP chain lengths (in Pi units) (14, 60, 130, 300) in comparison to charge matched heparin (18 µM) was tested. Experiments were repeated at least 3 times and data are shown +/- SD (Wickramasinghe, Lempart et al. 2019).*

5.10.4 The effect of polyP on tau structure is chain length dependent

Longer polyP chains bind more tightly to amyloids and are more effective in accelerating fiber formation. The Rhoades lab conducted smFRET measurements with distinct 2N4R constructs, monitoring either the NT region (C17-C149) or the

PRR and MTBR domain (C1490-C372) using $polyP_{14}$, $polyP_{60}$, $polyP_{130}$ and $polyP_{300}$ to investigate the effect of different chain length on the induction of structural changes in tau. $PolyP_{14}$ showed only a small increase in the ET_{eff} for the NT region and caused no change in the conformation of the PRR-MTBR domain. All other polyP chain lengths cause large shifts in the mean ET_{eff} for both, the NT and PRR-MTBR domain (Figure 26). This was a surprising observation given the fact that $polyP_{14}$ binds to the full length protein and isolated fragments and efficiently accelerates tau fiber formation (Figure 23 and 25). This experiment is consistent with our previous data on polyP chain length dependency, and suggests that long polyP chain are capable of inducing structural changes and potentially binding several monomers in a scaffolding fashion.

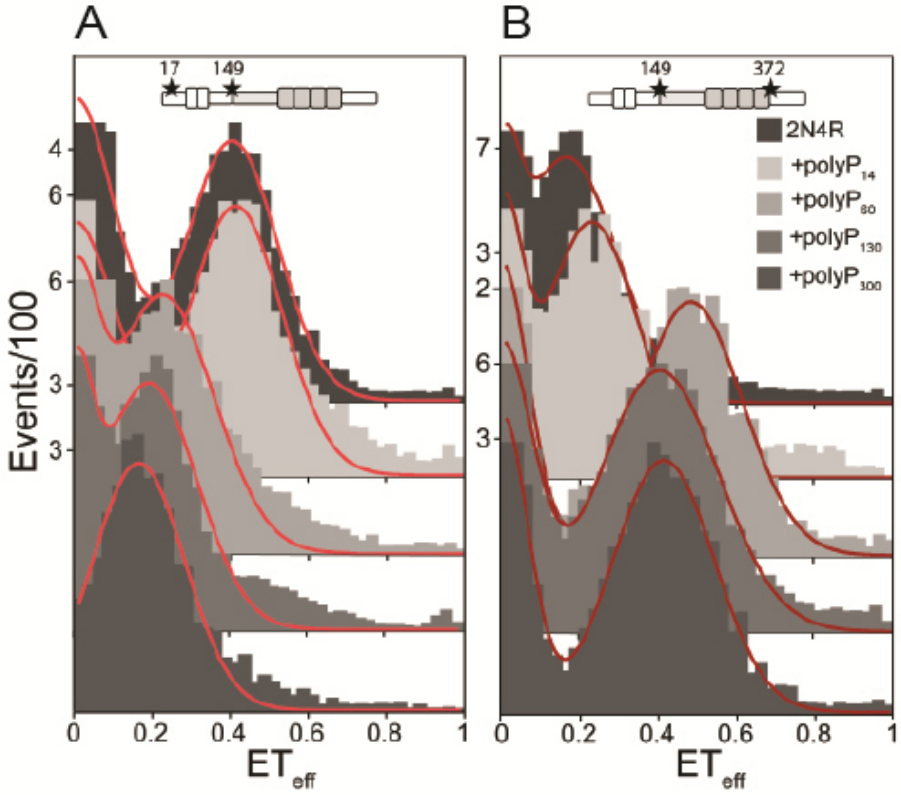

***Figure 26: Conformational changes of tau are polyP chain-length dependent**. SmFRET measurements of tau 2N4R labeled in the area of C17-C149 (A) or C149-C372 (B) in the absence or in the presence of 20 µM of different polyP chain length (14, 60, 130, 300). Experiments were repeated at least three times and representative histograms are shown (Wickramasinghe, Lempart et al. 2019).*

6 DISCUSSION

6.1 PolyP as a physiological modifier of amyloid formation

PolyP interacts with a multitude of different proteins. Dependent on the client protein, this interaction fulfills different functions. Gray et al. was the first to identify polyP as a protector against cellular stress by stabilizing unfolding proteins in a soluble β-sheet rich conformation (Gray, Wholey et al. 2014). Follow-up studies identified that polyP forms defined sized complexes with metastable folding intermediates, harboring amyloid-like features (Yoo, Dogra et al. 2018). By preventing irreversible protein aggregation, polyP even protects bacteria against extreme temperatures (Yoo, Dogra et al. 2018). In mammalian systems, polyP was shown to regulate blood coagulation through stabilizing proteins such as fibrin in a β-sheet like conformation (Litvinov, Faizullin et al. 2012). Although the exact mechanism for most of those interactions remains enigmatic, all of them share the common feature that polyP binding induces conformational changes and/or stabilizes certain structural features. The findings by Gray et al. ultimately led to the discovery of polyP's role in promoting the conversion of amyloidogenic peptides, like tau, Aβ and α-synuclein, into β-sheet rich fibrils. This activity suggested that polyP might serve as a modifier of neurodegeneration but leaves several mechanistic questions unanswered (Cremers, Knoefler et al. 2016). Studies investigating polyP induced amyloid fibril formation in amyloidosis suggest the underlying mechanism to lie in the ability of polyP to interaction with positively charged client proteins (Sasahara, Yamaguchi et al. 2019; Zhang, Yamaguchi et al. 2019). The group reasons that the charge neutralization leads to a structural destabilization that eventually causes the formation of amorphous aggregates once the solubility limit is reached (Sasahara, Yamaguchi et al. 2019; Zhang, Yamaguchi et al. 2019). However, the mechanistic idea that polyP interacts through charge is unable to explain the effect of polyP on proteins that lack positively charged amino acids (i.e. CsgA (Cremers, Knoefler et al. 2016)) and suggests that polyP might interact with the protein backbone (Cohlberg, Li et al. 2002). PolyP binding could then interfere with electrostatic interactions that otherwise stabilize amyloid monomers, making them more likely to undergo conformational rearrangements.

The degree to which polyP stimulated kinetics of fibril formation and fibril yield was highly dependent on the ability of the client protein to fibrillate on their own

(Cremers, Knoefler et al. 2016). Peptides like CsgA or Aβ, which are less responsive to the presence of polyP, are able to form fibrils rapidly and independently of any nucleators. On the other hand, fiber formation of tau and α-synuclein, which are unable to from fibrils in the absence of nucleators, were strongly dependent on polyP. In this work, I focused on those two proteins and was able to demonstrate that polyP has a different mechanism for α-synuclein fiber formation than it does for tau fiber formation. While polyP binds to tau monomers and induces structural changes that foster interactions and the formation of aggregation-competent oligomers, polyP does not interact with α-synuclein monomers (Figure 27). Instead, α-synuclein undergoes a concentration- and polyP independent nucleation step, which is necessary for binding to polyP (Figure 27).
Once the two interact, however, β-sheet-rich amyloids form that are structurally distinct from fibers formed in the absence of polyP. The initial rate limiting step of fibril formation is the conversion of a largely unfolded α-helical amyloid into a nucleation competent β-sheet conformation (Eichner and Radford 2011). Previous studies showed that α-synuclein forms ThT negative oligomers, which subsequently undergo conformational changes that lead to ThT positive oligomers and eventually fibers (Mehra, Ghosh et al. 2018). Results from this work suggest that polyP interacts with and scaffolds oligomers that are still ThT-negative, enabling the conversion into ThT positive oligomers and protofibrils (Figure 27). In support of this idea are previous studies, which showed that polyP does not promote the conversion of α-helical proteins into β-sheet structure but instead stabilizes folding intermediates once they have β-sheet conformation (Yoo, Dogra et al. 2018). Once polyP binds to β-sheet oligomers, it accelerates fiber formation through a variety of possible scenarios: polyP might serve as a scaffold, bringing several of these oligomeric species into close proximity and hence increasing the local concentration; alternatively, polyP's ability to induce structural rearrangement might make them prone to sequester additional monomers for fiber formation. It is also conceivable that polyP changes the balance within the reaction by pushing the equilibrium towards the formation of mature fibers. Further experiments have to be conducted to identify the exact mechanism of fiber elongation and the role that polyP plays in this process. Nevertheless, the fact that polyP affects fiber formation when added during any point of the process suggests continued and highly potent interactions of polyP with the amyloids.

In contrast to α-synuclein, polyP binds to tau monomers, inducing the compaction of the central MTBR and PRR domain and an elongation of end-to-end distances (Figure 27). Interestingly, the polyP-mediated compaction of the MTBR domain was only observed when the PRR was present as well. This effect is most likely due to polyP binding sites being present in both the PRR and the MTBR domains, causing noncovalent intramolecular cross-linking of tau monomers. Additionally, polyP could act as a scaffold bringing several monomeric or oligomeric species in close proximity, cross linking them and leading to accelerated amyloid formation (Figure 27). In support of this idea is the fact that longer polyP chains have a stronger effect on amyloid formation as they are capable of bringing more building blocks in close proximity.

However, the physiological effect of those acceleration mechanism as well as to what extent they serve a protective function of polyP *in vivo* stays enigmatic. With polyP being present in the intracellular and extracellular space in the brain (Holmstrom, Marina et al. 2013) it is conceivable that the molecule encounters both tau and α-synuclein *in vivo*. The lack of polyP- α-synuclein-monomer binding indicate that polyP only interacts with the peptide once toxicity has started and suggests that the protective effect only takes place under pathological conditions. Opposite to α-synuclein, polyP is capable of interacting with tau monomers suggesting an interaction of a different nature. In the healthy brain tau binds to microtubules, but when compromised by mutation or hyperphosphorylation, it could increase the cytoplasmatic pool available for polyP interaction marking the start of polyP dependent effects. Also possible is that polyP directly increases the amount of cytosolic tau by competing with microtubules for tau binding (Wickramasinghe, Lempart et al. 2019). Future studies are needed to answer these questions and identify whether tubulin-dissociated, polyP-bound tau isoforms might be a therapeutic target (Brunden, Trojanowski et al. 2009).

Overall, unraveling the mechanism of tau and α-synuclein fiber formation provides important insight on the influence of polyP in the context of neurodegeneration and builds the basis for future studies that need to investigate those effects in the context of a physiological system. This will ultimately help to identify polyP as a putative target to alter amyloid formation *in vivo*.

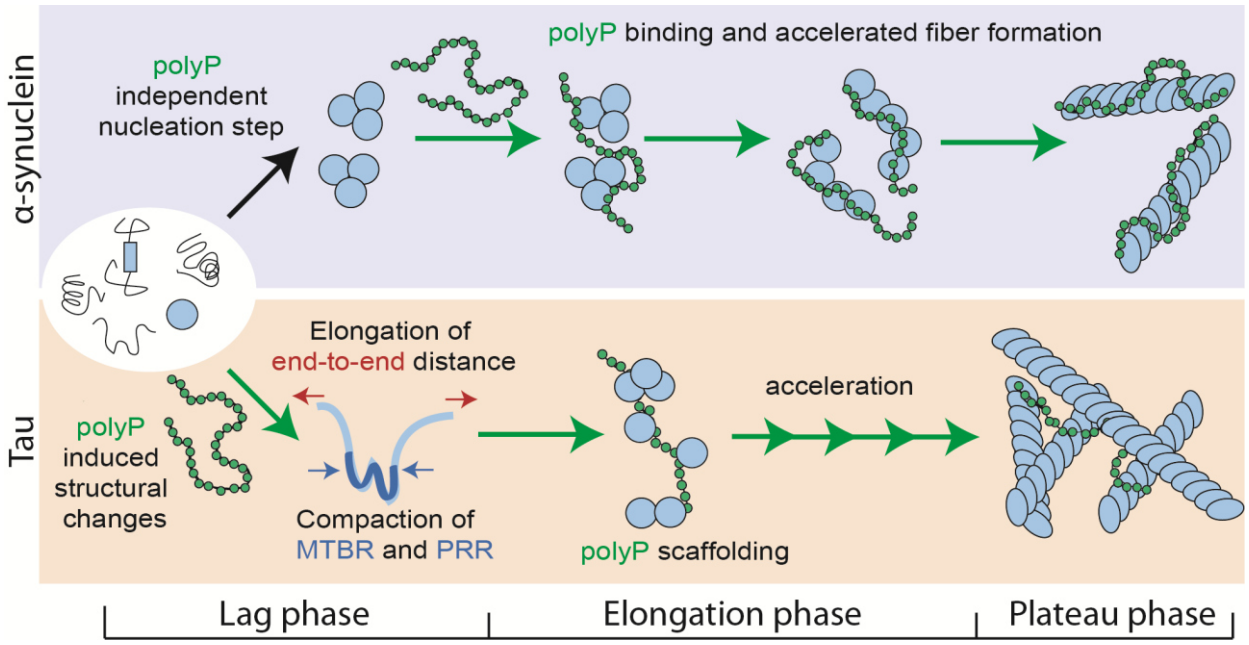

Figure 27: Model for the polyP induced accelerated fiber formation of α-synuclein and tau. *PolyP binds to amyloidogenic α-synuclein species after an initial polyP-independent step during the transition from lag phase to elongation phase. The interaction rapidly accelerates fiber formation and induces altered fiber morphology. Tau fiber formation is accelerated through polyP induced structural changes in the monomeric peptide and scaffolding of multiple monomers/oligomers.*

6.2 PolyP and its effects on amyloid fiber structure

The recently solved structure of α-synuclein fibrils revealed that two β-sheet containing monomers associate into protofibrils, which then interact with one another through salt bridges forming the characteristically twisted fibril (Figure 28) (Guerrero-Ferreira, Taylor et al. 2018). Dense, positively charged patches are located in the vicinity of the interface and run in parallel to the fibril axis. We now propose that polyP associates with the fibril, and interferes with the salt bridges at the interface of the two strands. This would cause dissociation of the protofibrils and explain the decreased fiber thickness that is observable when polyP is present during fiber formation or when the polyanion is added to the mature fibers. Additionally, I have found that the binding of polyP changes the packaging of β-sheet in the amyloid fibrils (Figure 11C-E) suggesting that the polyanion interaction might influence the orientation of individual peptides within the fibril strand.

The high affinity of polyP towards binding along the positively charged fibril strands would also explain polyP's low affinity for soluble α-synuclein monomers, and provide a rationale for the low binding stoichiometry of polyP binding to α-synuclein (5 Pi-units per one α-synuclein monomer). The fact that polyP can induce structural changes even after the fibers have formed is particularly interesting because it has previously been shown that fiber structure influences fiber stability, seeding capability, toxicity and the ability of oligomers to spread throughout the brain (Bousset, Pieri et al. 2013). This makes polyP a potential therapeutic target to treat neurodegenerative diseases.

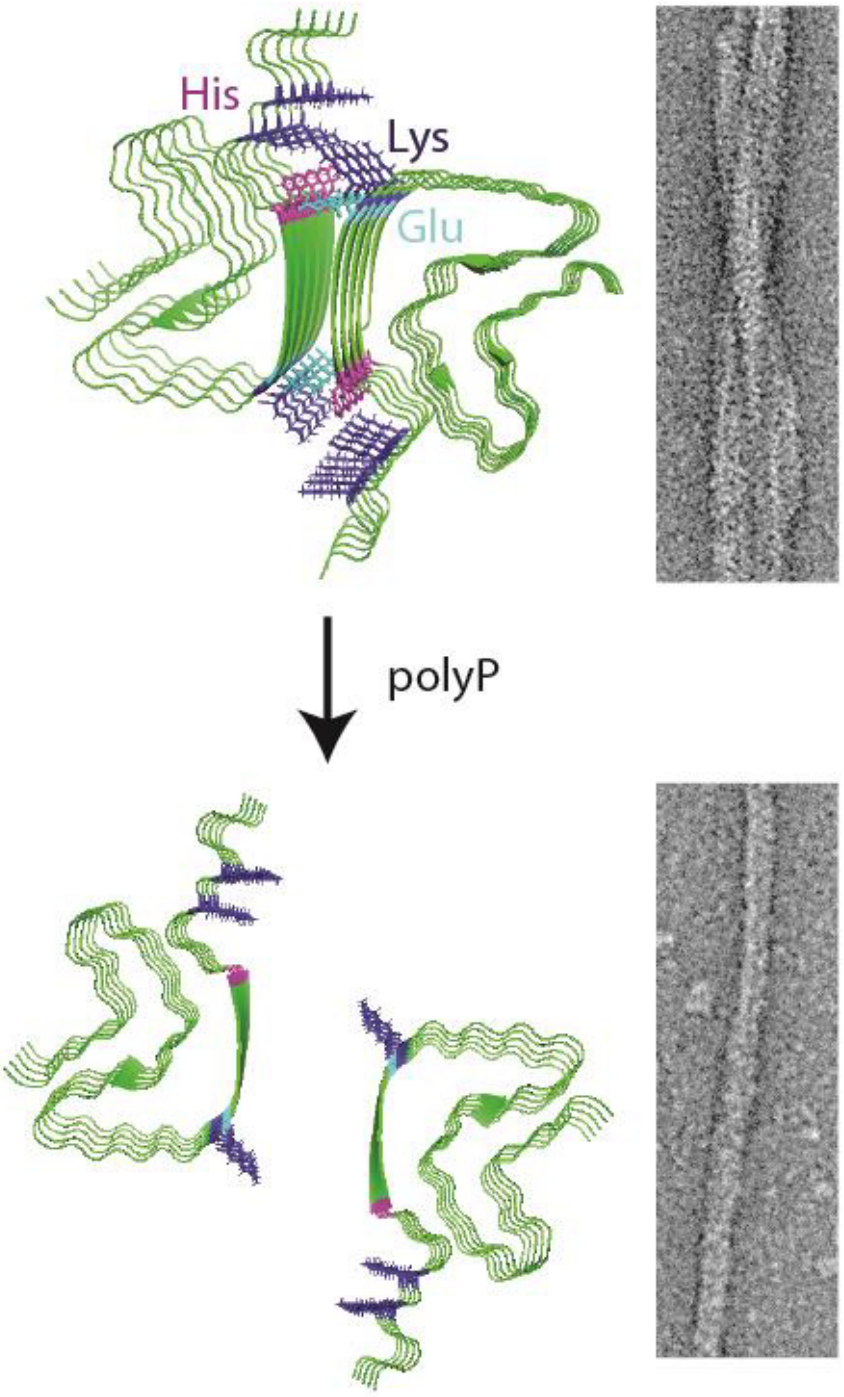

Figure 28: Comparison of the published α-synuclein fiber structured (PDB) and observed polyP-induced morphological changes (Guerrero-Ferreira, Taylor et al. 2018).

6.3 PolyP as a protector against α-synuclein toxicity – A mechanistic insight

Current therapies for neurodegeneration are limited to treating symptoms but not the cause (Szeto and Lewis 2016). With many aspects of the disease development remaining unknown, it is difficult to identify new drugs. One of the biggest risk factors of developing neurodegeneration is age. PolyP levels have previously been shown to decrease in the brain of rats with age (Lorenz, Munkner et al. 1997). Together with recent publications as well as our work, we propose a previously unrecognized connection between age-related decline in polyP and age-associated neurodegeneration (Cremers, Knoefler et al. 2016; Muller, Wang et al. 2017; Lempart, Tse et al. 2019). Several of polyP's physiological functions could be involved, including its role in energy homeostasis (Baev, Angelova et al. 2016; Wang, Schroder et al. 2016), apoptosis (Angelova, Baev et al. 2016) or a signaling molecule in the brain (Holmstrom, Marina et al. 2013) (Figure 7). As a highly energetic molecule, polyP has been associated with mitochondria and the energetic content of the cell (Hernandez-Ruiz, Gonzalez-Garcia et al. 2006; Baev, Angelova et al. 2016; Wang, Schroder et al. 2016). Both AD and PD pathology have been associated with defects in energy homeostasis. Whereas AD is characterized by altered energy levels in the brain tissue, familiar forms of PD show mitochondrial dysfunction that leads to changes in signal transition (Mounsey and Teismann 2010; Muller, Wang et al. 2017). And indeed, the group of Mueller et al identified that the protective effect of polyP against $A\beta_{25-35}$ toxicity lies in the ability of polyP to increase intracellular ATP levels and therefore reverse the β-amyloid-induced compromised energy status in neuronal cells (Muller, Wang et al. 2017). The increased energy can either originate from polyP directly or might be associated with its physiological role in energy homeostasis in mitochondria.

In vitro assays showed that the presence of polyP decreases the amount of nucleation and stabilizes the amyloid fibers in an altered conformation that is less prone to shed off toxic oligomers (Cremers, Knoefler et al. 2016). Over a time period of 48 hours, fibers formed in the presence of polyP only disassembles 60% in comparison to fibers formed in the absence of polyP (Cremers, Knoefler et al. 2016). The role of polyP as a glio-and neurotransmitter (Holmstrom, Marina et al. 2013) suggests its presence in the synaptic space where oligomers were shown to exert toxicity by inducing synapse damage (Yang, Li et al. 2017). One potential mechanism is that the formation of a polyP-oligomer complex prevents the toxic

interaction with the synaptosomes. It is also possible that the protective effect of polyP is due to the depletion of toxic oligomers from the synaptic sides by accelerating the formation of non-toxic mature fibers. Amyloids formed in the presence of polyP are in general more stable, less prone to shed off toxic intermediates and more susceptible to be degraded by proteases (Cremers, Knoefler et al. 2016). Apart from influencing the fibers and their toxicity directly, another explanation of the protective effect of polyP against amyloid toxicity could lie in its ability to influence the location, processing or turnover of the fibrils in a cellular context. A tremendous amount of recent publication identifies cell-to-cell spreading as one of the biggest contributing factors to the progression of neurodegenerative diseases (Braak and Braak 1991; Braak, Del Tredici et al. 2003; Braak, Muller et al. 2006; Jucker and Walker 2013; Guo and Lee 2014). In this work, I was able to show that increased extracellular polyP levels prevent the membrane association of α-syn$^{PFF\text{-}AF488}$ and reduce the internalization of the amyloid in cell culture experiments. The effect is highly specific for α-synuclein and polyP does not affect uptake of TAT-TAMRA. This result suggests that polyP might be capable of preventing cell-to-cell spreading of α-synuclein amyloids and reducing or preventing the prion-like propagation of α-synuclein induced toxicity. Previous studies using other negatively charged compounds, such as heparin, have shown that the negative charge is most likely the source of the uptake inhibition (Holmes, DeVos et al. 2013; Mehra, Ghosh et al. 2018). In our work, co-localization studies of polyP and α-synuclein revealed a similar mechanism and suggest that polyP binding to fibrils interfere with receptor binding (Nakase, Tadokoro et al. 2007; Holmes, DeVos et al. 2013; Gustafsson, Loov et al. 2018) (Figure 29).

Apart from binding and uptake of α-synuclein fibers through the heparan receptor, the literature reports amyloids to be capable of interacting with the cell membrane directly, leading to a destructive effect through interference with the integrity of the cell (Lashuel, Petre et al. 2002; Tsigelny, Sharikov et al. 2012). In addition, polyP-lipid interaction was reported to induce fiber formation process by serving as a nucleator for *de-novo* fiber formation (Galvagnion, Buell et al. 2015; Galvagnion, Brown et al. 2016). With polyP's ability to completely prevent the association of α-syn$^{PFF\text{-}AF488}$ with the cell membrane, it is possible that polyP protects against amyloid toxicity by blocking the fibers from binding, penetrating and damaging

membranes (Figure 29). A decreased association of the fibers to the membrane would inhibit the spreading of the toxicity throughout the brain and therefore the progression of the disease.

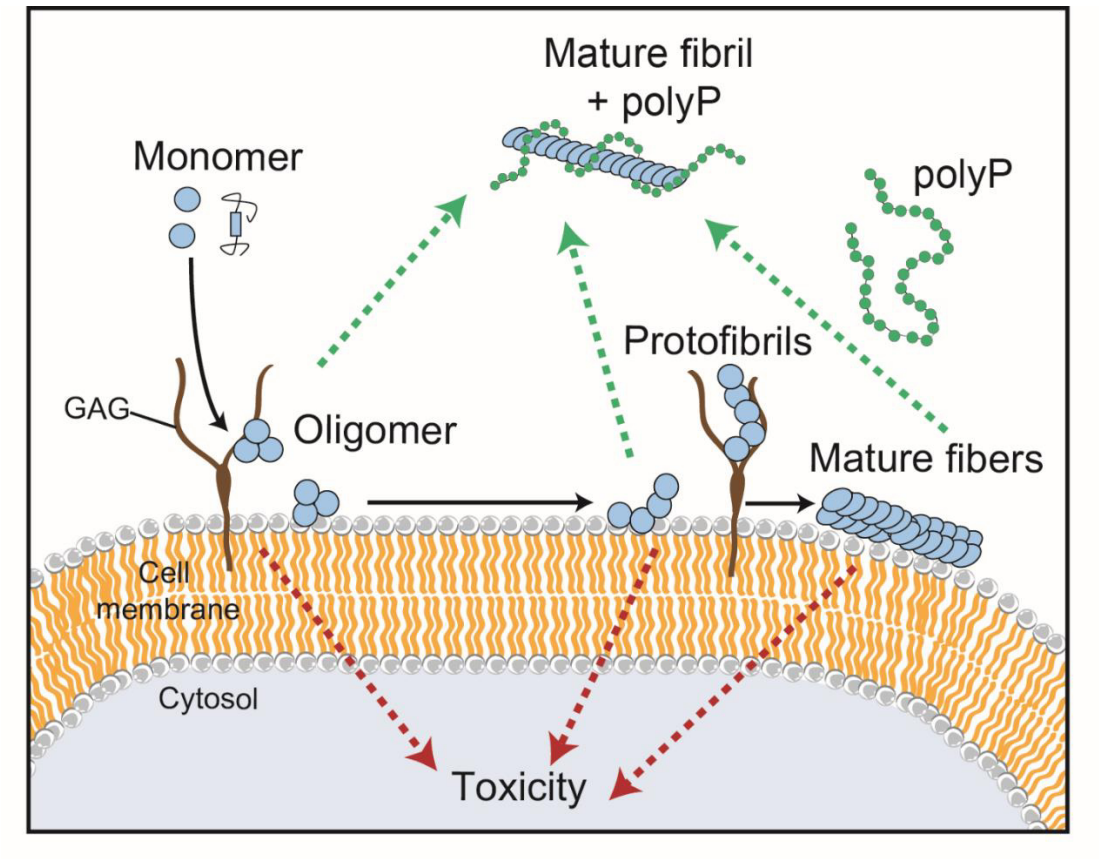

***Figure 29: Model for the uptake inhibition of polyP**. Oligomers, protofibrils and mature fibers interact with the cell membrane and GAG receptors and get internalized and spread toxicity. PolyP prevents the association with the membrane/receptors and supports formation of mature fibers with altered fiber morphology (Lempart, Tse et al. 2019).*

7 CONCLUSION

Accumulating evidence suggests that polyP serves as modifier of neurodegeneration and that age and/or disease-associated changes in polyP levels make the brain more susceptible to develop neurodegeneration (Hernandez-Ruiz, Gonzalez-Garcia et al. 2006; Holmstrom, Marina et al. 2013; Baev, Angelova et al. 2016). Studies on mice have reinforced this idea by showing that induction of an AD phenotypes leads to decreased polyP levels in their brains compared to their wildtype littermates (Cremers, Knoefler et al. 2016). This work started to unravel how polyP works and suggests that polyP supplementation might serve as a novel therapeutic strategy to prevent the cellular spreading of amyloidogenic α-synuclein. Studies using antibodies to prevent prion-like spreading show first success in rodent models (Schofield, Irving et al. 2019). With polyP being a physiological polymer that is already used as a food additive and considered to be safe for clinical application (Masters and Selkoe 2012; Muller, Tolba et al. 2015), this molecule could harbor several advantages over antibodies. Without knowing the cellular system responsible for polyP synthesis, however, many of the ideas remain speculations, and therapeutic attempts unapproachable. Nevertheless, this work builds the foundation for future studies by providing important insights into the mechanism of the protective effect of polyP against amyloid toxicity and insight into polyP induced fiber formation.

8 REFERENCES

Abramov, A. Y., C. Fraley, et al. (2007). "Targeted polyphosphatase expression alters mitochondrial metabolism and inhibits calcium-dependent cell death." Proc Natl Acad Sci U S A **104**(46): 18091-18096.

Abramowski, D., K. H. Wiederhold, et al. (2008). "Dynamics of Abeta turnover and deposition in different beta-amyloid precursor protein transgenic mouse models following gamma-secretase inhibition." J Pharmacol Exp Ther **327**(2): 411-424.

Akiyama, M., E. Crooke, et al. (1992). "The polyphosphate kinase gene of Escherichia coli. Isolation and sequence of the ppk gene and membrane location of the protein." J Biol Chem **267**(31): 22556-22561.

Alonso, A. C., I. Grundke-Iqbal, et al. (1996). "Alzheimer's disease hyperphosphorylated tau sequesters normal tau into tangles of filaments and disassembles microtubules." Nat Med **2**(7): 783-787.

Angelova, P. R., B. K. Agrawalla, et al. (2014). "In situ investigation of mammalian inorganic polyphosphate localization using novel selective fluorescent probes JC-D7 and JC-D8." ACS Chem Biol **9**(9): 2101-2110.

Angelova, P. R., A. Y. Baev, et al. (2016). "Role of inorganic polyphosphate in mammalian cells: from signal transduction and mitochondrial metabolism to cell death." Biochem Soc Trans **44**(1): 40-45.

Angelova, P. R., K. Z. Iversen, et al. (2018). "Signal transduction in astrocytes: Localization and release of inorganic polyphosphate." Glia.

Archibald, F. S. and I. Fridovich (1982). "Investigations of the state of the manganese in Lactobacillus plantarum." Arch Biochem Biophys **215**(2): 589-596.

Arvai, A. (2015). "A Program to Display X-ray Diffraction Images." from https://www.scripps.edu/tainer/arvai/adxv.html.

Baev, A. Y., P. R. Angelova, et al. (2016). Role of Inorganic Polyphosphate in the Cells of the Mammalian Brain. Inorganic Polyphosphates in Eukaryotic Cells. T. Kulakovskaya, E. Pavlov and E. N. Dedkova. Cham, Springer International Publishing**:** 115-121.

Ballatore, C., V. M. Lee, et al. (2007). "Tau-mediated neurodegeneration in Alzheimer's disease and related disorders." Nat Rev Neurosci **8**(9): 663-672.

Barghorn, S. and E. Mandelkow (2002). "Toward a unified scheme for the aggregation of tau into Alzheimer paired helical filaments." Biochemistry **41**(50): 14885-14896.

Bendor, J. T., T. P. Logan, et al. (2013). "The function of alpha-synuclein." Neuron **79**(6): 1044-1066.

Biancalana, M., K. Makabe, et al. (2009). "Molecular mechanism of thioflavin-T binding to the surface of beta-rich peptide self-assemblies." J Mol Biol **385**(4): 1052-1063.

Bousset, L., L. Pieri, et al. (2013). "Structural and functional characterization of two alpha-synuclein strains." Nat Commun **4**: 2575.

Braak, H. and E. Braak (1991). "Neuropathological stageing of Alzheimer-related changes." Acta Neuropathol **82**(4): 239-259.

Braak, H., K. Del Tredici, et al. (2003). "Staging of brain pathology related to sporadic Parkinson's disease." Neurobiol Aging **24**(2): 197-211.

Braak, H., C. M. Muller, et al. (2006). "Pathology associated with sporadic Parkinson's disease--where does it end?" J Neural Transm Suppl(70): 89-97.

Brandt, R., J. Leger, et al. (1995). "Interaction of tau with the neural plasma membrane mediated by tau's amino-terminal projection domain." J Cell Biol **131**(5): 1327-1340.

Brothers, H. M., M. L. Gosztyla, et al. (2018). "The Physiological Roles of Amyloid-beta Peptide Hint at New Ways to Treat Alzheimer's Disease." Front Aging Neurosci **10**: 118.

Bru, S., B. Samper-Martin, et al. (2017). "Polyphosphate is a key factor for cell survival after DNA damage in eukaryotic cells." DNA Repair (Amst) **57**: 171-178.

Brunden, K. R., J. Q. Trojanowski, et al. (2009). "Advances in tau-focused drug discovery for Alzheimer's disease and related tauopathies." Nat Rev Drug Discov **8**(10): 783-793.

Burchell, V. S., S. Gandhi, et al. (2010). "Targeting mitochondrial dysfunction in neurodegenerative disease: Part I." Expert Opin Ther Targets **14**(4): 369-385.

Burchell, V. S., S. Gandhi, et al. (2010). "Targeting mitochondrial dysfunction in neurodegenerative disease: Part II." Expert Opin Ther Targets **14**(5): 497-511.

Burre, J., M. Sharma, et al. (2010). "Alpha-synuclein promotes SNARE-complex assembly in vivo and in vitro." Science **329**(5999): 1663-1667.

Castuma, C. E., R. Huang, et al. (1995). "Inorganic polyphosphates in the acquisition of competence in Escherichia coli." J Biol Chem **270**(22): 12980-12983.

Chen, S. W., S. Drakulic, et al. (2015). "Structural characterization of toxic oligomers that are kinetically trapped during alpha-synuclein fibril formation." Proc Natl Acad Sci U S A **112**(16): E1994-2003.

Choi, B. K., M. G. Choi, et al. (2013). "Large alpha-synuclein oligomers inhibit neuronal SNARE-mediated vesicle docking." Proc Natl Acad Sci U S A **110**(10): 4087-4092.

Choi, S. H., J. N. Collins, et al. (2010). "Phosphoramidate end labeling of inorganic polyphosphates: facile manipulation of polyphosphate for investigating and modulating its biological activities." Biochemistry **49**(45): 9935-9941.

Christ, J. J. and L. M. Blank (2018). "Enzymatic quantification and length determination of polyphosphate down to a chain length of two." Anal Biochem **548**: 82-90.

Chung, J. A. and J. L. Cummings (2000). "Neurobehavioral and neuropsychiatric symptoms in Alzheimer's disease: characteristics and treatment." Neurol Clin **18**(4): 829-846.

Cohlberg, J. A., J. Li, et al. (2002). "Heparin and other glycosaminoglycans stimulate the formation of amyloid fibrils from alpha-synuclein in vitro." Biochemistry **41**(5): 1502-1511.

Costanzo, M. and C. Zurzolo (2013). "The cell biology of prion-like spread of protein aggregates: mechanisms and implication in neurodegeneration." Biochem J **452**(1): 1-17.

Cremers, C. M., D. Knoefler, et al. (2016). "Polyphosphate: A Conserved Modifier of Amyloidogenic Processes." Mol Cell **63**(5): 768-780.

CROMPTON, M. (1999). "The mitochondrial permeability transition pore and its role in cell death." Biochemical Journal **341**(2): 233-249.

Cuervo, A. M., L. Stefanis, et al. (2004). "Impaired degradation of mutant alpha-synuclein by chaperone-mediated autophagy." Science **305**(5688): 1292-1295.

Danzer, K. M., L. R. Kranich, et al. (2012). "Exosomal cell-to-cell transmission of alpha synuclein oligomers." Mol Neurodegener **7**: 42.

Danzer, K. M., S. K. Krebs, et al. (2009). "Seeding induced by alpha-synuclein oligomers provides evidence for spreading of alpha-synuclein pathology." J Neurochem **111**(1): 192-203.

Dawson, T. M. (2000). "New Animal Models for Parkinson's Disease." Cell **101**(2): 115-118.

Derisbourg, M., C. Leghay, et al. (2015). "Role of the Tau N-terminal region in microtubule stabilization revealed by new endogenous truncated forms." Sci Rep **5**: 9659.

Dinarvand, P., S. M. Hassanian, et al. (2014). "Polyphosphate amplifies proinflammatory responses of nuclear proteins through interaction with receptor for advanced glycation end products and P2Y1 purinergic receptor." Blood **123**(6): 935-945.

Diogenes, M. J., R. B. Dias, et al. (2012). "Extracellular alpha-synuclein oligomers modulate synaptic transmission and impair LTP via NMDA-receptor activation." J Neurosci **32**(34): 11750-11762.

Docampo, R., V. Jimenez, et al. (2011). "The role of acidocalcisomes in the stress response of Trypanosoma cruzi." Adv Parasitol **75**: 307-324.

Domert, J., C. Sackmann, et al. (2016). "Aggregated Alpha-Synuclein Transfer Efficiently between Cultured Human Neuron-Like Cells and Localize to Lysosomes." PLoS One **11**(12): e0168700.

Dunnett, S. B. and A. Björklund (1999). "Prospects for new restorative and neuroprotective treatments in Parkinson's disease." Nature **399**(6738): A32-A39.

Eichner, T. and S. E. Radford (2011). "A diversity of assembly mechanisms of a generic amyloid fold." Mol Cell **43**(1): 8-18.

Elbaum-Garfinkle, S. and E. Rhoades (2012). "Identification of an aggregation-prone structure of tau." J Am Chem Soc **134**(40): 16607-16613.

Gabel, N. W. and V. Thomas (1971). "Evidence for the occurrence and distribution of inorganic polyphosphates in vertebrate tissues." J Neurochem **18**(7): 1229-1242.

Galvagnion, C., J. W. Brown, et al. (2016). "Chemical properties of lipids strongly affect the kinetics of the membrane-induced aggregation of alpha-synuclein." Proc Natl Acad Sci U S A **113**(26): 7065-7070.

Galvagnion, C., A. K. Buell, et al. (2015). "Lipid vesicles trigger alpha-synuclein aggregation by stimulating primary nucleation." Nat Chem Biol **11**(3): 229-234.

George, J. M., H. Jin, et al. (1995). "Characterization of a novel protein regulated during the critical period for song learning in the zebra finch." Neuron **15**(2): 361-372.

Giehm, L. and D. E. Otzen (2010). "Strategies to increase the reproducibility of protein fibrillization in plate reader assays." Anal Biochem **400**(2): 270-281.

Goedert, M., R. Jakes, et al. (1996). "Assembly of microtubule-associated protein tau into Alzheimer-like filaments induced by sulphated glycosaminoglycans." Nature **383**(6600): 550-553.

Goedert, M., M. G. Spillantini, et al. (1989). "Multiple isoforms of human microtubule-associated protein tau: sequences and localization in neurofibrillary tangles of Alzheimer's disease." Neuron **3**(4): 519-526.

Goode, B. L., M. Chau, et al. (2000). "Structural and functional differences between 3-repeat and 4-repeat tau isoforms. Implications for normal tau function and the onset of neurodegenetative disease." J Biol Chem **275**(49): 38182-38189.

Gray, M. J., W. Y. Wholey, et al. (2014). "Polyphosphate is a primordial chaperone." Mol Cell **53**(5): 689-699.

Guerrero-Ferreira, R., N. M. Taylor, et al. (2018). "Cryo-EM structure of alpha-synuclein fibrils." Elife **7**.

Guo, J. L. and V. M. Lee (2014). "Cell-to-cell transmission of pathogenic proteins in neurodegenerative diseases." Nat Med **20**(2): 130-138.

Gustafsson, G., C. Loov, et al. (2018). "Secretion and Uptake of alpha-Synuclein Via Extracellular Vesicles in Cultured Cells." Cell Mol Neurobiol **38**(8): 1539-1550.

Hansen, C., E. Angot, et al. (2011). "alpha-Synuclein propagates from mouse brain to grafted dopaminergic neurons and seeds aggregation in cultured human cells." J Clin Invest **121**(2): 715-725.

Hawkes, C. H., K. Del Tredici, et al. (2010). "A timeline for Parkinson's disease." Parkinsonism Relat Disord **16**(2): 79-84.

Hed, J., G. Hallden, et al. (1987). "The use of fluorescence quenching in flow cytofluorometry to measure the attachment and ingestion phases in phagocytosis in peripheral blood without prior cell separation." J Immunol Methods **101**(1): 119-125.

Helzner, E. P., N. Scarmeas, et al. (2008). "Survival in Alzheimer disease: a multiethnic, population-based study of incident cases." Neurology **71**(19): 1489-1495.

Hernandez-Ruiz, L., I. Gonzalez-Garcia, et al. (2006). "Inorganic polyphosphate and specific induction of apoptosis in human plasma cells." Haematologica **91**(9): 1180-1186.

Heuck, C. C., U. Schiele, et al. (1985). "The role of surface charge on the accelerating action of heparin on the antithrombin III-inhibited activity of alpha-thrombin." J Biol Chem **260**(8): 4598-4603.

Holmes, B. B., S. L. DeVos, et al. (2013). "Heparan sulfate proteoglycans mediate internalization and propagation of specific proteopathic seeds." Proc Natl Acad Sci U S A **110**(33): E3138-3147.

Holmstrom, K. M., N. Marina, et al. (2013). "Signalling properties of inorganic polyphosphate in the mammalian brain." Nat Commun **4**: 1362.

Hoyer, W., T. Antony, et al. (2002). "Dependence of alpha-synuclein aggregate morphology on solution conditions." J Mol Biol **322**(2): 383-393.

Hufnagel, D. A., C. Tukel, et al. (2013). "Disease to dirt: the biology of microbial amyloids." PLoS Pathog **9**(11): e1003740.

Ingelsson, M., H. Fukumoto, et al. (2004). "Early Abeta accumulation and progressive synaptic loss, gliosis, and tangle formation in AD brain." Neurology **62**(6): 925-931.

Iwai, A., E. Masliah, et al. (1995). "The precursor protein of non-A beta component of Alzheimer's disease amyloid is a presynaptic protein of the central nervous system." Neuron **14**(2): 467-475.

Jain, N., K. Bhasne, et al. (2013). "Structural and dynamical insights into the membrane-bound alpha-synuclein." PLoS One **8**(12): e83752.

Jakes, R., M. G. Spillantini, et al. (1994). "Identification of two distinct synucleins from human brain." FEBS Lett **345**(1): 27-32.

Jameson, D. M. and J. C. Croney (2003). "Fluorescence polarization: past, present and future." Comb Chem High Throughput Screen **6**(3): 167-173.

Jimenez-Nunez, M. D., D. Moreno-Sanchez, et al. (2012). "Myeloma cells contain high levels of inorganic polyphosphate which is associated with nucleolar transcription." Haematologica **97**(8): 1264-1271.

Jucker, M. and L. C. Walker (2013). "Self-propagation of pathogenic protein aggregates in neurodegenerative diseases." Nature **501**(7465): 45-51.

Kamp, F., N. Exner, et al. (2010). "Inhibition of mitochondrial fusion by alpha-synuclein is rescued by PINK1, Parkin and DJ-1." EMBO J **29**(20): 3571-3589.

Kaplan, I. M., J. S. Wadia, et al. (2005). "Cationic TAT peptide transduction domain enters cells by macropinocytosis." J Control Release **102**(1): 247-253.

Karpowicz, R. J., Jr., C. M. Haney, et al. (2017). "Selective imaging of internalized proteopathic alpha-synuclein seeds in primary neurons reveals mechanistic insight into transmission of synucleinopathies." J Biol Chem **292**(32): 13482-13497.

Keasling, J. D., L. Bertsch, et al. (1993). "Guanosine pentaphosphate phosphohydrolase of Escherichia coli is a long-chain exopolyphosphatase." Proc Natl Acad Sci U S A **90**(15): 7029-7033.

Kellogg, E. H., N. M. A. Hejab, et al. (2018). "Near-atomic model of microtubule-tau interactions." Science **360**(6394): 1242-1246.
Kempf, M., A. Clement, et al. (1996). "Tau binds to the distal axon early in development of polarity in a microtubule- and microfilament-dependent manner." J Neurosci **16**(18): 5583-5592.
Kim, D. and E. J. Cavanaugh (2007). "Requirement of a soluble intracellular factor for activation of transient receptor potential A1 by pungent chemicals: role of inorganic polyphosphates." J Neurosci **27**(24): 6500-6509.
Kordower, J. H., Y. Chu, et al. (2008). "Lewy body-like pathology in long-term embryonic nigral transplants in Parkinson's disease." Nat Med **14**(5): 504-506.
Kornberg, A. (1999). "Inorganic polyphosphate: a molecule of many functions." Prog Mol Subcell Biol **23**: 1-18.
Kornberg, A., N. N. Rao, et al. (1999). "Inorganic polyphosphate: a molecule of many functions." Annu Rev Biochem **68**: 89-125.
Krebs, M. R., E. H. Bromley, et al. (2005). "The binding of thioflavin-T to amyloid fibrils: localisation and implications." J Struct Biol **149**(1): 30-37.
Kruger, R., W. Kuhn, et al. (1998). "Ala30Pro mutation in the gene encoding alpha-synuclein in Parkinson's disease." Nat Genet **18**(2): 106-108.
Kulaev, I. S. and V. M. Vagabov (1983). "Polyphosphate metabolism in micro-organisms." Adv Microb Physiol **24**: 83-171.
Kulakovskaya, T. V., V. M. Vagabov, et al. (2012). "Inorganic polyphosphate in industry, agriculture and medicine: Modern state and outlook." Process Biochemistry **47**(1): 1-10.
Kumble, K. D. and A. Kornberg (1995). "Inorganic polyphosphate in mammalian cells and tissues." J Biol Chem **270**(11): 5818-5822.
LaPointe, N. E., G. Morfini, et al. (2009). "The amino terminus of tau inhibits kinesin-dependent axonal transport: implications for filament toxicity." J Neurosci Res **87**(2): 440-451.
Lasagna-Reeves, C. A., D. L. Castillo-Carranza, et al. (2012). "Alzheimer brain-derived tau oligomers propagate pathology from endogenous tau." Sci Rep **2**: 700.
Lasagna-Reeves, C. A., D. L. Castillo-Carranza, et al. (2012). "Identification of oligomers at early stages of tau aggregation in Alzheimer's disease." FASEB J **26**(5): 1946-1959.
Lashuel, H. A., B. M. Petre, et al. (2002). "Alpha-synuclein, especially the Parkinson's disease-associated mutants, forms pore-like annular and tubular protofibrils." J Mol Biol **322**(5): 1089-1102.
Lee, H. J., J. E. Suk, et al. (2010). "Direct transfer of alpha-synuclein from neuron to astroglia causes inflammatory responses in synucleinopathies." J Biol Chem **285**(12): 9262-9272.
Lempart, J. and U. Jakob (2019). "Role of Polyphosphate in Amyloidogenic Processes." Cold Spring Harb Perspect Biol.
Lempart, J., E. Tse, et al. (2019). "Mechanistic insights into the protective roles of polyphosphate against amyloid cytotoxicity." Life Sci Alliance **2**(5).
Li, J. Y., E. Englund, et al. (2008). "Lewy bodies in grafted neurons in subjects with Parkinson's disease suggest host-to-graft disease propagation." Nat Med **14**(5): 501-503.
Li, W. and V. M. Lee (2006). "Characterization of two VQIXXK motifs for tau fibrillization in vitro." Biochemistry **45**(51): 15692-15701.
Litvinov, R. I., D. A. Faizullin, et al. (2012). "The alpha-helix to beta-sheet transition in stretched and compressed hydrated fibrin clots." Biophys J **103**(5): 1020-1027.
Loike, J. D. and S. C. Silverstein (1983). "A fluorescence quenching technique using trypan blue to differentiate between attached and ingested glutaraldehyde-fixed

red blood cells in phagocytosing murine macrophages." J Immunol Methods **57**(1-3): 373-379.
Lorenz, B., J. Munkner, et al. (1997). "Changes in metabolism of inorganic polyphosphate in rat tissues and human cells during development and apoptosis." Biochim Biophys Acta **1335**(1-2): 51-60.
Luk, K. C., V. Kehm, et al. (2012). "Pathological alpha-synuclein transmission initiates Parkinson-like neurodegeneration in nontransgenic mice." Science **338**(6109): 949-953.
Luk, K. C., V. M. Kehm, et al. (2012). "Intracerebral inoculation of pathological alpha-synuclein initiates a rapidly progressive neurodegenerative alpha-synucleinopathy in mice." J Exp Med **209**(5): 975-986.
Luk, K. C., C. Song, et al. (2009). "Exogenous alpha-synuclein fibrils seed the formation of Lewy body-like intracellular inclusions in cultured cells." Proc Natl Acad Sci U S A **106**(47): 20051-20056.
Masters, C. L. and D. J. Selkoe (2012). "Biochemistry of amyloid beta-protein and amyloid deposits in Alzheimer disease." Cold Spring Harb Perspect Med **2**(6): a006262.
Masuda-Suzukake, M., T. Nonaka, et al. (2013). "Prion-like spreading of pathological alpha-synuclein in brain." Brain **136**(Pt 4): 1128-1138.
Mehra, S., D. Ghosh, et al. (2018). "Glycosaminoglycans have variable effects on alpha-synuclein aggregation and differentially affect the activities of the resulting amyloid fibrils." J Biol Chem **293**(34): 12975-12991.
Morfini, G. A., M. Burns, et al. (2009). "Axonal transport defects in neurodegenerative diseases." J Neurosci **29**(41): 12776-12786.
Morrissey, J. H., S. H. Choi, et al. (2012). "Polyphosphate: an ancient molecule that links platelets, coagulation, and inflammation." Blood **119**(25): 5972-5979.
Mounsey, R. B. and P. Teismann (2010). "Mitochondrial dysfunction in Parkinson's disease: pathogenesis and neuroprotection." Parkinsons Dis **2011**: 617472.
Mulcahy, L. A., R. C. Pink, et al. (2014). "Routes and mechanisms of extracellular vesicle uptake." J Extracell Vesicles **3**.
Mullan, A., J. P. Quinn, et al. (2002). "A nonradioactive method for the assay of polyphosphate kinase activity and its application in the study of polyphosphate metabolism in Burkholderia cepacia." Anal Biochem **308**(2): 294-299.
Muller, F., N. J. Mutch, et al. (2009). "Platelet polyphosphates are proinflammatory and procoagulant mediators in vivo." Cell **139**(6): 1143-1156.
Muller, W. E., E. Tolba, et al. (2015). "Retinol encapsulated into amorphous Ca(2+) polyphosphate nanospheres acts synergistically in MC3T3-E1 cells." Eur J Pharm Biopharm **93**: 214-223.
Muller, W. E. G., S. Wang, et al. (2017). "Rebalancing beta-Amyloid-Induced Decrease of ATP Level by Amorphous Nano/Micro Polyphosphate: Suppression of the Neurotoxic Effect of Amyloid beta-Protein Fragment 25-35." Int J Mol Sci **18**(10).
Naiki, H., K. Higuchi, et al. (1989). "Fluorometric determination of amyloid fibrils in vitro using the fluorescent dye, thioflavin T1." Anal Biochem **177**(2): 244-249.
Nakamura, K., V. M. Nemani, et al. (2011). "Direct membrane association drives mitochondrial fission by the Parkinson disease-associated protein alpha-synuclein." J Biol Chem **286**(23): 20710-20726.
Nakase, I., A. Tadokoro, et al. (2007). "Interaction of arginine-rich peptides with membrane-associated proteoglycans is crucial for induction of actin organization and macropinocytosis." Biochemistry **46**(2): 492-501.
Ohi, M., Y. Li, et al. (2004). "Negative Staining and Image Classification - Powerful Tools in Modern Electron Microscopy." Biol Proced Online **6**: 23-34.

Outeiro, T. F. and S. Lindquist (2003). "Yeast cells provide insight into alpha-synuclein biology and pathobiology." Science **302**(5651): 1772-1775.

Panda, D., J. C. Samuel, et al. (2003). "Differential regulation of microtubule dynamics by three- and four-repeat tau: implications for the onset of neurodegenerative disease." Proc Natl Acad Sci U S A **100**(16): 9548-9553.

Paumier, K. L., K. C. Luk, et al. (2015). "Intrastriatal injection of pre-formed mouse alpha-synuclein fibrils into rats triggers alpha-synuclein pathology and bilateral nigrostriatal degeneration." Neurobiol Dis **82**: 185-199.

Pavlov, E., E. Zakharian, et al. (2005). "A large, voltage-dependent channel, isolated from mitochondria by water-free chloroform extraction." Biophys J **88**(4): 2614-2625.

Pick, U. and M. Weiss (1991). "Polyphosphate Hydrolysis within Acidic Vacuoles in Response to Amine-Induced Alkaline Stress in the Halotolerant Alga Dunaliella salina." Plant Physiol **97**(3): 1234-1240.

Pokhrel, A., J. C. Lingo, et al. (2019). "Assaying for Inorganic Polyphosphate in Bacteria." J Vis Exp(143).

Polymeropoulos, M. H., C. Lavedan, et al. (1997). "Mutation in the alpha-synuclein gene identified in families with Parkinson's disease." Science **276**(5321): 2045-2047.

Puig, K. L. and C. K. Combs (2013). "Expression and function of APP and its metabolites outside the central nervous system." Exp Gerontol **48**(7): 608-611.

Rao, N. N., M. R. Gomez-Garcia, et al. (2009). "Inorganic polyphosphate: essential for growth and survival." Annu Rev Biochem **78**: 605-647.

Rashid, M. H., N. N. Rao, et al. (2000). "Inorganic polyphosphate is required for motility of bacterial pathogens." J Bacteriol **182**(1): 225-227.

Rashid, M. H., K. Rumbaugh, et al. (2000). "Polyphosphate kinase is essential for biofilm development, quorum sensing, and virulence of Pseudomonas aeruginosa." Proc Natl Acad Sci U S A **97**(17): 9636-9641.

Rasola, A. and P. Bernardi (2011). "Mitochondrial permeability transition in Ca(2+)-dependent apoptosis and necrosis." Cell Calcium **50**(3): 222-233.

Reisberg, B., J. Borenstein, et al. (1987). "Behavioral symptoms in Alzheimer's disease: phenomenology and treatment." J Clin Psychiatry **48 Suppl**: 9-15.

Reusch, R. N. and H. L. Sadoff (1988). "Putative structure and functions of a poly-beta-hydroxybutyrate/calcium polyphosphate channel in bacterial plasma membranes." Proc Natl Acad Sci U S A **85**(12): 4176-4180.

Reyes, J. F., T. T. Olsson, et al. (2015). "A cell culture model for monitoring alpha-synuclein cell-to-cell transfer." Neurobiol Dis **77**: 266-275.

Sakatani, A., M. Fujiya, et al. (2016). "Polyphosphate Derived from Lactobacillus brevis Inhibits Colon Cancer Progression Through Induction of Cell Apoptosis." Anticancer Res **36**(2): 591-598.

Santarella, R. A., G. Skiniotis, et al. (2004). "Surface-decoration of microtubules by human tau." J Mol Biol **339**(3): 539-553.

Sasahara, K., K. Yamaguchi, et al. (2019). "Polyphosphates diminish solubility of a globular protein and thereby promote amyloid aggregation." J Biol Chem.

Savage, M. J., S. P. Trusko, et al. (1998). "Turnover of amyloid beta-protein in mouse brain and acute reduction of its level by phorbol ester." J Neurosci **18**(5): 1743-1752.

Schofield, D. J., L. Irving, et al. (2019). "Preclinical development of a high affinity alpha-synuclein antibody, MEDI1341, that can enter the brain, sequester extracellular alpha-synuclein and attenuate alpha-synuclein spreading in vivo." Neurobiol Dis: 104582.

Seidlmayer, L. K., M. R. Gomez-Garcia, et al. (2012). "Inorganic polyphosphate is a potent activator of the mitochondrial permeability transition pore in cardiac myocytes." J Gen Physiol **139**(5): 321-331.

Selkoe, D. J. (1991). "The molecular pathology of Alzheimer's disease." Neuron **6**(4): 487-498.

Selkoe, D. J. (2002). "Alzheimer's disease is a synaptic failure." Science **298**(5594): 789-791.

Shoffner, S. K. and S. Schnell (2016). "Estimation of the lag time in a subsequent monomer addition model for fibril elongation." Phys Chem Chem Phys **18**(31): 21259-21268.

Soto, C. (2003). "Unfolding the role of protein misfolding in neurodegenerative diseases." Nat Rev Neurosci **4**(1): 49-60.

Spillantini, M. G., M. L. Schmidt, et al. (1997). "α-Synuclein in Lewy bodies." Nature **388**(6645): 839-840.

Stotz, S. C., L. O. Scott, et al. (2014). "Inorganic polyphosphate regulates neuronal excitability through modulation of voltage-gated channels." Mol Brain **7**: 42.

Szeto, J. Y. and S. J. Lewis (2016). "Current Treatment Options for Alzheimer's Disease and Parkinson's Disease Dementia." Curr Neuropharmacol **14**(4): 326-338.

Tipping, K. W., T. K. Karamanos, et al. (2015). "pH-induced molecular shedding drives the formation of amyloid fibril-derived oligomers." Proc Natl Acad Sci U S A **112**(18): 5691-5696.

Tomoda, H., Y. Kishimoto, et al. (1989). "Temperature effect on endocytosis and exocytosis by rabbit alveolar macrophages." J Biol Chem **264**(26): 15445-15450.

Tran, H. T., C. H. Chung, et al. (2014). "Alpha-synuclein immunotherapy blocks uptake and templated propagation of misfolded alpha-synuclein and neurodegeneration." Cell Rep **7**(6): 2054-2065.

Trexler, A. J. and E. Rhoades (2010). "Single molecule characterization of alpha-synuclein in aggregation-prone states." Biophys J **99**(9): 3048-3055.

Tsigelny, I. F., Y. Sharikov, et al. (2012). "Role of alpha-synuclein penetration into the membrane in the mechanisms of oligomer pore formation." FEBS J **279**(6): 1000-1013.

Unal-Cevik, I., Y. Gursoy-Ozdemir, et al. (2011). "Alpha-synuclein aggregation induced by brief ischemia negatively impacts neuronal survival in vivo: a study in [A30P]alpha-synuclein transgenic mouse." J Cereb Blood Flow Metab **31**(3): 913-923.

Volpicelli-Daley, L. A., K. C. Luk, et al. (2014). "Addition of exogenous alpha-synuclein preformed fibrils to primary neuronal cultures to seed recruitment of endogenous alpha-synuclein to Lewy body and Lewy neurite-like aggregates." Nat Protoc **9**(9): 2135-2146.

von Bergen, M., P. Friedhoff, et al. (2000). "Assembly of tau protein into Alzheimer paired helical filaments depends on a local sequence motif ((306)VQIVYK(311)) forming beta structure." Proc Natl Acad Sci U S A **97**(10): 5129-5134.

Wadia, J. S., R. V. Stan, et al. (2004). "Transducible TAT-HA fusogenic peptide enhances escape of TAT-fusion proteins after lipid raft macropinocytosis." Nat Med **10**(3): 310-315.

Wan, C. P., C. S. Park, et al. (1993). "A rapid and simple microfluorometric phagocytosis assay." J Immunol Methods **162**(1): 1-7.

Wang, L., U. Das, et al. (2014). "alpha-synuclein multimers cluster synaptic vesicles and attenuate recycling." Curr Biol **24**(19): 2319-2326.

Wang, X., H. C. Schroder, et al. (2016). "Polyphosphate as a metabolic fuel in Metazoa: A foundational breakthrough invention for biomedical applications." Biotechnol J **11**(1): 11-30.

Whyte, C. S., I. N. Chernysh, et al. (2016). "Polyphosphate delays fibrin polymerisation and alters the mechanical properties of the fibrin network." Thromb Haemost **116**(5): 897-903.

Wickramasinghe, S. P., J. Lempart, et al. (2019). "Polyphosphate Initiates Tau Aggregation through Intra- and Intermolecular Scaffolding." Biophys J.

Winner, B., R. Jappelli, et al. (2011). "In vivo demonstration that alpha-synuclein oligomers are toxic." Proc Natl Acad Sci U S A **108**(10): 4194-4199.

Wood, H. G. and J. E. Clark (1988). "Biological aspects of inorganic polyphosphates." Annu Rev Biochem **57**: 235-260.

Wood, S. J., J. Wypych, et al. (1999). "alpha-synuclein fibrillogenesis is nucleation-dependent. Implications for the pathogenesis of Parkinson's disease." J Biol Chem **274**(28): 19509-19512.

Wu, C., M. Biancalana, et al. (2009). "Binding modes of thioflavin-T to the single-layer beta-sheet of the peptide self-assembly mimics." J Mol Biol **394**(4): 627-633.

Wurst, H. and A. Kornberg (1994). "A soluble exopolyphosphatase of Saccharomyces cerevisiae. Purification and characterization." J Biol Chem **269**(15): 10996-11001.

Xue, C., T. Y. Lin, et al. (2017). "Thioflavin T as an amyloid dye: fibril quantification, optimal concentration and effect on aggregation." R Soc Open Sci **4**(1): 160696.

Yang, T., S. Li, et al. (2017). "Large Soluble Oligomers of Amyloid beta-Protein from Alzheimer Brain Are Far Less Neuroactive Than the Smaller Oligomers to Which They Dissociate." J Neurosci **37**(1): 152-163.

Yoo, N. G., S. Dogra, et al. (2018). "Polyphosphate Stabilizes Protein Unfolding Intermediates as Soluble Amyloid-like Oligomers." J Mol Biol **430**(21): 4195-4208.

Yoo, N. G., S. Dogra, et al. (2018). "Polyphosphate Stabilizes Protein Unfolding Intermediates as Soluble Amyloid-like Oligomers." J Mol Biol.

Zakharian, E., B. Thyagarajan, et al. (2009). "Inorganic polyphosphate modulates TRPM8 channels." PLoS One **4**(4): e5404.

Zhang, C. M., K. Yamaguchi, et al. (2019). "Possible mechanisms of polyphosphate-induced amyloid fibril formation of beta2-microglobulin." Proc Natl Acad Sci U S A **116**(26): 12833-12838.

9 APPENDIX

9.1 Abbreviation

AD	Alzheimer's disease
AF	Alexa Fluor
α-syn$^{PFF-AF488}$	α-synuclein PFF labeled with AF488
ATP	adenosine triphosphate
BSA	bovine serum albumin
°C	degree Celsius
Da	Dalton
DNA	desoxyribonucleic acid
DTT	dithiothreitol
EDAC	1-ethyl-3-(3-dimethylaminopropyl) carbodiimide
E. coli	*Eschericia coli*
EDTA	Ethylenediaminetetraacetic acid
FP	Fluorescence polarization
FRET	Förster resonance energy transfer
GAG	glucoseaminoglycans
x g	gravity
g	gram
HCl	Hydrochloric acid
H_2O	dihydrogen monoxide (water)
IPTG	Isopropyl β-D-1-thiogalactopyranoside
KCl	Potassium chloride
k	kilo

KPi	Potassium phosphate
l	liter
m	milli
M	molar
min	minute
µ	micro
mPTP	mitochondrial permeability transition pore
n	nano
NaCl	Sodium chloride
NaOH	Sodium hydroxyde
OD_{600}	optical density at 600 nm
PD	Parkinson's disease
PFF	Preformed fibrils
PHB	polyhydoxybutyrate
Pi	inorganic phosphate
PPK	Polyphosphate kinase
PPX	polyphosphatase
polyP	polyphosphate
$polyP_{300\text{-}AF647}$	$PolyP_{300}$ labeled with AF647
S. cerevisiae	*Saccharomyces cerevisiae*
SDS	sodium dodecyl sulfate
TB	Trypan blue
TBO	Toluidine blue
TEM	Transmission electron microscopy

ThT	Thioflavin T
WT	Wild type

9.2 Index of figures

9.3 Publications

Mechanistic insights into the protective roles of polyphosphate against amyloid cytotoxicity.
Lempart J, Tse E, Lauer JA, Ivanova MI, Sutter A, Yoo N, Huettemann P, Southworth D, Jakob U.
Life Sci Alliance. 2019 PMID: 31533964

Polyphosphate Initiates Tau Aggregation through Intra- and Intermolecular Scaffolding.
Wickramasinghe SP, Lempart J, Merens HE, Murphy J, Huettemann P, Jakob U, Rhoades E.
Biophys J. 2019 PMID: 31400913

Role of Polyphosphate in Amyloidogenic Processes.
Lempart J, Jakob U.
Cold Spring Harb Perspect Biol. 2019, Review PMID: 30617049

The anti-inflammatory drug mesalamine targets bacterial polyphosphate accumulation.
Dahl JU, Gray MJ, Bazopoulou D, Beaufay F, Lempart J, Koenigsknecht MJ, Wang Y, Baker JR, Hasler WL, Young VB, Sun D, Jakob U.
Nat Microbiol. 2017 PMID: 28112760

Polyphoshpate: A Universally Conserved Modifier of Amyloidogenic Processes
Cremers C, Knoefler D, Marin N, Dahl JU, Gates S, Xie L, Lempart J, Chapman MR, Southworth DR, Galvan V, Jakob U.
Mol. Cell. 2016 PMID: 27570072

Evidence for a regulatory role of Cullin-RING E3 ubiquitin ligase 7 in insulin signaling
Scheufele, Wolf, Kruse, Hartmann, Lempart, Muehlich, Pfeiffer, Field, Charron, Pan, Engelhardt, Sarikas,
Cellular Signaling, 2014 PMID: 24219910

Oncogenes and tumor suppressor genes in squamous cell carcinoma of the tongue in young patients
Knopf, Lempart, Bas, Slotta-Huspenina, Mansour, Fritsche,
Oncotarget, 2015 PMID: 25633809

9.4 Meetings and Conferences

Midwest Stress Response and Molecular Chaperone Meeting (January 2019), Northwestern University, Evanston, USA
Polyphosphate – A Novel Modifier of Neurodegeneration
Justine Lempart, Eric Tse, James Lauer, Philipp Huettemann and Ursula Jakob
(oral presentation)

Neurobiology of brain disorders (August 2018), Rey Don Jaime Grand Hotel in Castelldefels, Spain
Polyphosphate - A Modifier of Neurodegeneration?
Justine Lempart, Eric Tse, James Lauer, Jacob Murphy and Ursula Jakob
(poster presentation)

MCDB department retreat (October 2017), Marriott Resort, Ypsilanti, USA
Polyphosphate - A Modifier of Neurodegeneration?
Justine Lempart, Eric Tse, James Lauer, Jacob Murphy and Ursula Jakob
(oral presentation)

Stress proteins in growth, development & disease (July 2017), Grand Summit Hotel at Sunday River, Newry ME, USA
Polyphosphate - A Modifier of Neurodegeneration?
Justine Lempart, Stephanie Gates, Melissa Birol and Ursula Jakob
(poster presentation)

10 ACKNOWLEDGEMENTS

Zuerst möchte ich mich bei meiner Familie bedanken. Meine Eltern Birgit und Olaf Lempart haben stets alles für mich gegeben. Danke, dass ihr immer an mich geglaubt habt und mich dazu erzogen habt nie aufzugeben. Ohne euch wäre ich nie so weit gekommen.
Danke auch an meine Oma, Evi, Manfred und Daniel. Eure Unterstützung und eurer Glaube an mich bedeutet mir so viel!

Especially, I would like to thank my supervisor Dr. Ursula Jakob - an incredible scientist and mentor. I am beyond grateful that she enabled my work on this very intriguing project. Her never-ending support, encouragement and guidance helped me to exceed my own expectations and push me to my greatest.

I also want to thank Dr. Johannes Buchner for being my advisor in München, without him, this dissertation would never have been possible.

I would like to express my gratitude to the entire Jakob and Bardwell lab. During my PhD thesis I was truly blessed to have awesome co-worker/friends inside of the lab. The collegiality and teamwork in our group is truly inspiring. In particular I want to thank Claudia Cremers, Daniela Knoefler and Daphne Bazoupoulou for initial supervision and help. I want to thank Ellen Quarles, Jan Dahl, Anke Kaufmann, Will Voth, Bryndon Oleson, Nicholas Yoo, Akash Rai and Lihan Xie for their scientific support but more importantly for their friendship.

I would like to thank James Lauer, Jacob Murphy and Philipp Huettemann, the students I had the pleasure to supervise during my time in Ann Arbor. There is nothing more inspiring than the enthusiasm of young scientists. I am grateful for their contribution and hard work as well as for the chance to teaching and mentoring them.

I would like to thank the Böhringer Ingelheim Founds for supporting me financially and intellectually through the journey of my PhD. I am deeply honored to have been selected as a scholar and greatly benefited from courses and conferences offered through the program.

The friends I made before or throughout my PhD journey have made hard moments more bearable and the great times even more fun. There are too many to mention them all, but special thanks to Jacqueline Isaac, Jeannette Tieno, Ellen Quarles, Nicolette Ognjanovski and Regina Baur. I am so grateful to call such smart, inspiring and strong women my best friends.

I would also like to thank my American family. James and Denise (as well as the whole Ruhlman and Brown family), I am so blessed to have you as bonus family. Thank you for your support!

Last but no least I want to thank my awesome husband James Ruhlman Brown. He is my rock, my foundation and my better half, who accompanied me though the whole journey of my PhD. His imperturbable support and his belief in me were more than I could have ever asked for. I am thankful for the hundreds of hours that he invested by listening to my practice talks. Thank you for your patience and understanding.